

Bodo's Power Systems®

Electronics in Motion and Conversion

December 2025



Pulsed Inductance Measurement on Power Inductors up to the MVA Range

**The Power Choke Tester DPG10 Series
in Small Series and Mass Production**

POWER CHOKE TESTER DPG10/20 SERIES

Inductance measurement
from 0.1 A to 10 kA

KEY FEATURES

Measurement of the

- Differential inductance $L_{diff}(i)$ and $L_{diff}(Udt)$
- Amplitude inductance $L_{amp}(i)$ and $L_{amp}(Udt)$
- Flux linkage $\psi(i)$
- Magnetic co-energy $W_{co}(i)$
- Flux density $B(i)$
- DC resistance

Also suitable for 3-phase inductors

WIDE RANGE OF MODELS

7 models available with maximum test current from 100A to 10000A and maximum pulse energy from 1350J to 15000J

KEY BENEFITS

- Very easy and fast measurement
- Lightweight, small and affordable price-point despite of the high measuring current up to 10000A
- High sample rate and very wide pulse width range
=> suitable for all core materials

APPLICATIONS

Suitable for all inductive components from small SMD inductors to very large power reactors in the MVA range

- Development, research and quality inspection
- Routine tests of small batch series and mass production



INTRODUCING

UX3 SERIES HIGH TEMPERATURE UNLYTIC® 125°C



The UX31 / UX32 / UX34 / UX35 UNLYTIC HIGH TEMPERATURE UX3 SERIES represents the best choice for high power DC application featuring operation to 125°C with no voltage derating and **acts as a drop in replacement** to existing standard polypropylene capacitors.



Content

Viewpoint	4
Why Power is so important	
Events	4
News	6-12
Product of the Month	14
Compact, High-Density, Fully Integrated, Scalable Power Module	
Blue Product of the Month	16
Optically Isolated Probing Solution for Analyzing Fastest Switching Operations	
Cover Story	18-23
Pulsed Inductance Measurement Replaces Reactance Measurement in the Production of Large Power Chokes <i>By Hubert Kreis, Chief Executive Officer, ed-k and Robert Rohn, Development, Hans von Mangoldt GmbH</i>	
Wide Bandgap	24-26
Three-Phase Module Based on Monolithic GaN Half-Bridge ICs <i>By Federico Unnia, Manager of Applications Engineering, and Marco Palma, Director of Applications Engineering, Efficient Power Conversion</i>	
Power Modules	28-30
The Next Leap in EV Powertrain Efficiency: The Rise of 3-Level Inverters <i>By Antonio Poveda Serrano, Automotive Application Engineer, and Sebastian Pawusch, Field Application Engineer Automotive Semiconductors, Fuji Electric</i>	
Diodes and Rectifiers	32-35
SiC-MPS Diodes Under Stress: Robust Performance Under Extreme Current and Temperature Conditions <i>By Simon Ginzel, Professorship of Power Electronics, Helmut-Schmidt-University, Hamburg/Germany; Zhe Yu, Principal Power Application Engineer, and Bengt Sprätz, Product Application Engineer, both Nexperia, Hamburg/Germany</i>	

Power Supply	36-37
Power Pulsating Buffer to meet peak power demands in AI server PSUs without disturbing the grid <i>By Sam Abdel-Rahman, System Architect Server SMPS, Infineon Technologies</i>	
Wide Bandgap	38-41
Selecting the Right SiC MOSFET Device: A Key to Efficient Zero-Voltage Switching <i>By Thomas Lehmeier, Yan Zhou, Martin März, Institute of Power Electronics, Friedrich-Alexander-Universität Erlangen-Nürnberg, and Ajay Poonjal Pai, Head of WBG Innovation, Munich, Sanan Semiconductor</i>	
DC/DC Converter	42-45
Solving DC/DC Power Challenges in Military Avionics Through Modularity (Part 2) <i>By Christian Jonglas, Technical Support Manager, GAIA Converter</i>	
Packaging	46-47
An Exploration of Surface Mount Power Packaging Technologies for SiC MOSFETs <i>By Vipin Gaonkar, Principal Applications Engineer, High-Power Solutions Business Unit, Microchip Technology</i>	
DC/DC Converter	48-51
Configuring Four-Switch Buck-Boost µModule Regulators for Step-Up, Step-Down, or Inverting Output <i>By Ling Jiang, Senior Manager, Wesley Ballar, Senior Engineer, and Anjan Panigrahy, Product Applications Engineer, Analog Devices; and Henry Zhang, ADI Fellow</i>	
New Products	52-56

Bodo's Power systems®
Electronics in Motion and Conversion



Follow us on LinkedIn:
[linkedin.com/company/bodo-s-power-systems](https://www.linkedin.com/company/bodo-s-power-systems)

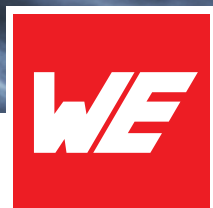
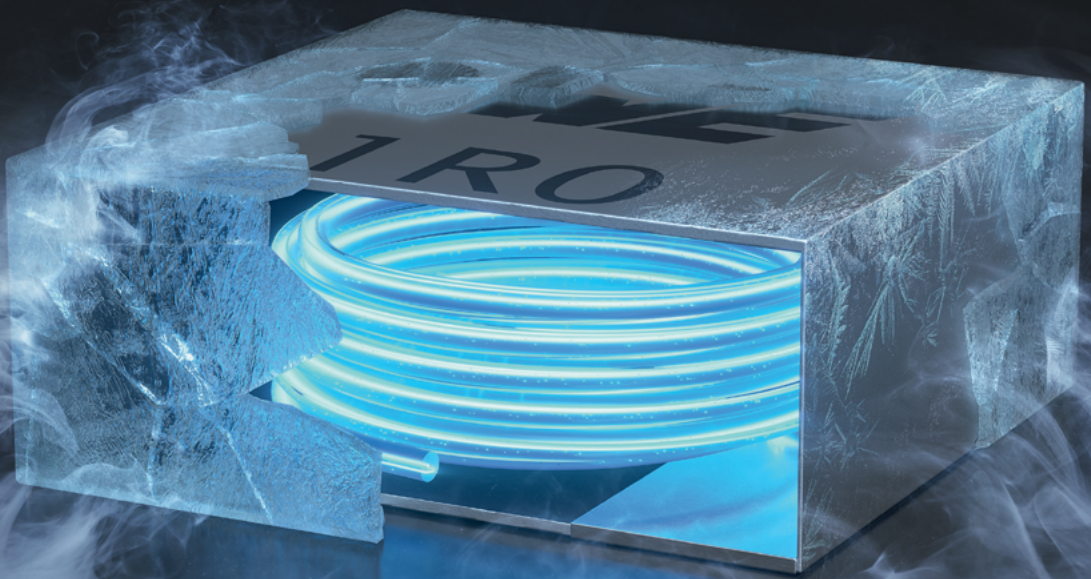
Supporters & Friends



WÜRTH ELEKTRONIK MORE THAN YOU EXPECT

ULTRA LOW LOSSES

WE-MXGI



WE are here for you!

Join our free webinars on:
www.we-online.com/webinars

With the WE-MXGI Würth Elektronik offers the newest molded power inductor series. It combines an innovative iron alloy material that provides high permeability for lowest R_{DC} values combined with an optimized wire geometry.

Ready to Design-In? Take advantage of personal technical support and free samples ex-stock.

www.we-online.com/WE-MXGI

Highlights

- Extremely high power density
- Ultra low R_{DC} values and AC losses
- Magnetically shielded
- Optimized for high switching frequencies beyond 1 MHz

#UltraLowLosses

A Media

Katzbek 17a
24235 Laboe, Germany
Phone: +49 4343 42 17 90
Fax: +49 4343 42 17 89
info@bodospower.com
www.bodospower.com

Founder

Bodo Arlt, Dipl.-Ing.
bodo@bodospower.com

Editor in Chief

Alfred Vollmer, Dipl.-Ing.
alfred@bodospower.com

Correspondent Editor Bavaria

Roland R. Ackermann, Dipl.-Ing.
roland@bodospower.com

Editor China

Min Xu – xumin@i2imedia.net

US Support

Rusty Dodge
rusty@eetech.com

Creative Direction & Production

Bianka Gehlert
b.gehlert@t-online.de

Publisher

Holger Moscheik
holger@bodospower.com

Free Subscription to qualified readers
Bodo's Power Systems is available for
the following subscription charges:
Annual charge (12 issues) is
150 € world wide · Single issue is 18 €
subscription@bodospower.com

**Printing by:**

Dierichs Druck+Media
GmbH & Co. KG
34121 Kassel, Germany

A Media and Bodos Power Systems

assume and hereby disclaim any
liability to any person for any loss or
damage by errors or omissions in the
material contained herein regardless
of whether such errors result from
negligence accident or any other
cause whatsoever.

Why Power is so important



These days we hear a lot about power in the news: political power, military power, market power, company power, purchasing power, electrical power, power plants, power grid etc. And it was brought to everybody's attention, just how important even the extremely tiny power semiconductor devices are for final products like cars, for example. For many years these tiny power devices were often smiled at, but not appreciated. At the same time, there was extreme price pressure; buyers often haggled over less than 0.1 cents. Now as we have seen in the news just what can happen, when political power, market power, company power and purchasing power clash. We have witnessed the implication of such an event recently which shows us, how important ALL individual components of a system are.

When we consider pure design solutions in the broad field of electrical power engineering, we see lots of focal activities around and with wide bandgap semiconductors. That's why we once again organized Bodo's Wide Bandgap Event, this year on December 2 and 3, 2025. But we, at Bodo's Power, also want to bring efficient power solutions forward – independent from the technology and the kind of semiconductors used (Si, SiC, GaN). We all think that we owe it to our (grand)children to use energy (and power) carefully and to use resources sparingly and sustainably. That's why we always appreciate efficient and clever designs.

With our magazine (printed and online), our website, the newsletter and the WBG Event we are making our contribution to the power community.

In December we also feel the power of Christmas, Hanukkah, the holiday season or whatever you're celebrating. Spending a few days with the family, having a few days away from work—that is the biggest common denominator worldwide for these last days of the year. These are days when we, as humans, can recharge our batteries so that we can work at full power again in the new year on the power solutions of the future. With this in mind, the entire team of Bodo's Power Systems would like to wish you all a Merry Christmas and an excellent start to the New Year.

Bodo's magazine is delivered by postal service to all places in the world. It is the only magazine that spreads technical information on power electronics globally. We have EETech as a partner serving our clients in North America. If you speak the language, or just want to have a look, don't miss our Chinese version at bodospowerchina.com. An archive, of every issue of the magazine, is available for free at our website bodospower.com.

My Green Tip of the Month:

If you have any remaining incandescent light bulbs replace them with energy-saving LED lighting solutions. When you choose light sources with a color rendering index (CRI) of >80 the colors will be good in every day life but not perfect, while a CRI of >90 will provide very good color rendering. And with a color temperature in the range of 2.700 K to 3.300 K (warmwhite) the light will be cozy and relaxing, similar to the old incandescent light; whereas 4.000 K to 6.500 K has an energizing and refreshing effect, similar to daylight, but also looks somewhat bluish or cold.

Alfred Vollmer

Events

Bodo's WBG Event 2025

Munich, Germany December 2 – 3
www.bodoswbm.com

IEEE IEDM 2025

San Francisco, CA, USA December 6 – 10
www.ieee-iedm.org

PCIM Asia New Delhi 2025

New Delhi, India December 9 – 10
www.pcim.in

SEMICON Japan 2025

Tokyo, Japan December 17 – 19
www.semiconjapan.org

DesignCon 2026

Santa Clara, CA, USA February 24 – 26
www.designcon.com

PLECS Conference 2026

Zurich, Switzerland March 3 – 4
www.plexim.com

CIPS 2026

Dresden, Germany March 10 – 12
www.cips.eu

Wide-Bandgap Developer Forum 2026

Online March 10
www.infineon.com

APEC 2026

San Antonio, TX, USA March 22 – 26
www.apec-conf.org



MERRY CHRISTMAS

**Season's Greetings from
the Team at**

***Bodo's POWER* Systems®**

**We wish you and your family
a prosperous and successful
New Year!**

Alfred Bollmer

Bodo Holt

Holger Mönch



Win a Power Analyzer Set for your Research Lab

Just in time for Christmas, HIOKI EUROPE GmbH is giving away a complete Power Analyzer Set with a retail value of around EUR 35,000 consisting of ex-demo devices. This special giveaway campaign is open exclusively to universities and research institutions across the European Union specialising in power electronics or energy efficiency. Are these your areas of expertise? Join the competition at shop.hioki.eu/win-PW6001-Power-Analyzer by briefly describing how you would use power analysis in your application – the most convincing idea wins! Among all participants, the HIOKI jury will award a Power Analyzer Set. With a bit of luck, you could find this special present under your institution's Christmas tree this year. Deadline for entries: 19 December 2025.

www.hioki.eu



GaN Technology Licensed to Accelerate U.S.-Manufactured Power Portfolio

GlobalFoundries (GF) announced that it has entered into a technology licensing agreement with TSMC for 650V and 80V Gallium Nitride (GaN) technology. This strategic move will accelerate GF's next generation of GaN products for datacenter, industrial and automotive power applications and provide U.S.-based GaN capacity for a global customer base. As traditional silicon CMOS technologies hit their performance limits, GaN is emerging as the next-generation solution for meeting the increasing demand for higher efficiency, power density and compactness in power systems. GF is developing a comprehensive GaN portfolio, including high-performance 650V and 80V technologies aimed at enabling electric vehicles, datacenters, renewable energy systems and fast-charging electronics. GF's GaN solutions are designed for harsh environments, with a holistic approach to GaN reliability that spans process development, device performance and application integration. GF will qualify the licensed GaN technology at its manufacturing facility in Burlington, Vermont, leveraging the site's expertise in high-voltage



GaN-on-Silicon technology to accelerate volume production for customers seeking next-generation power devices. Development is set for early 2026, with production to begin later in the year.

www.gf.com

Power Architecture for AI Factories with SiC and GaN, Power MOSFET, and Power IC Solutions

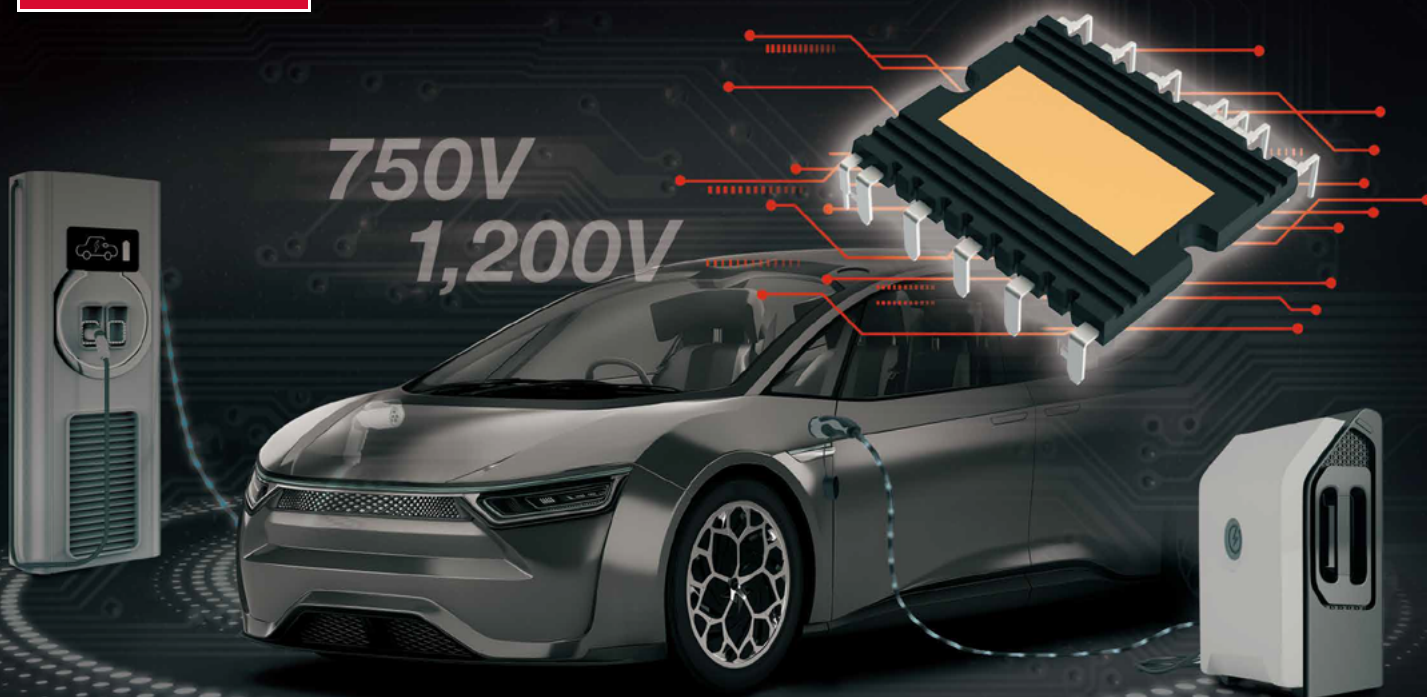
Alpha and Omega Semiconductor Limited (AOS) announced support for the power requirements of the innovative 800 V_{DC} architecture announced by NVIDIA. This architecture is set to power the next generation of AI data centers, which will feature megawatt-scale racks to meet the exponential growth of AI workloads.

The shift from traditional 54V power distribution to an 800 V_{DC} system is a fundamental change in data center design, aimed at overcoming the physical limits of existing infrastructure. By reducing power conversion steps and enabling more efficient power delivery, the 800 V_{DC} architecture promises significant efficiency gains, reduced copper usage, and improved reliability. This paradigm shift requires advanced power semiconductors, particularly Silicon Carbide (SiC) and Gallium Nitride (GaN), to handle higher voltages and frequencies with maximum efficiency.

"As a key supplier to the high-performance data center market, our portfolio of SiC and GaN products is strategically aligned with the core technical demands of next generation AI factories with 800 V_{DC} power architecture," said Ralph Monteiro, Sr. VP, Power IC and Discrete Product lines at AOS. "We are collaborating with NVIDIA to design 800 V_{DC} power semiconductors to provide the high efficiency and power density necessary for the new power distribution modules, from the initial AC-to-DC conversion to the final DC-to-DC stages within the racks."



www.aosmd.com



New High Power Density EcoSiC™ Modules

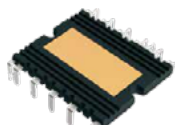
Compact high heat dissipation design sets a new standard for OBCs

ROHM has developed the new 4-in-1 and 6-in-1 SiC molded modules in the HSDIP20 package optimized for PFC and LLC converters in onboard chargers (OBC) for xEVs (electric vehicles). The lineup includes six models rated at 750V (BSTxxx1P4K01) and seven products rated at 1200V (BSTxxx2P4K01).

Lineup ideal for configuring high-power power supply circuit topologies such as PFC and LLC circuits

Adopting high thermal conductivity insulating materials ensures superior heat dissipation, facilitating insulation design

Delivers higher output compared to power modules of similar size

Part No.	Absolute Max. Ratings (Tj=25°C)			Topology	Module Package
	V _{DSS} [V]	R _{DS(on)} [mΩ]	I _D [A] ¹		
BST91B1P4K01	750	13	90	4in1	 HSDIP20 [38.0mm x 31.3mm x 3.5mm]
BST47B1P4K01		26	47		
BST31B1P4K01		45	31		
BST91T1P4K01		13	90	6in1	
BST47T1P4K01		26	47		
BST31T1P4K01		45	31		
BST70B2P4K01	1,200	18	70	4in1	
BST38B2P4K01		36	38		
BST25B2P4K01		62	25		
BST70T2P4K01		18	70	6in1	
BST38T2P4K01		36	38		
BST25T2P4K01		62	25		
BST70M2P4K01 ²		18 ³ / _{36⁴}	70 ³ / _{38⁴}		

^{*1}: Tc=25°C VGS=18V ^{*2}: Combines chips with different ON resistances

^{*3}: Q1, Q4 pins ^{*4}: Q2, Q3, Q5, Q6 pins

EcoSiC™ is a trademark or registered trademark of ROHM Co., Ltd.

Semiconductor Manufacturer signs long-term Contract for green Electricity Supply

Infineon Technologies has concluded Power Purchase Agreements (PPA) with PNE and Statkraft for green electricity. Over the next ten years, Infineon will purchase green electricity from PNE AG's Schlenzer and Kittlitz III wind farms in Brandenburg in Germany to supply its sites in Dresden, Regensburg, Warstein and Neubiberg near Munich. Seven turbines in the PNE AG wind farms offer a total capacity of 24 MW and a contracted electricity volume of 550 GWh. Statkraft will additionally supply German locations with renewable electricity from solar parks in Spain with a total volume of 220 GWh over the next five years. Infineon aims to switch its global operations to 100 % green electricity this year and become CO₂-neutral for Scope 1 and 2 emissions by 2030. Infineon has been using green electricity in Germany and Europe since the 2021 fiscal year. By concluding Power Purchase Agreements for specific wind and solar power plants in Brandenburg and Spain, the company is now securing its long-term green electricity requirements and supporting the expansion of renewable energies.



www.infineon.com

Entering the Semiconductor Industry

Kurtz Ersa has taken over the business operations of the insolvent equipment manufacturer ATV Technologie. For Kurtz Ersa, this is the strategic step into the market for production systems for the semiconductor industry that has been announced for some time. All ATV employees will be taken over. ATV will continue to do business under the name Kurtz Ersa Semicon GmbH. The company is specialized in the development and distribution of high-quality vacuum solder-



ing systems providing precise temperature control and high homogeneity – essential for the requirements of the semiconductor and microelectronics industry. The interdisciplinary team, consisting of engineers, physicists, and specialists in precision mechanics and electrical engineering, delivers customized solutions for universities, research institutes, laboratories, and manufacturing companies.

www.kurtzersa.com

Vertical GaN Sample Prototypes – already in 2025!

Vertical Semiconductor (Vertical), a semiconductor company spun out of the Massachusetts Institute of Technology (MIT), received \$11 million in seed funding led by Playground Global to help accelerate development of vertical GaN transistors. Additional investors



include JIMCO Technology Fund, milemark•capital, and Shin-Etsu Chemical. The company's technology is said to reduce energy loss, cut heat, and simplify infrastructure, improving efficiency by up to 30% and enabling a 50% smaller power footprint in AI data center racks. Vertical Semiconductor has demonstrated its vertical GaN technology on 8-inch wafers using standard silicon CMOS semiconductor manufacturing methods, enabling seamless integration with existing process technology and making it ready for real-world deployment for devices from 100 V to 1.2 kV. With a prototype in development and commercial milestones ahead, the company plans to start early sampling for its first prototype packaged devices by the end of the year and a fully integrated solution in 2026.

www.verticalsemi.com

Job Promotion: Focus on Solution for Power Electronics



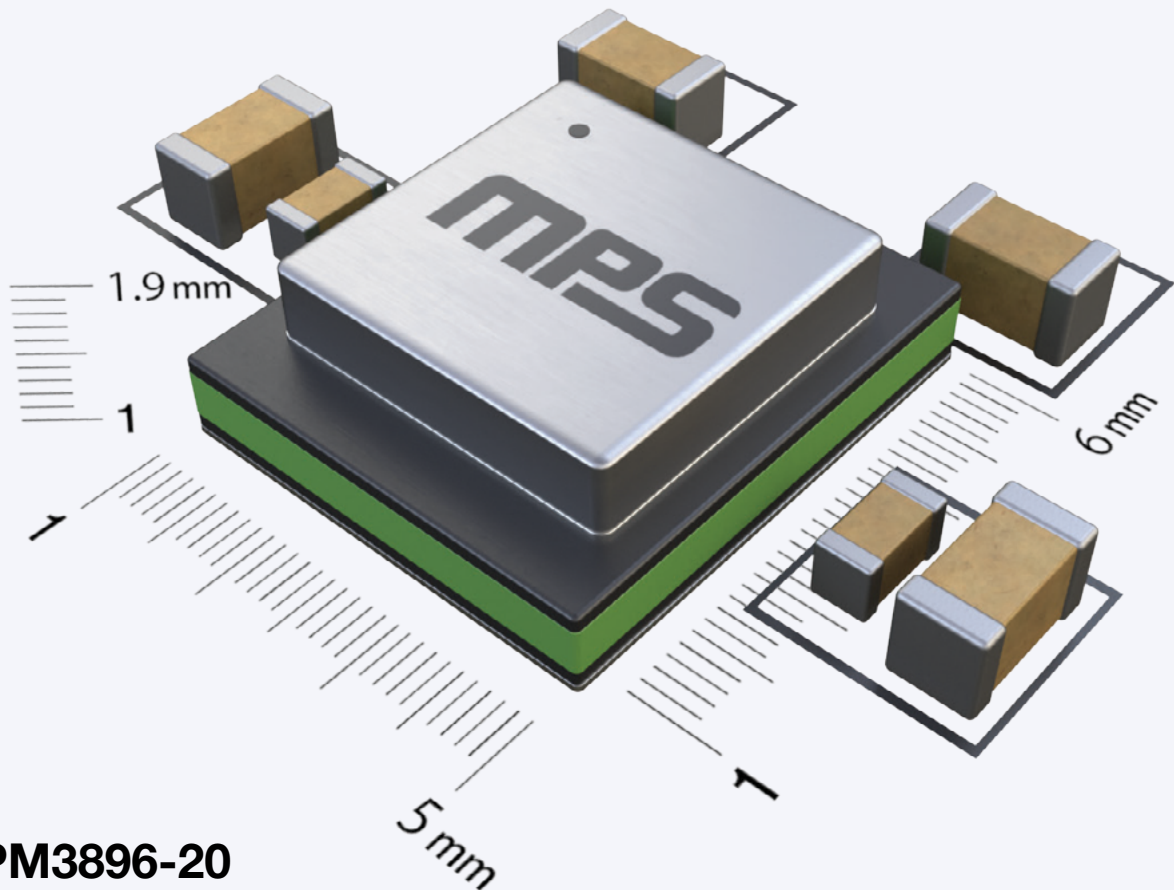
Indium Corporation has promoted Joseph Hertline to Senior Product Manager, Engineered Solder Materials (ESM). In his new role, as Senior Product Manager, Hertline is now responsible for driving the growth of Indium Corporation's global ESM initiatives through the development of marketing strategies. He will continue to lead the company's efforts in the power electronics application

segment with a broader scope of products, applications, and customer segments. He will also continue to lead ESM Application Engineering efforts for all ESM product lines. Hertline has more than a decade of experience in engineering and product management within the electronics industry and joined Indium Corporation in 2020 as Product Manager, Power Electronics.

www.indium.com

Power Modules. Simple as that.

Shorten your design cycle.



MPM3896-20

5V, 20A, 5mm x 6mm x 1.9mm

Key Benefits:

- Small-Sized, Fully Integrated Solution
- Reduced Overall Solution Size
- High Efficiency for Various Applications
- Ease of Use: Simple & Flexible → Designer-Oriented
- EMI Class-B Certification and Fast Time-to-Market
- Anytime Support from MPS
- Broadest Portfolio:
 - Voltages from <7V Up to >50V
 - Currents from <1A Up to >100A

Suitable Applications:

- Industrial & Test Equipment
- FPGAs
- Drones & Robotics
- Optical Communications
- Datacenters & AI

Learn More



MPS

Digital Power Joint Lab

GigaDevice has launched a Digital Power Joint Lab in collaboration with Navitas Semiconductor. By combining GigaDevice's GD32MCU expertise with Navitas' advantages in high-frequency, high-speed, and highly integrated GaN technologies, and its GeneSiC™ technology leveraging 'trench-assisted planar' technology, the collaboration aims to deliver intelligent and high-efficiency digital power solutions for emerging markets such as AI data centers, photovoltaic inverters, energy storage systems, charging infrastructure, and electric vehicles. Before its official launch, the lab achieved several important technological milestones, including 4.5 kW and 12 kW server power supply solutions and a 500 W single-stage PV micro-inverter. The lab will focus on developing comprehensive system-level reference designs and application-specific solutions to enable smarter, greener, and more energy-efficient power systems across data centers, renewable energy, and electric mobility.

www.navitassemi.com



Web-Based Tools for Power Design

Analog Devices launched ADI Power Studio, a comprehensive family of products that offers modeling, component recommendations and efficiency analysis with simulation. In addition, ADI is introducing two new web-based tools with a modernized user experience



under the Power Studio umbrella: ADI Power Studio Planner and ADI Power Studio Designer. These new tools, together with the full ADI Power Studio portfolio, including LTspice®, SIMPLIS®, LTpowerCAD®, LTpowerPlanner®, EE-Sim®, LTpowerPlay® and LTpowerAnalyzer™, streamline the entire power system design process. The Power Studio tools support engineers from initial concept through measurement and evaluation, empowering engineers to design with confidence and efficiency. ADI Power Studio Planner is a web-based tool for system-level power tree planning, which gives engineers an interactive view of their system architecture. ADI Power Studio Designer is also a web-based tool, however, for IC-level power supply design. It provides component recommendations, performance estimates, and tailored efficiency analysis. These tools represent the first phase of ADI's vision to deliver a fully connected power design workflow for customers.

www.analog.com

Power Company opened its Italian Headquarters

RECOM Power Solutions (RPS), part of the RECOM Group, officially celebrated the opening of its company headquarters in Mareno di Piave, Italy. The event brought together employees from around the world, customers, and representatives from politics and business to mark this milestone. The celebration embodied the company's core values – teamwork, passion, and a shared vision. In an atmosphere filled with energy and inspiring conversations, the event marked not only the inauguration of the new site but also the beginning of another chapter in the company's history.

www.recom-power.com



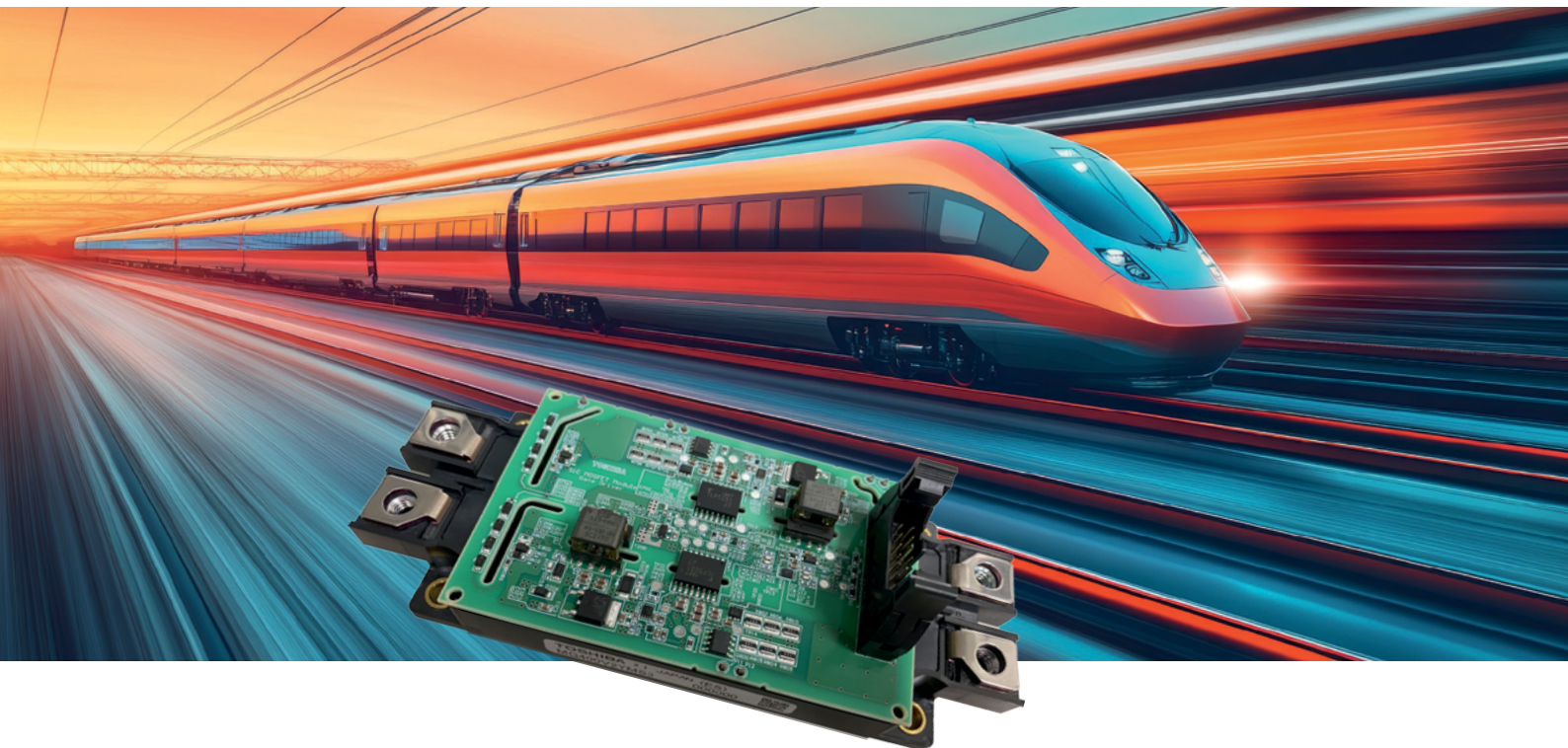
APEC 2026 Registration has started

The registration for APEC 2026, which will take in San Antonio, Texas (USA) on March 22-26, 2026, is now open. The IEEE Applied Power Electronics Conference and Exposition (APEC) offers a wide range of educational and social activities. APEC attendees can choose the registration category that best fits their needs and interests. Early bird registration will close on January 26, 2026.

www.apec-conf.org

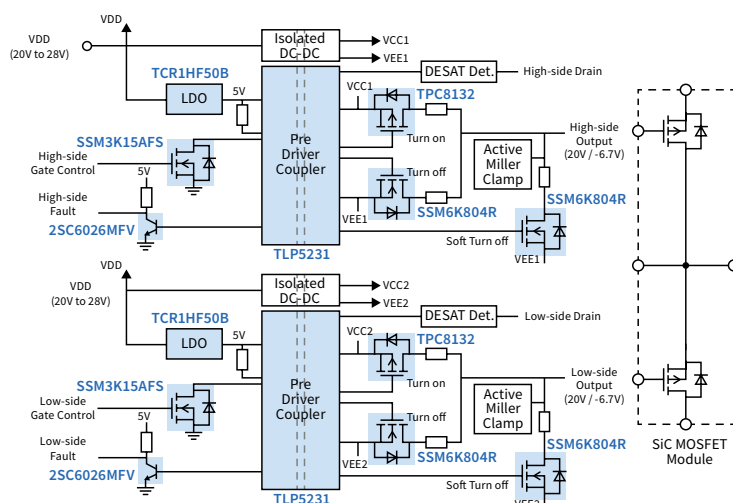


Gate Drive Circuit Solution for SiC MOSFET Module



Highlights

- Built-in implementation on a SiC MOSFET Module
- Output voltage +20V (typ.) / -6.7V (typ.)
- Output current $\pm 9.8\text{A}$ (max.)
- Max. PWM frequency 50kHz
- Independent open-collector fault signal output of high-side and low-side



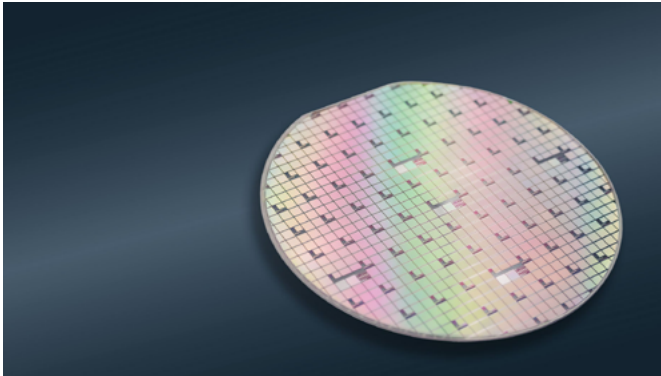
Featured Products

- **TLP5231** – isolated pre-gate driver
 - Split output
 - UVLO protection
 - Over current protection
 - Fault signal feedback
 - Soft shutdown
 - Active Miller clamp using DESAT
- **SSM6K804R** – n-ch MOSFET
 - 40V, 18mΩ @ $V_{GS} = 4.5\text{V}$, 1.5W, TSOP6F package
- **TPC8132** – p-ch MOSFET
 - -40V, 20mΩ @ $V_{GS} = -10\text{V}$, 1.9W, SOP-8 package
- **TCR1HF50B** – LDO Regulator
 - $V_{IN} = 4 \sim 36\text{V}$, $V_{OUT} = 1.8\text{V}$ to 5.0V, $V_{OUT} = \pm 1\%$ ($T_a = 25^\circ\text{C}$)
 - Overcurrent protection, thermal shutdown, inrush current reduction
- **SSM3K15AFS** – n-ch MOSFET
 - 30V, 3.6Ω @ $V_{GS} = 4\text{V}$, 100mW, SOT-416 package
- **2SC6026MFV** – npn transistor
 - 50V, 150mA (max.), SOT-723 package



Vertical GaN Semiconductors

As global energy demand surges from AI data centers, electric vehicles, and other energy intensive applications, onsemi has introduced vertical gallium nitride (vGaN) power semiconductors, setting a new benchmark for power density, efficiency and ruggedness



for these applications. These next-generation GaN-on-GaN power semiconductors conduct current vertically through the compound semiconductor, enabling higher operating voltages and faster switching frequencies, leading to energy savings to deliver smaller and lighter systems across AI data centers, electric vehicles (EVs), renewable energy, and aerospace, defence and security. onsemi's vGaN technology is designed to handle high voltages in a monolithic die – 1,200 volts and beyond – switching high currents at high frequency with superior efficiency. High end power systems built with this technology can reduce losses by almost 50% and by operating at higher frequencies can also reduce the size, including passives like capacitors and inductors by a similar amount. Additionally, compared to commercially available lateral GaN, vGaN devices are approximately three times smaller. This makes onsemi's vGaN ideal for critical high-power applications where power density, thermal performance and reliability are paramount.

www.onsemi.com

EPCIA President appointed

According to Murata Manufacturing, Christophe Pottier, Vice President of Sales for Murata Europe, has been appointed as President of the European Passive Components Industry Association (EPCIA), effective immediately. Mr. Pottier brings over three decades of deep experience within the electronics industry to his new role, with a strong focus on strategic sales and automotive sector initiatives. His experience at Murata, where he has contributed across multiple domains, including strategic sales in telecom and collaborative initiatives in the automotive industry, has shaped his understanding of how these components quietly

power advanced technologies. As EPCIA President, Mr. Pottier's mission is to promote a stronger, more connected passive components ecosystem across Europe by focusing on three key areas. The first area is elevating the role of passive components as these elements regulate, protect, and optimize electronic signals, making them indispensable to chip performance and system reliability. The second focal point is fostering collaboration which means working with adjacent industries to meet demands for miniaturization, high-speed data, and energy efficiency as integration into semiconductor packaging accelerates.



Strengthening ties with research institutes is the third key area: Driving innovation in materials science, sustainability, and advanced manufacturing through partnerships with Europe's academic and research institutions.

www.murata.com

Report: Graphene in electronic Applications

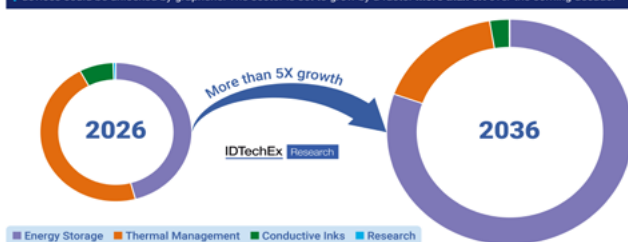
Graphene was initially celebrated as a sci-fi material destined to transform electronics, quantum devices, and futuristic sensors. While expectations soared, commercial reality proved more modest. Rather than enabling transparent phones or levitating trains, graphene first succeeded in practical roles such as enhancing polymer composites in tires, coatings, and sporting goods through improved strength and conductivity. Now, with advances in manufacturing and renewed interest from major electronics and energy

companies, the question resurfaces: are we finally approaching the breakthrough era once promised? IDTechEx has now released a report, dubbed "Graphene & 2D Materials 2026-2036: Technologies, Markets, Players", which includes granular 10-year graphene market forecasts, based on profiles of 90+ key players and leverages extensive coverage of many end-use markets for graphene. Graphene is increasingly used in consumer electronics for thermal management, leveraging its exceptional heat conductivity to improve device cooling and reliability. Beyond passive materials, its high surface area and conductivity also make it a strong candidate for energy storage applications, particularly in next-generation batteries and supercapacitors, where faster charging and longer lifetimes are sought. IDTechEx believes that thermal management applications is a key early area for graphene adoption. There is increasing demand for high-performance heat spreaders, and the graphene properties and morphology are well-suited. The thermal conductivity of carbon materials tend to be higher than that seen in metals, with graphene oxide (GO) reporting a thermal conductivity in excess of 3,000 W/m·K.

www.IDTechEx.com

Small Material, Big Impact: Graphene in Electronic Applications

The electronic applications of graphene have received a lot of hype and bordered on science fiction over the past two decades. Tangible success is now being achieved in thermal management, while the next generation of energy storage devices could be unlocked by graphene. The sector is set to grow by a factor more than 5X over the coming decade.



Japanese precision since 1935

HIOKI

WATT a X-mas!

**WIN
A POWER
ANALYZER
SET!***



**Win precision measurement instruments –
exclusive for universities and research labs**

- 1 x fully equipped **PW6001-16 Power Analyzer**
- 4 x **CT6843-05 AC/DC Current Clamps**

Participate online now!

shop.hioki.eu/win-PW6001



*The Power Analyzer Set consists of ex-demo instruments with a new-item retail value of 35,000 Euro that are used but in great condition. Promotion organized by HIOKI EUROPE GmbH, Eschborn, Germany. Participation limited exclusively to universities and research institutions within the EU. No purchase necessary. Closing date: 19 December 2025. Terms and conditions: <https://shop.hioki.eu/win-PW6001-terms>

Compact, High-Density, Fully Integrated, Scalable Power Module



Monolithic Power Systems' MPM3695-20 is a fully integrated, synchronous, step-down power module that delivers high current and fast transient response in a really small ECLGA-29 package (5 mm x 6 mm x 4.4 mm). Designed to simplify board-level power delivery, the module supplies up to 25 A of continuous output current (I_{OUT}) and supports a 0.5 V to 5.5 V output voltage (V_{OUT}), covering today's processor cores, FPGAs, ASICs, and input/output (I/O) rails with minimal external components.

The MPM3695-20 offers real input flexibility and output accuracy. It accepts a wide input range and supports both internal and external VCC configurations, enabling operation from common intermediate-bus voltages. MPS specifies tight reference accuracy ($\pm 1\%$ across industrial temperature ranges), and the module supports true remote sense and pre-biased outputs for accurate regulation at the load. These characteristics reduce design iterations and help meet stringent power supply requirements in telecom, datacom, and computing applications.

High integration brings board-level benefits. By embedding the power stage, magnetics, and switching components inside a single module, the MPM3695-20 reduces the BOM count and helps designers avoid complex layout. Only a handful of external passive components and configuration parts are required, accelerating time-to-prototype and trimming the PCB area in space-constrained designs where power density is critical.

An additional advantage of MPS's power modules is their control flexibility and telemetry, which expand system-level utility. The module's constant-on-time (COT) adaptive control provides ultra-fast transient response and stable operation without complicated external compensation. Designers can configure operating param-

eters, soft start (SS) behavior, the switching frequency (f_{SW} , selectable up to 1 MHz), and the current limit by utilizing the MPS's graphical user interface, Virtual Bench 4.0. The integrated multiple-time programmable (MTP) memory preserves customized parameters across power cycles, while telemetry readback provides status and fault indication for the input voltage (V_{IN}), output voltage (V_{OUT}), output current (I_{OUT}), and temperature, enabling robust monitoring and system management.

Protection and scalability are built-in. The MPM3695-20 includes comprehensive protection features — including over-current protection (OCP), over-voltage protection (OVP), under-voltage protection (UVP), and over-temperature protection (OTP) — enabling safe operation under fault conditions. Paralleling capability lets designers aggregate current beyond a single module's 25 A when system demands increase, enabling scalable solutions for higher-power rails.

Evaluation and deployment are straightforward. MPS offers the EVM3695-20 evaluation board to quickly validate performance, and the module's selectable f_{SW} and telemetry options make it suitable for low-noise and high-efficiency designs. Efficiency, compactness, and configurability make the MPM3695-20 well-suited for AI, datacom line cards, accelerator cards, optical modules, edge servers, and other applications where tight space, high current, and reliable regulation matter.

The MPM3695-20 condenses a high-current power stage, precise regulation, and digital configurability into a tiny production-ready package. It reduces design time and overall BOM count while offering system-level telemetry and protection.

www.monolithicpower.com

Are wide-bandgap switches still *too fast* for your HIL simulator?



**Have no fear, the
RT Box is up to the task.**



High fidelity controller HIL testing,
even when switching at 1 MHz.

www.plexim.com/nanostep



plexim
electrical engineering software

Optically Isolated Probing Solution for Analyzing Fastest Switching Operations



Faster switching times, higher voltages, and increasingly systems: GaN and SiC devices are pushing power electronics to new limits. Applications such as EV inverters, motor drives, and high-efficiency converters demand reliable high-voltage measurements at unprecedented switching speeds with small, hard-to-reach test points. PMK's galvanically and optically isolated FireFly® probe is designed precisely for these challenges. FireFly delivers accurate, high-bandwidth measurements without loading or influencing the device under test. Its optical isolation ensures safe and precise signal acquisition, even in the most demanding wide-bandgap applications.

To achieve increases in efficiency, MOSFETs are switched faster, with steeper switching edges and reduced dead times. If the signal is not correctly characterized, the reduced safety margins in the switching times between the high and low sides of a half-bridge, can lead to safety issues, such as inadvertent "shoot-through" conduction. The high switching speeds also introduce voltage overshoots within the circuit that must be accurately monitored to avoid false turn-on and/or breakdown. The FireFly series from PMK offers features with over 1.5 GHz bandwidth and more than 180 dB common-mode rejection ratio (CMRR), allowing for the precise characterization of switching processes. FireFly, and its dedicated connectivity accessories, enable reliable and repeatable measurements of high-speed power devices with the highest signal quality.

Measuring the gate and drain-source voltages is only part of the process. Complete characterization of the power semiconductor also requires the measurement of currents. For example, the current flowing into the gate or through the source terminal. Often, these currents are in the triple-digit ampere range and exceed the bandwidths of Rogowski coils. Due to inductance, traditional shunts often load the circuit, altering its behavior.

Often, they do not accurately represent the true current waveform. Measuring both in-circuit current and voltage accurately was not possible until now. However, through the combination of the FireFly together with the new Ultra-Fast Current Shunts UFCS, also from PMK, unprecedented $>2000 A_{PEAK}$ current measurements with lowest inductive loading of $< 200 p\Omega$ and $>1 GHz$ bandwidth is now possible. Various UFCS models between 1 m Ω and 52 m Ω are available for different use cases.

High flexibility, exceptional temperature stability

The FireFly series offers high flexibility. A wide range of connection adapters allow for signal acquisition under even the most challenging conditions. With a universal BNC connector, the probe can be used with any oscilloscope, ensuring future-proof and flexible operation. The FireFly, with its patented DC drift stability scheme, is also extremely stable over temperature. It has a best-in-class $<0.05 \%/^{\circ}C$ temperature drift. Together with the Power-over-Fiber option, the system excels in long-term 24/7 operation and measurements.

Banner Specifications:

- Bandwidth: $>1.5 GHz$ (-3 dB)
- Rise Time: $<250 ps$
- Input Voltages: $\pm 1V$ to $\pm 2500 V$
- Common Mode Voltage: $\pm 60 kV$ (DC + Peak AC)
- Input Current: $>2000 A_{PEAK}$ (with UFCS-Shunt)
- Insertion Inductance (UFCS): $< 200 p\Omega$
- CMRR: $>180 dB$ @ DC, $118 dB$ @ 1 GHz
- Temperature Drift: $<0.05 \%/^{\circ}C$
- Output Connector: Universal BNC for use with any oscilloscope

It's Your Choice

Innovative packages
that push the limits of SiC



Semikron Danfoss introduces a range of power modules and IPMs, equipped with the latest 2kV SiC technology. The SEMITOP E2, SEMITRANS 3, and SEMITRANS 20 enable flexible converter development. The SKiIP 4 SiC integrates power modules, driver, current sensors and heatsink in a single, high-power unit. **Whether you prefer a standard package or a ready-to-use IPM solution, it's your choice.**

**Exceeding the Standard
for Superior Performance**

SEMITOP® E2
with 2kV SiC
100kW up to 215kW



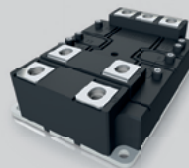
**Latest Technology in
a Proven Package**

SEMITRANS® 3
with 2kV SiC
200kW up to 400kW



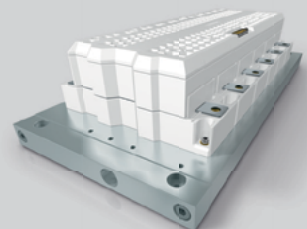
**Industry Standard Power Module
for Extreme Power Density**

SEMITRANS® 20
with 2kV SiC
from 500kW



**Intelligent Power Module
for Reducing Time-to-Profit**

SKiIP® 4 SiC
with 2kV SiC
500kW up to 2MW



AC | DC

Pulsed Inductance Measurement Replaces Reactance Measurement in the Production of Large Power Chokes

Application of the Power Choke Tester DPG10 Series up to the MVA Range

The pulse measurement method of the Power Choke Tester DPG10 series has decisive advantages over conventional reactance measurement for determining inductance and can be used for all types of power chokes, from small, PCB-mounted chokes to chokes weighing several tons in the MVA range. Hans von Mangoldt GmbH has, therefore, switched its inductance measurement in production to pulse measurement with the Power Choke Tester DPG10 series.

*By Hubert Kreis, Chief Executive Officer, ed-k
and Robert Rohn, Development, Hans von Mangoldt GmbH*

Introduction

For historical reasons, the inductance of chokes with sheet metal cores is still often determined by measuring their reactance during production. In this method, the choke is subjected to line current and line voltage, and the reactance is calculated based on the RMS values of current and voltage. From this, the inductance is derived. However, this approach has several significant disadvantages compared to the pulse measurement method. Therefore, Hans von Mangoldt GmbH is in the process of switching its inductance measurement in production to pulse measurement using the Power Choke Tester DPG10 series.

This article outlines both the pulse measurement principle and the conventional reactance-based method, highlighting the advantages of pulse measurement.

In addition, the practical application of the Power Choke Tester DPG10 series at Hans von Mangoldt GmbH in the series production of wound products with sheet metal cores, covering a power range from 1 kVA to over 1 MVA, is presented.

Finally, it will be shown how the Power Choke Tester DPG10 series can be integrated into fully automated production lines for mass-produced winding goods using the new InterfaceBox INT1, without having to write own software.

Pulse Measuring Principle of the Power Choke Tester DPG10 Series

With this measuring principle, a square-wave voltage pulse is applied to the test specimen, as in most real power electronics applications. This results in a ramp-shaped current increase in the test object (Figure 1), whose slew rate di/dt is dependent on the current-dependent inductance $L(i)$. The measuring pulse is cut off again when a preset maximum current or a preset pulse duration is reached.

From the curves of the current $i(t)$ and the voltage $v(t)$ on the test specimen, the following variables can be calculated with a single pulse:

- Differential inductance $L_{diff}(i)$ (Figure 2) and $L_{diff}(JUdt)$
- Amplitude inductance $L_{amp}(i)$ and $L_{amp}(JUdt)$ (also called secant inductance)
- Flux linkage $\psi(i)$
- Magnetic co-energy $W_{co}(i)$
- Flux density $B(i)$, if the core cross-section and number of turns are specified

The DC resistance is measured separately. The Power Choke Tester DPG10 Series is also suitable for 3-phase chokes with the optional 3-Phase Extension Unit.

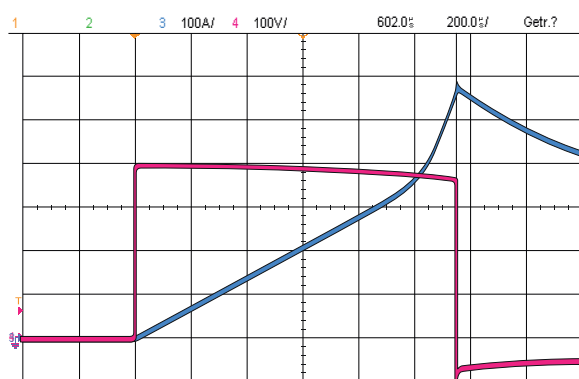


Figure 1: Current and voltage curve of the measuring pulse
CH1: Current 100A/div
CH2: Voltage 100V/div

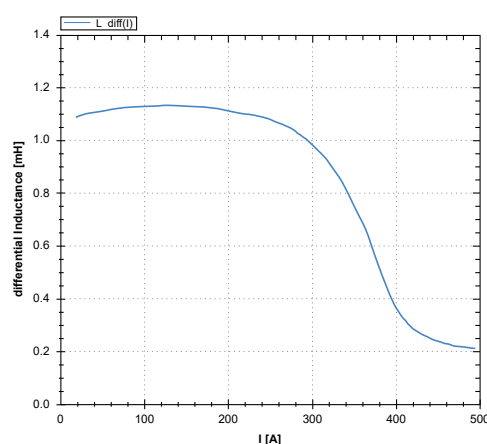


Figure 2: Diagram of the differential inductance $L_{diff}(i)$ of a filter reactor

„THE MOST EFFICIENT LINK BETWEEN YOUR NEEDS AND THE MARKET: GVA”

gva-power.de



ELECTRONICON
always in charge



Fuji Electric

HITACHI



NEOGRAF
SOLUTIONS

özdisan
heatsink



SENSORS
PETERCEM

POSEICO
POWER ELECTRONICS

power
integrations™

Zait Akcam, GVA expert in components

What makes component procurement efficient for you? If it's the perfect mix of personal consulting, systemic expertise, delivery reliability and an optimal price-performance ratio, you should get in touch with us. We look forward to hearing from you!



Your GVA expert:
Zait Akcam
+49 (0)621 / 78992-24
z.akcam@gva-power.de



YouTube

GVA

POWER ELECTRONICS EXPERTS

Advantages of the Power Choke Tester DPG10 Series at a Glance

- Extremely wide range of applications that cannot be achieved with any other commercially available inductance meter; suitable for almost all types of inductive power components from small SMD chokes to power chokes in the MVA range weighing several tonnes.
- Very wide current range, currently available from < 0.1 A to 10000 A
- Suitable for all core materials from < 5 Hz to many hundreds of kHz
- Very simple operation, test results within seconds
- Small and lightweight, even the 10 kA model can be used mobile on a trolley
- Affordable price point despite the very high measurement currents
- Pulse energy currently available up to 15 kJ
- No thermal influence on the DUT
- Also suitable for 3-phase chokes by means of the 3-Phase Extension Unit

Conventional Measurement of Reactance with Mains Voltage and Mains Current

When measuring the reactance, the rated current and rated voltage (50 Hz or 60 Hz) are usually applied to the test specimen. Electromechanical variable transformers or regulated inverters with sine filters are used for this purpose. The RMS values of the current and voltage are measured. According to general AC theory and neglecting the ohmic resistance, the inductance is then calculated as

$$L = \frac{V_{rms}}{2\pi f * I_{rms}} \quad (1)$$

Taking the ohmic resistance into account the equation results in

$$L = \frac{\left(\sqrt{\left(\frac{V_{rms}}{I_{rms}}\right)^2 - R^2}\right)}{2\pi f} \quad (2)$$

The fundamental problem with this is that no sinusoidal voltages and currents are present due to the extremely non-linear behaviour of the core material. This applies especially to iron core materials, which usually have a very much lower permeability at the origin of the B-H curve than in the normal operating range, which then decreases again as the saturation increases.

When a sinusoidal current is applied to the test specimen, the resulting voltage deviates from a pure sinusoidal waveform. Conversely, applying a sinusoidal voltage leads to a current response that is non-sinusoidal.

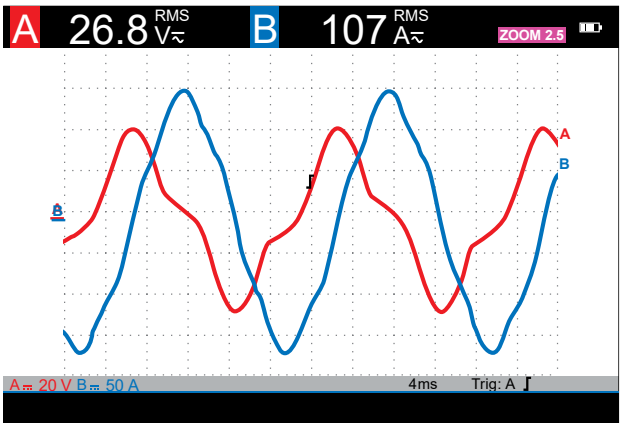


Figure 3: Current and voltage shape for a measurement with 50Hz mains voltage
CH1: Voltage 20V/div
CH3: Current 5A/div

In practice, neither sinusoidal currents nor sinusoidal voltages are typically observed with this measurement method unless the supply is provided by an electronically controlled inverter. The measured signals exhibit significant harmonic distortion. The typically smooth crests of the sinusoidal current become pointed, and in extreme cases even needle shaped (Figure 3).

With such distorted curves, a RMS value measurement of voltage and current and the subsequent calculation of the inductance according to equation (1) or (2) are incorrect for two reasons:

- The equations are derived from the general AC theory. However, this is only valid for sinusoidal variables and linear relationships.
- For the RMS value measurement, the measured variable is by definition quadratically evaluated and integrated over one period. This is based on the heating effect of alternating current in a resistive load. The RMS value of an alternating current is equivalent to the heating effect of a corresponding direct current. This has nothing to do with magnetism! Due to the high crest factor, this method systematically yields values for current and voltage that are significantly higher than those of the fundamental waveform.

In principle, therefore, this measurement method is of little use in the non-linear range. Due to a lack of better alternatives, this measurement method was justified in the past, at least up to the saturation limit of the core material. With the advent of the pulse measurement method, however, a measurement method is now available that is more precise, faster, simpler and, starting from certain power ratings, also more cost-effective.

When comparing the measurement results, the conventional reactance measurement most closely corresponds to the amplitude inductance $L_{amp(i)}$ determined with the pulse measurement method (up to the saturation limit). However, the additionally available curve of the differential inductance $L_{diff(i)}$ can provide valuable insights into the characteristics of the components and the magnetic circuit.

Comparison Power Choke Tester DPG10 Measurement ↔ Conventional Reactance Measurement at a Glance

	DPG10 Series Pulse Measurement	Reactance Measurement
Applicability	Delivers correct results even in the non-linear range.	Only allowed in the linear range, incorrect measurement results in the non-linear, saturated range.
Duration of a Measurement	A complete measurement curve takes only a few seconds, since only a single measuring pulse is necessary for a single-phase measurement.	Creating a complete measurement curve takes a long time because many measurement points have to be measured individually.
Mobility	Even the largest models of the DPG10/20 series are mobile, so that the measuring station can be easily brought to the test object.	For larger currents and power levels, a large, heavy, stationary power supply via a variable transformer or a converter with a sine-wave filter is required. Therefore, the test object must be brought to the stationary test station, even if it is very large.

Revolutionize solar power with TI GaN

Power a more sustainable future with TI GaN technology.
Minimize losses, increase efficiency and reduce the
overall system costs of your next solar design.

▶ Discover more at [TI.com/solar](https://www.ti.com/solar)

Practical use of the Power Choke Tester DPG10 series at Hans von Mangoldt GmbH

Founded in 1941, Hans von Mangoldt GmbH has consistently stood for excellence in quality and innovation in the manufacturing of inductive components. With more than eight decades of experience, it remains a reliable partner, especially where customized solutions are required.

The product portfolio encompasses a broad range of inductive components used in various applications: from industrial power supplies and grid systems to power electronics, as well as demanding environments such as maritime and desert conditions. The challenge lies not only in manufacturing, but especially in the individual design of the components - always tailored to the specific requirements of each customer. Just as important as the technical expertise is the reliability of the products. Customers depend on on-time delivery and consistently high quality.

To ensure consistent quality, Hans von Mangoldt GmbH relies on the Power Choke Tester DPG10 from ed-k and is currently in the final stages to replace the old testing transformers and power meters, which were not only complex to use, but also not mobile and required high maintenance effort due to their moving components. With the DPG10, this is no longer relevant. The compact design allows flexible use in the production line - without elaborate modifications or long set-up times.

Figure 4 showcases the comparison between the old transformer-based test bench and the new DPG10-4000B/F with an optional 3-Phase Extension Unit. The conventional test system consists of a variable transformer with 100 A and another fixed ratio transformer to increase testing capabilities up to 500 ARMS.



Figure 4: Conventional testing system up to 500A with variable transformer, top right the Power Choke Tester DPG10-4000B/F with 3-Phase Extension Unit in comparison

Figure 5, furthermore, shows the old direct current linearity test bench developed in the early 1990s by Hans von Mangoldt GmbH. It is a thyristor-based system housed in four cabinets and capable of 5000 A. In comparison, the Power Choke Tester DPG10-4000B/F with the 3-phase extension unit EXT2, which replaces this system, can be seen in the foreground on the lower floor of the cart. The size comparison is remarkable and demonstrates the advantage of the DPG10, which can be used for mobile applications at any time. The DPG10 can replace both systems, contributing to the standardization of equipment and streamlining operations.



Figure 5: Control cabinets of the DC linearity test bench in the background, in front trolley with DPG10-4000B/F and PC

The versatility of the Power Choke Tester DPG10 is particularly noteworthy. It is suitable for inductance measurements across a wide power range and can reliably test a wide variety of product groups. The DPG10 delivers precise and reproducible measurement results whether small sine filter chokes with inductances of a few microhenries or smoothing reactors weighing several tonnes with several hundreds of millihenries are being tested. This range is of central importance to Hans von Mangoldt GmbH, as company's product diversity continues to grow and the demands on measurement technology increase accordingly.



Figure 6: Mobile usage in production

Another advantage of the Power Choke Tester DPG10 is its mobility. Thanks to its compact dimensions and low weight, the device can be easily used at different production stations. This enables immediate quality control in the production process, saving valuable time. At the same time, the effort of training employees is reduced, as the operation is intuitive and user-friendly.

A locking contact enables door switches to be monitored, allowing testing to be performed by electrically unqualified personnel within a test cabin. This eliminates the need to transport the product to a separate test facility, as was previously required, and paves the way for final testing at the end of the assembly line.

A software API enables the DPG10 to be controlled from a custom software environment, allowing seamless integration into tailored process chains. This was also a key criterion for Hans von Mangoldt GmbH, as numerous product characteristics, beyond inductance, are recorded during the final inspection and documented using an in-house developed software system. This ensures that every product is tested in accordance with the customer-specific requirements. The software guides the operator through every step of the testing process, ensuring that no measurement is overlooked.

Fully automated testing of mass-produced wound components using the new InterfaceBox INT1

PCB-mounted wound components or wound components for the automotive industry are manufactured in extremely large quantities. These cost-sensitive products are, therefore, often manufactured on fully automated production lines.

With the new InterfaceBox INT1, inductance measurement can now be performed on a fully automated production line without the need to develop custom software to control the Power Choke Tester DPG10.

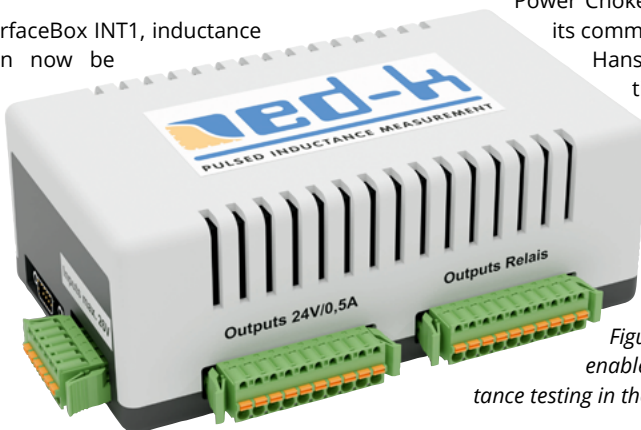


Figure 7: InterfaceBox INT1 to enable fully automated inductance testing in the production line

The InterfaceBox INT1 provides the interface between the Power Choke Tester PC software and a fully automated production line. Three universal inputs and five universal outputs enable the interaction with the production line's PLC. For example, the PLC can signal the DPG10 software that:

- a new test item has been contacted or a new measurement can be started
- the production line has been stopped

Furthermore, the DPG10 software can signal the production line PLC via five universally configurable outputs that:

- a measurement is in progress
- the limit curve test has failed (FAIL, part is rejected)
- the DPG10 system is ready for a new measurement
- the measurement is completed, and the test item can then be ejected from the test line

Warning lights, horns, or foot switches can also be connected. The active 24 VDC outputs deliver up to 12 W per output. Relay outputs (250VAC/8A or 30VDC/5A) are also available.

All inputs and outputs are individually configurable via the software, meaning each output can be assigned a separate activation delay and activation time. The existing functions can be assigned to any output.

Summary

In a market defined by rapid change and rising expectations, Hans von Mangoldt GmbH has made a strategic decision to adopt the Power Choke Tester DPG10 from ed-k. A move that underscores its commitment to innovation and quality. The collaboration of Hans von Mangoldt GmbH with ed-k has proven to be particularly effective, driven by a shared vision: to develop cutting-edge solutions that streamline manufacturing processes while upholding the highest quality standards of precision and reliability. This technology choice positions Hans von Mangoldt GmbH to meet future challenges with confidence and agility and underscores ed-k's market leadership in the field of pulsed inductance measurement.

www.ed-k.de
www.mangoldt.com

OUR MAIN COMPONENT IS **TRUST**

ITG delivers common mode choke solutions for every application.

You'll get quick turnarounds, custom solutions, and one-on-one support from the industry's top, high-volume magnetics manufacturer. Our design engineers offer a full-range of solutions for a wide variety of industries and applications.

- | | | |
|------------------------|-----------------------|---------------------|
| • Appliances | • DC-to-DC Converters | • Power Supplies |
| • Automotive | • LED Lighting | • Renewable Energy |
| • Cloud Computing | • Medical | • Storage Devices |
| • Consumer Electronics | • Military | • Telecommunication |



Trusted Innovation

Magnetics & EMI Filters

www.ITG-Electronics.com

Engineering Electronics Partnership since 1963

Three-Phase Module Based on Monolithic GaN Half-Bridge ICs

EPC33110 is a three-phase module that utilizes gallium nitride (GaN) monolithic integrated circuits, enabling the development of smaller, lighter motor drive inverters. Its compact design is ideal for drone and humanoid robot applications, supporting higher switching frequencies with respect to traditional silicon-based inverters, ultimately improving system size, weight, and performance.

*By Federico Unnia, Manager of Applications Engineering,
and Marco Palma, Director of Applications Engineering, Efficient Power Conversion*

The EPC33110 is a cutting-edge three-phase module leveraging gallium nitride (GaN) technology, representing an innovative solution in power electronics for motor drive applications. GaN devices, known for their superior electrical properties compared to traditional silicon-based components, enable the EPC33110 to deliver exceptional performance in a compact form factor.

GaN technology enables the integration of the logic functions and gate driver on the same substrate as the power FETs, thanks to the lateral conduction of the power devices, allowing the realization of monolithic power half-bridge chips. The EPC33110 implements the co-packaging of three half-bridges, keeping the excellent electrical and thermal performance of GaN devices, while optimizing the overall size of the inverter.

This module is specifically designed to meet the stringent requirements of applications such as drones and humanoid robots, where size, weight, efficiency, and thermal management are critical constraints. Its compact form and ease of use simplify the designer's approach to miniature motor drive inverters in complex structures, such as multi-axis motor drives in humanoid arms.

EPC33110 description

The EPC33110 is a three-phase co-packaged module that integrates three monolithic gallium nitride (GaN) half-bridges, each featuring integrated gate drivers, bootstrap circuits, and level shifters. This integration results in a compact, high-power-density solution optimized for motor control applications. The module operates with a maximum recommended input voltage of 80 V and exhibits a typical on-resistance of 8.7 mΩ at room temperature per each power GaN FET.

Designed to support logic-level inputs at 3.3 V or 5 V, the EPC33110 simplifies system design by eliminating the need for discrete gate driver components. By embedding the gate driver within the module, it enables a logic-input-to-power-output configuration, which reduces the component count and overall system complexity. This design approach requires only a minimal set of external components: small bypass capacitors to stabilize the power supply of the three legs, a single decoupling capacitor for the low-side power FETs driving stage, and three bootstrap capacitors to drive the high-side FETs. Co-packaging three integrated half-bridges ICs enhances power density and exhibits a good thermal performance thanks to the excellent top-side cooling obtained by the exposed dies.

The EPC33110 is housed in a 6x6.5 mm QFN package featuring 21 pads, which include 7 signal pins, 7 supply pins, 7 power pads and is represented in Figure 1. It supports six complementary PWM signals and includes a fast, active-low shutdown pin to disable the module during fault conditions.

The whole module is supplied at 5 V by a single pin V_{DRV} , which powers internally the three supplies of the logic circuits V_{DD} , that must be locally decoupled by small capacitors. The V_{DRV} also charges the bootstrap capacitors through a synchronous boot FET; the bootstrap pins are conveniently positioned close to their respective switching node pads. Additionally, the device has three switching node power pads, two power pads for ground (GND), and two power pads for V_{IN} . The complementary input PWM signals are designed to optimize dead time based on the application. Meanwhile, the large V_{IN} , power GND, and switching node pads reduce PCB trace resistance and inductance, thereby enhancing thermal dissipation through the PCB.

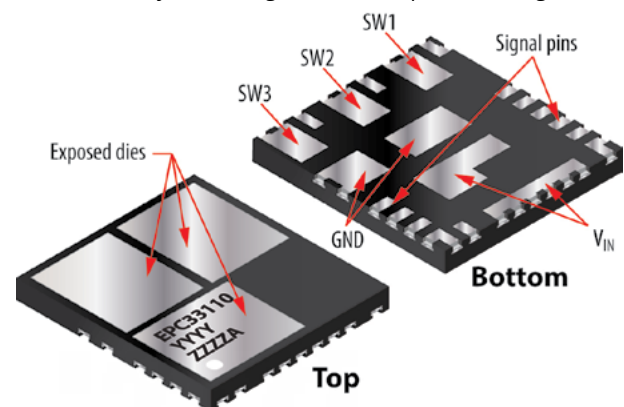


Figure 1: Overview of the top side (left) and bottom side (right) of the EPC33110 module.

Motor drive application

The EPC33110 is specifically designed for driving three-phase permanent magnet motors, which are widely used in applications such as drones and humanoid robots due to their efficiency, compact size, and precise control capabilities.

Complementing the EPC33110 module, the EPC91122 reference design board serves as a practical implementation platform tailored for humanoid robot joints and small drone applications, as shown in Figure 2. This board is engineered to operate with a wide input DC battery voltage range from 15 V to 55 V, accommodating various power sources typical in portable and mobile robotics. EPC91122 is equipped with all the features and functions of a complete motor drive inverter, including regulated off-line power supplies, DC voltage sensing, on-board magnetic encoder for rotor shaft position and speed control, and current sensor ICs with embedded overcurrent fault signal triggered at 30 A. The inverter is controlled by an on-board microcontroller, which can be programmed and operated in real-time through a JTAG connector or through an RS-485 port.



CLEAN CHIMNEYS FOR SANTA CLAUS!

POWER SEMICONDUCTORS
FOR CLEAN TECHNOLOGIES
IN HOME APPLIANCES



Get all information about
the DIIPM™ family

The extended SLIMDIP™ family line-up for compact 3-Phase DC/AC inverter stage

- // SLIMDIP™ (5A to 30 A/600 V) with RC-IGBT
- // Hybrid SiC SLIMDIP™ (15 A/600 V) with RC-IGBT and SiC MOSFET for high efficiency at partial load
- // Full SiC SLIMDIP™ (15 A/600 V) with SiC MOSFET for highest efficiency at partial and full load
- // Optimized terminal layout for compact PCB design
- // Integrated driver ICs (HVIC and LVIC)
- // Unipolar 15 V driving voltage for both RC-IGBT and SiC MOSFET
- // Integrated bootstrap diodes and current-limiting-resistors
- // Short circuit protection through external shunt resistor
- // Power supply under-voltage protection
- // Over temperature protection
- // Temperature output function as analog voltage signal
- // Low electromagnetic emissions

More Information:

semis.info@meg.mee.com / www.meu-semiconductor.eu

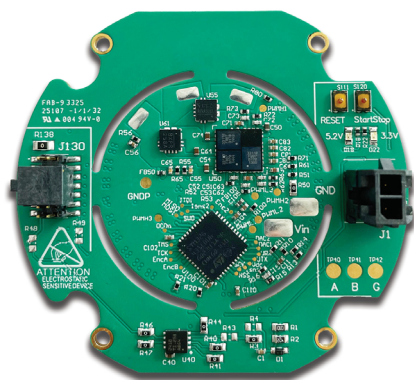


Figure 2: Overview of EPC91122 board – three-phase inverter for drones and humanoid motor joints.

In addition to the existing single-motor reference design board EPC91122, the compact size of the EPC33110 module indeed facilitates the design of multi-axis drivers by enabling dense integration on a small PCB footprint. For instance, four of these modules would compose a quadcopter drone electronic speed controller capable of carrying a payload of a few kilograms on each axis. The layout depicted in Figure 3 illustrates a practical example of a 4-axis driver on a 30 mm x 30 mm PCB. Placing a microcontroller centrally allows for efficient routing and control of the four three-phase inverters, while the EPC33110 modules and relative current sensors are placed symmetrically at the four corners of the PCB.

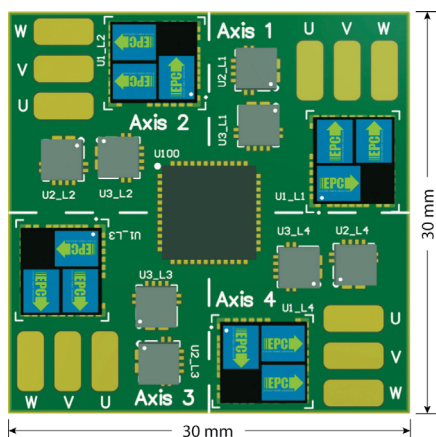


Figure 3: Layout example of a rectangular 30x30 mm multi-axis motor drive, including power stage, current sensors, and microcontroller.

EPC33110 performance

EPC33110 performance was tested in a humanoid joint motor application with load conditions up to 300 W (20 Nm load torque and 135 rpm motor speed) on a dynamometric bench. Operated at 100 kHz PWM and 25 ns deadtime, the board was able to deliver a repetitive 2-seconds pulsed phase current of 20 A_{RMS}.

In the case of the motor used in the tests, which had a torque per ampere constant of 1 Nm/A_{RMS}, the 20 Nm maximum load resulted in 20 A_{RMS}, 28 A_{PK} current in each leg of the inverter, as shown in Figure 4, at the motor's maximum speed.

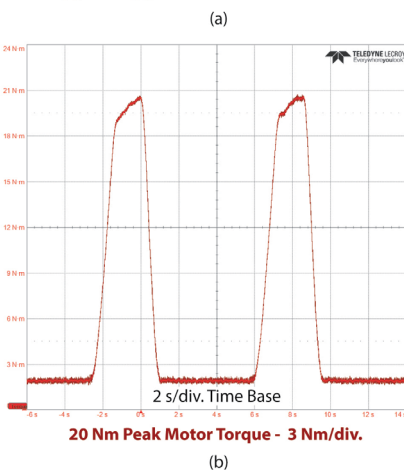
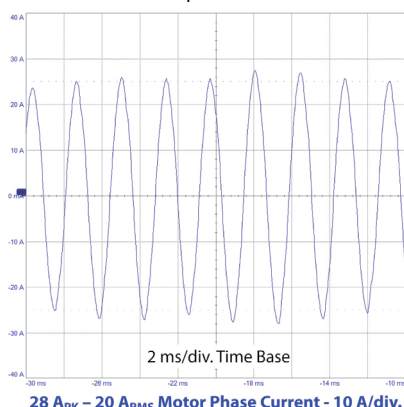


Figure 4: Output current capabilities of EPC33110 operated at 100 kHz PWM in a humanoid robot joint:

(a) detail of the motor phase current reaching 20 A_{RMS}

(b) overview of the load torque 2 second pulses at 20 Nm peak

In addition to the dynamometric bench measurements, steady-state measurements on a passive load were performed to identify the maximum current that can be delivered continuously at the thermal regime. The board was tested at 100 kHz with a 25 ns deadtime and a passive heatsink under natural convection cooling.

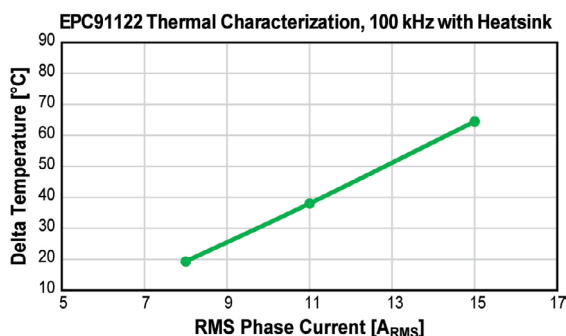


Figure 5: Steady state thermal performance of EPC33110 operated at 100 kHz PWM under natural convection cooling.

The graph represented in Figure 5 reports the results showing that the EPC33110 module reached a temperature increase of 50 °C from ambient temperature while delivering 13 A_{RMS} to each phase of the motor.

While in the case of humanoid robot joints natural convection cooling is the only choice, drone applications the propellers generate a strong airflow yielding thrust and an effective cooling to the whole system, that increases the inverter current capabilities.

Conclusions

The EPC33110 is a compact three-phase module integrating three GaN half-bridges with built-in gate drivers, bootstrap circuits, and level shifters, optimized for motor control. A single 5 V power supply can power the module to operate up to 80 V with a typical on-resistance of 8.7 mΩ, supporting 3.3 V or 5 V logic inputs. This simplifies system design by reducing the need for external components. Housed in a 6 x 6.5 mm QFN package with 21 pads, it features complementary PWM inputs, a fast shutdown pin, and power supply pins arranged to minimize PCB resistance and inductance, and enhance thermal dissipation.

The EPC33110 is designed for driving three-phase permanent magnet motors commonly used in drones and humanoid robots. The EPC91122 reference board supports these applications with a wide 15–65 V input range and includes complete motor drive features such as regulated power supplies, DC voltage sensing, magnetic encoder, and current sensors. The EPC33110, thanks to its compact size and easy layout, also enables multi-axis driver designs which are particularly effective in small drones such as quadcopters with a few kilograms payload or in humanoid robot arms.

Thanks to the top side cooling optimized by the exposed dies, EPC33110 can deliver up to 20 A_{RMS} per phase, as verified in 2-second pulses in a humanoid joint motor. Operated at 100 kHz PWM and 25 ns dead-time under natural convection cooling, the EPC33110 can deliver 13 A_{RMS} continuously while

keeping the temperature increase with respect to ambient temperature below 50 °C and 8 A_{RMS} keeping the temperature increase with respect to ambient temperature below 20 °C; such thermal increase is significantly reduced while operated under forced air cooling conditions, which is typical for aerial drones.



Vincotech

SIMULATE SMARTER, DESIGN FASTER

Accurate data provided by VINcoSIM

Designed for engineers, VINcoSIM is a web-based integrated simulation environment that delivers rapid, data-driven insights into module performance under real-world operating conditions.

Starting from simple configuration of key parameters such as voltages, currents, and switching frequencies, the software gives a proper estimation for junction temperature and loss calculations. The results are based on real measurements taken from each module, enabling faster and more reliable design validation.

Main benefits

- / Measurement-based accuracy
- / Multi-topology evaluation [e.g., inverter, PFC, buck/boost]
- / Comprehensive thermal modeling



www.vincotech.com/VINcoSIM

EMPOWERING YOUR IDEAS

The Next Leap in EV Powertrain Efficiency: The Rise of 3-Level Inverters

Battery-electric vehicles are evolving rapidly and nowhere is that progress more visible than in the powertrain. Over just a few years, the industry has moved from early silicon (Si) IGBT traction inverters to silicon-carbide (SiC) MOSFET-based systems that deliver higher efficiency, better thermal performance, and greater power density.

By Antonio Poveda Serrano, Automotive Application Engineer, and Sebastian Pawusch, Field Application Engineer Automotive Semiconductors, Fuji Electric

This shift has already redefined what electric vehicles can achieve, shrinking components while unlocking new levels of performance and driving range. Yet, as electric mobility continues to mature, engineers are looking beyond semiconductor improvements to the very topology of the inverter itself, the next leap in powertrain efficiency is now emerging through the adoption of 3-level inverter architectures.

Today, the vast majority of battery-electric vehicles rely on a 2-level voltage-source inverter (VSI) to control their traction motors. In this familiar configuration, each inverter leg alternates the DC-link voltage directly between the positive and negative rails, producing a pulse width modulated (PWM) waveform that regulates motor torque and speed. The introduction of SiC MOSFETs has already delivered major benefits compared to traditional Si IGBTs, reducing switching and conduction losses, increasing switching frequencies, and improving thermal behavior. Despite these gains, there are still meaningful opportunities to improve efficiency, particularly in reducing parasitic losses, mitigating electromagnetic interference (EMI), and lessening the electrical stress experienced by both the inverter and motor.

These challenges become more critical as EV platforms move toward higher battery voltages, often 800 V or more in the latest and upcoming generations of vehicles.

In a 2-level inverter, the PWM voltage waveform inherently contains high harmonic content. These harmonics contribute to unwanted copper, iron, and stray losses within the electric machine, converting useful energy into heat. That heat not only reduces efficiency but also limits the duration for which the motor can deliver peak power. Moreover, when high DC-bus voltages combine with the ultrafast switching transitions typical of modern SiC devices, the result is extreme steep voltage slew rates (dV/dt). These rapid voltage changes can wear away motor insulation over time, create bearing currents, and increase EMI, posing significant challenges to long-term reliability, noise, vibration, and overall electromagnetic compatibility.

To overcome these issues, engineers are turning to multi-level inverter architectures, and particularly the 3-level T-type inverter. This topology introduces a neutral connection and adds two semiconductor devices per phase, effectively splitting the DC-link voltage into two equal halves. The result is that each switching event changes the output voltage by only half the step of a conventional 2-level design. While this adjustment might seem simple, the performance implications are profound. The halved voltage step produces an output waveform that much more closely resembles a pure sine wave, dramatically reducing harmonic distortion and current ripples at the motor terminals.

The effects of this cleaner waveform cascade through the entire system. Lower harmonic content means reduced copper and core losses, as well as diminished eddy-current and hysteresis effects in the motor's magnetic materials. The machine runs cooler, more efficiently, and more quietly. Torque ripple is reduced, which improves driving smoothness and minimizes acoustic noise, a benefit felt directly by the driver. Meanwhile, the smaller voltage transitions reduce common-mode voltage and dV/dt, dropping the electrical stress on motor insulation and bearings while also lowering EMI emissions. In practice, this means improved reliability, longer component life, and potentially smaller and simpler EMI filters.

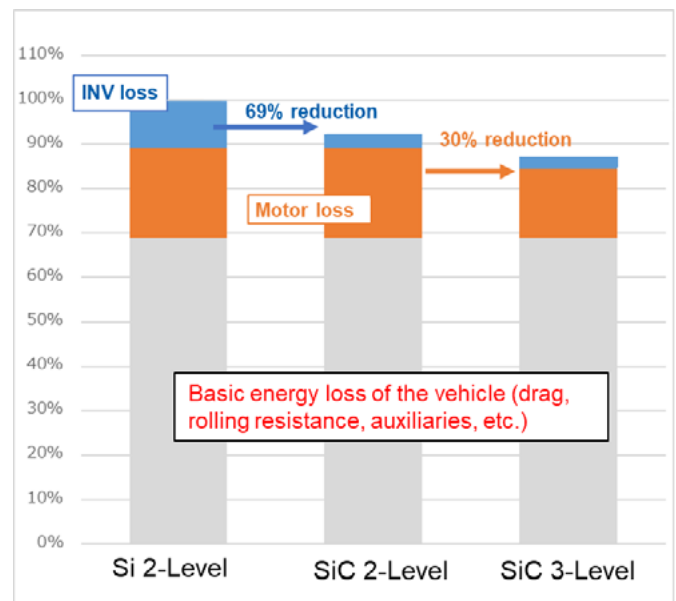
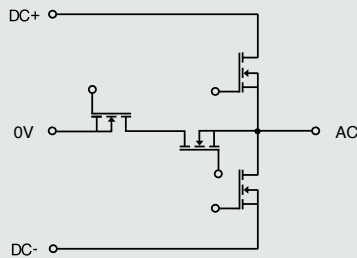
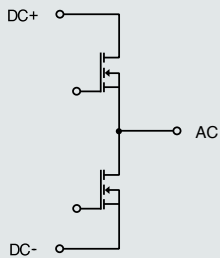
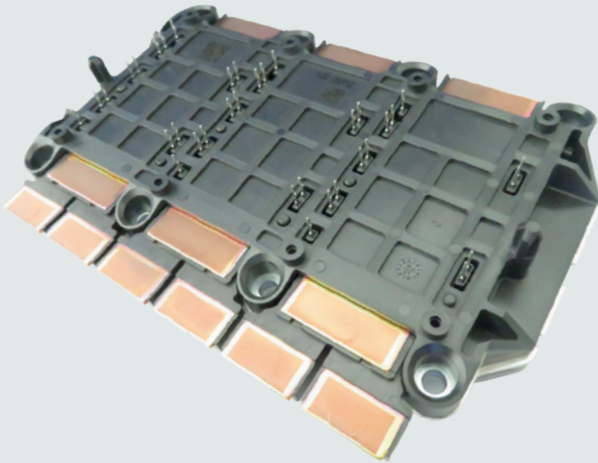


Figure 1: Loss comparison with different inverter topologies and technologies

Experimental data and simulation results strongly support these theoretical advantages. Studies show that upgrading from a SiC-based 2-level inverter to a SiC-based 3-level T-type inverter can reduce motor-related losses by as much as 30 %, depending on the operating conditions and chosen modulation strategy. At the overall vehicle level, efficiency improvements of around 7 % have been observed; similar in magnitude to the gains realized during the industry's transition from Si to SiC technology a few years ago. For automakers, such improvements translate into tangible benefits: extended driving range, smaller and lighter cooling systems, or higher sustained power output without compromising reliability.

Automotive SiC Power Modules

The next level of efficiency,
power density and reliability



MAIN FEATURES

- Fuji Electric 1200 V 3G SiC MOSFET
- Scalable current rating up to 1000 A
- Revolutionary 3D wiring structure
- Very low stray inductance
- High temperature operation up to 200 °C
- AQC 324 qualified
- 2 level and 3 level options
- Flexible half-bridge design
- Universal fit due to adapter frame
- Available with or without cooler
- Cu or Al PinFin or closed water coolers



However, as with any new technology, the 3-level approach comes with its own set of challenges. The added semiconductor devices and gate drivers increase component count and system cost. The control system must also manage voltage balancing across the split DC-link capacitors, which introduces additional sensing and modulation requirements. Advanced pulse-width modulation strategies or redundant switching states are also employed to maintain balance and optimize efficiency. Furthermore, under certain load conditions, the additional devices can introduce slightly higher conduction losses. These design considerations require careful engineering, but ongoing advances in packaging, thermal management, and digital control are steadily reducing their impact.

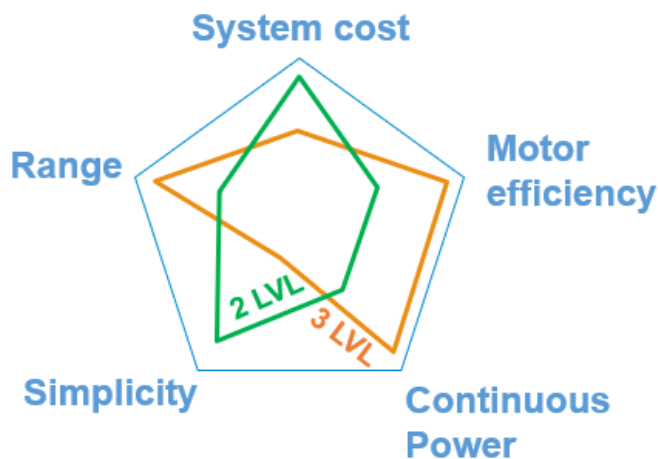


Figure 2: Comparison of key parameters between 2- and 3-Level Inverters

In the broader context, the move toward 3-level inverter technology aligns perfectly with the industry's pursuit of higher efficiency and lower EMI as battery voltages rise. It represents a natural next step in the ongoing evolution of the electric drivetrain. Just as the switch from Si to SiC transformed inverter performance, the transition from 2-level to 3-level topologies promises another significant leap forward in range, power density, and system reliability.

Fuji Electric is among the leaders driving this innovation. The company has developed the M1206, a cutting-edge 3-level T-type SiC module designed for 800 V battery systems. The AQG324-certified module integrates all key components into a compact, low-inductance package capable of delivering up to 300 kW of power. This high level of integration simplifies implementation for OEMs, reducing the complexity typically associated with multi-level systems. By offering a ready-to-use, high-performance building block, Fuji Electric is making the adoption of 3-level inverter technology more practical and accessible for next-generation BEVs. With the module expected to reach the market in 2026, the next major improvement in electric vehicle efficiency, range, and overall driving performance is already on the horizon.

www.fujielectric.com

Messe Frankfurt Group

mesago

pcim

9 – 11.6.2026
NUREMBERG, GERMANY

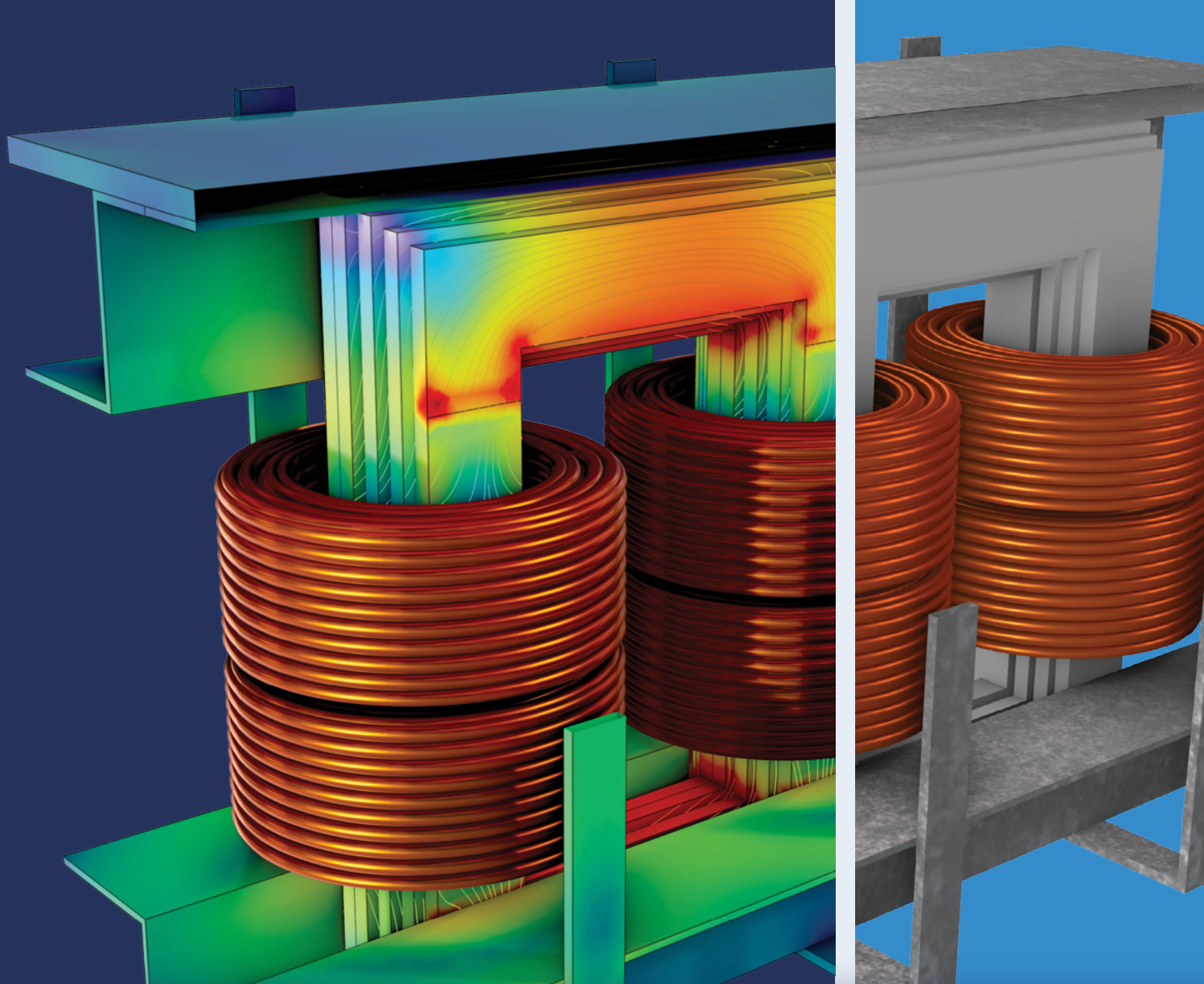
WHAT'S NEXT
IN POWER
ELECTRONICS?
SHOW & TELL!

Become an exhibitor at the
leading exhibition now.

Innovation happens where passion meets expertise and exchange opens up new perspectives. That is exactly what the PCIM Expo brings together in one place, making it the central meeting point for the international power electronics community.

Become an exhibitor now:
pcim.mesago.com/exhibit-now

   #pcim



Power Innovation in Electrical Design

with COMSOL Multiphysics®

Electrification success calls for smart design innovation and fast-paced product development. To achieve this, industry leaders are turning to multiphysics simulation to accurately test, optimize, and predict the performance of high-voltage equipment and power systems.

» comsol.com/feature/electrical-innovation

SiC-MPS Diodes Under Stress: Robust Performance Under Extreme Current and Temperature Conditions

What is the reverse recovery behavior of SiC-MPS diodes in scenarios that challenge their thermal and dynamic robustness? This article provides a closer look.

By Simon Ginzel, Professorship of Power Electronics, Helmut-Schmidt-University, Hamburg/Germany; Zhe Yu, Principal Power Application Engineer, and Bengt Sprätz, Product Application Engineer, both Nexperia, Hamburg/Germany

Power electronic systems, such as on-board chargers (OBCs) and insulated DC/DC converters, impose stringent requirements on component reliability, particularly under thermal and electrical stress. SiC-Merged-PiN-Schottky (MPS) diodes, which combine the characteristics of a Schottky barrier and a P-N junction, offer significant advantages in terms of both switching performance and robustness [1]. This study explores the reverse recovery behavior of various SiC-MPS diodes from Nexperia in scenarios that challenge their thermal and dynamic robustness. The primary objective is to assess their performance limits and evaluate their suitability for demanding industrial applications.

Test Concept & Measurement Conditions

Double-pulse tests were carried out on Nexperia's 650 V SiC-MPS diodes [2] with nominal current ratings (I_N) of 6 A, 10 A, 16 A, and 20 A. The applied stress conditions included forward conducting currents of up to 120 A and case temperatures up to 175 °C, representing a challenging operating regime for the devices under test. The test samples covered a broad range of package types, including wire-bonded TO247, TO220, DPAK and D2PAK (e.g. PSC1065J) as well as innovative clip-bonded variants such as CFP40 and CFP60.

In order to evaluate the impact of switching speed on device robustness, the diode turn-off current slope (di_F/dt) was increased up to approximately 9 A/ns. These test conditions were chosen to emulate realistic worst-case scenarios in power electronic systems, particularly under transient overcurrent and thermal stress, enabling a reliable assessment of the diodes' reverse recovery behavior.

The reverse recovery charge Q_{rr} , used as a key parameter for characterizing reverse behavior, was determined according to equation (1), in which the parameter i_F equals the diode forward current [3].

$$Q_{rr} = \int_{t_0}^{t_1} (-i_F) dt \quad (1)$$

Here, t_0 denotes the time of the first zero-crossing of the forward current i_F , and t_1 is defined as a steady-state point in time after the completion of the switching transition.

Measurement Results & Observations

Figure 1 illustrates the reverse recovery charge Q_{rr} as a function of diode turn-off current for a commutation speed of up to 4 A/ns and a case temperature of 175 °C. The measurements were conducted on D2PAK-packaged SiC-MPS diodes with nominal current ratings of 10 A, 16 A, and 20 A. All devices are based on the same die technology but differ in die size, with the 20A-die featuring the largest active area.

Up to a certain current threshold, Q_{rr} remains nearly constant, even at elevated temperatures of 175 °C, as shown in figure 1. Until this threshold, the reverse recovery appears to be primarily influenced by capacitive effects, where against bipolar carrier injection playing only a minor role.

This corresponds to a nearly idealized unipolar condition, where the reverse recovery charge is dominated by the junction capacitance, which can be approximated by:

$$Q_c = \int C(V) dV + Q_0 \quad (2)$$

Assuming the diode capacitance is unaffected by commutation, temperature, or other dynamic effects, equation (2) describes a charge primarily influenced by the blocking voltage. Here, Q_0 represents an integration constant. Moreover, equation (2) implies that the capacitive charge Q_c and thus Q_{rr} in this operating range, scales with the die area.

A clear influence of die size is also visible in Figure 1. Due to their smaller active area, devices with smaller dies exhibit reduced parasitic capacitances, which leads to lower Q_{rr} values. This effect becomes particularly apparent at a forward current of 10 A ($I_F = 10$ A), where the 10A-die shows the lowest reverse recovery charge.

However, these smaller dies also demonstrate increased sensitivity to temperature. The temperature-induced rise in Q_{rr} begins at significant lower forward current levels compared to devices with larger die areas. For instance, the 10A-die shows a noticeable increase in recovery charge already at $I_F = 25$ A and 175 °C, whereas

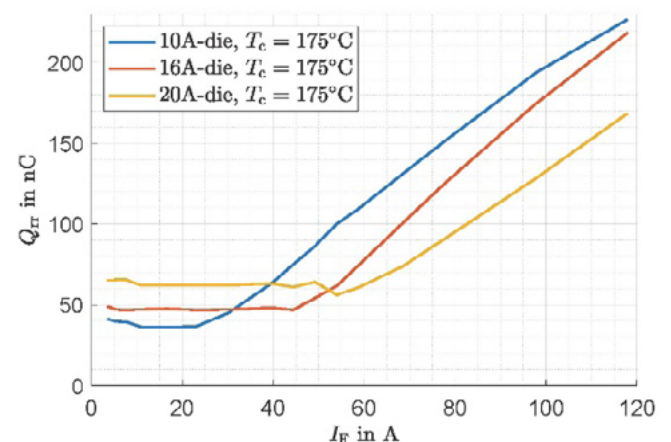


Figure 1: Reverse recovery charge Q_{rr} at $T_c = 175^\circ\text{C}$ for different and die sizes.



Accelerate next-generation solar designs with Infineon's advanced system solutions

Watch our on-demand webinar and discover how you can simplify solar PV development, increase efficiency and reliability, optimize price/performance, and reduce time-to-market.

Key takeaways:

- Silicon MOSFETs in power optimizers and IGBT solutions in hybrid inverters
- GaN-based innovations for compact, efficient power optimizer and microinverter designs
- SiC modular hybrid inverter platform with single-phase HERIC topology plus three-phase NPC2 topology
- Modular design concepts
- Control and connectivity card integration for seamless system implementation

Whether you're working on single-phase, three-phase, or next-generation solar systems, we have the expertise, tools, and reference designs to help you succeed.



Register now



the 20A-die variant maintains stable behavior up to approximately $I_F = 60$ A at the same temperature. This trend can be attributed to the higher current densities in smaller dies, which accelerate the onset of bipolar carrier injection in the drift region. In contrast, larger dies provide greater thermal robustness and delay the activation of such bipolar effects.

Further insight into the reverse recovery behavior is provided in figure 2, which presents the measured current waveforms during diode turn-off. In figure 2a, using $I_F = 10$ A, the reverse recovery current shape remains nearly unchanged across the entire temperature range, confirming the absence of significant bipolar injection below the threshold. In contrast, figure 2b highlights the behavior at 175 °C as the forward current increases. At $I_F = 60$ A, a pronounced increase in reverse recovery charge is observed, consistent with the onset of charge carrier injection beyond the critical threshold. Importantly, even in this regime, the behavior does not indicate thermal runaway. The results underline that bipolar effects remain controlled and only become significant beyond specific operating points, supporting the robustness of the investigated SiC-MPS diodes under extreme conditions.

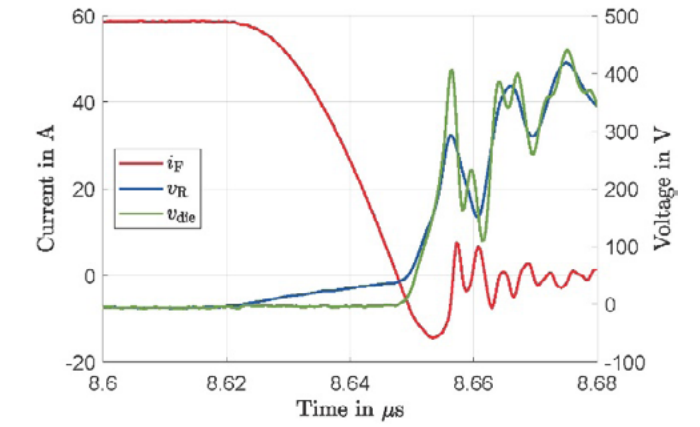
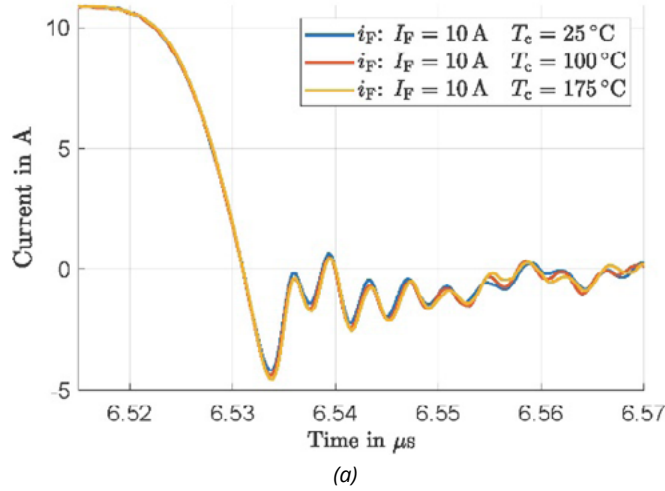


Figure 4: Waveforms of $v_R(t)$, $v_{die}(t)$ and $i_F(t)$ during reverse recovery.

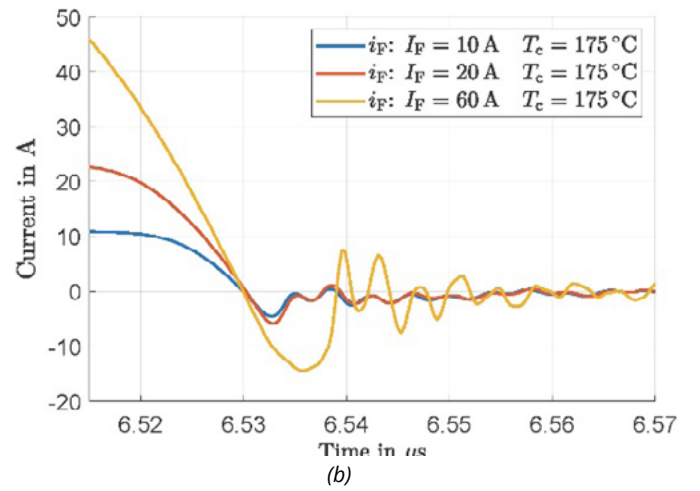


Figure 2: Reverse recovery current waveforms (a) at $I_F = 10$ A for different temperatures (b) at $T_c = 175^\circ\text{C}$ for varying I_F .

The devices were subjected to extreme stress conditions, including reverse currents up to 20 times the nominal rating, case temperatures of 175 °C and current slopes of up to 9 A/ns. Despite these conditions, none of the tested diodes showed any signs of electrical or thermal failure.

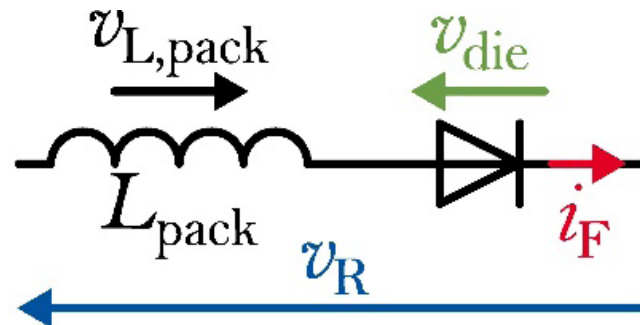


Figure 3: Diode parameter definition.

Using the definitions in figure 3, the internal die voltage $v_{die}(t)$ can be reconstructed over time. This is based on the measured package voltage $v_R(t)$, the known package inductance and the current through the diode, as described in equation (3) [4].

$$v_{die}(t) = v_R(t) + L_{pack} \cdot \frac{di_F(t)}{dt} \quad (3)$$

Figure 4 illustrates the waveforms of the measured voltage $v_R(t)$, the reconstructed die voltage $v_{die}(t)$ and the diode current $i_F(t)$. A significant voltage overshoot at the die level was observed during steep current transitions. This overshoot is influenced not only by the di/dt but also by the corresponding package inductance.

Package inductance parasitics have an impact on the voltage stress at the chip level. Higher inductance causes increased voltage overshoot during commutation events. Transient voltages, derived as described in equation (3), reached up to 900 V on devices rated for 650 V. Nevertheless, no destructive overvoltage conditions were observed.

Discussion: Implications for Application Engineers

The experimental results highlight the robustness of Nexperia's SiC-MPS diodes under demanding electrical and thermal stress. Although the reverse recovery behavior changes beyond certain current and temperature thresholds, it remains nearly constant across a broad operating range. None of the tested devices experienced electrical or thermal failure, even under extreme conditions, underscoring their resilience.

Advert

This suggests that the diodes can tolerate short-term dynamic overloads without functional interruption. Such conditions may arise temporarily, for example during cold-start events or transient overcurrent peaks. While these findings do not replace formal specification limits, they offer valuable insight into safe operating behavior under real-world conditions.

For system design, this reveals potential benefits in pulsed or fault-tolerant applications. The ability to withstand brief overstress events with stable switching behavior may provide additional design margin and support more compact, cost-efficient solutions. However, package parasitics, especially their impact on voltage overshoot, have to be carefully considered. Appropriate gate resistor selection and optimized PCB layout are essential to limit transient voltage spikes and ensure reliable operation.

The observed performance under combined high current and temperature conditions supports the applicability of these diodes in safety-critical systems such as automotive on-board chargers. In operating regimes where bipolar carrier injections occurs, the devices continued to switch reliably. Although changes in reverse recovery characteristics were observed, the bipolar effects themselves appear to contribute to stable thermal behavior under elevated stress.

Ultimately, application-specific validation remains essential. While the results indicate a certain degree of design headroom, system-level testing is necessary to address the dynamic conditions of real-world use. These insights may contribute to a more differentiated approach to derating and component selection, helping to optimize cost, size, and thermal performance in practical designs.

Conclusion

These investigations demonstrate that SiC-MPS diodes from Nexperia exhibit robust switching behavior under demanding electrical and thermal stress. In all tested scenarios, the devices withstood elevated transient conditions, confirming their suitability for use in environments with high reliability demands. These findings may support greater design flexibility, particularly in applications in which short-term current peaks have to be managed safely. The results highlight the diodes' potential for safety-critical systems such as automotive on-board chargers. Further work could address system-level validation and compare measured device behavior with simulation results of corresponding models to support robust design under dynamic stress.

References

- [1] Nexperia, Diode Application Handbook: Fundamentals, Characteristics, Applications. 2022.
- [2] Nexperia, "PSC1065J 650 V, 10 A SiC Schottky Diode in D2PAK R2P: Product Data Sheet," 2024.
- [3] J. Lutz, H. Schlangenotto, U. Scheuermann, and R. W. de Doncker, Semiconductor Power Devices: Physics, Characteristics, Reliability (Electrical Engineering), Second edition. Cham: Springer, 2018.
- [4] S. Ginzl, K. Hoffmann, Z. Yu, S. Fahlbusch and S. Habenicht, "SiC MPS Diodes – Impacts of Package Inductance and Charge Carriers on Dynamic Switching Behavior" in Proceedings of PCIM Europe 2025; International Exhibition and Conference for Power Electronics, Intelligent Motion, Renewable Energy and Energy Management, 2025, pp. 1–7.

www.nexperia.com

POWER SUPPLIES

Heavy-Duty
Industrial
Quality

Cost-effective
solutions to tough
design challenges



ABSOPULSE
ELECTRONICS LTD.

www.absopulse.com
Since 1982

IGCT highest power density for most compact equipment

The IGCT is the semiconductor of choice for demanding high-power applications such as wind power converters, medium-voltage drives, pumped hydro, marine drives, co-generation, interties and FACTS. Hitachi Energy's range of 4500 to 6500 volt asymmetric and reverse conducting IGCTs deliver highest power density and reliability together with low on-state losses.

hitachienergy.com/semiconductors



HITACHI

Power Pulsating Buffer to meet peak power demands in AI server PSUs without disturbing the grid

GPU peak power demand imposes new architectures and concepts to absorb dynamic load reflections caused by AI accelerators, smoothing out power demand from the electricity grid.

By Sam Abdel-Rahman, System Architect Server SMPS, Infineon Technologies

The rise of artificial intelligence (AI) has resulted in a significant increase in power demand in data centers. AI server racks will rise to higher power levels reaching 1 MW. Aside from the significant nominal-power rise of the AI PSU, the GPU also draws a higher peak power and generates high load transients, as shown in Figure 1. This high power and high load transient dictates new architectural changes in AC and DC distribution of data center racks to accommodate the significantly higher currents, while also considering the grid power capabilities. As a part of this new architecture, we introduce concepts of energy buffer (also known as Power Pulsation Buffer or PPB) to support AI peak loads without overloading the grid side. This article will also provide an overview of trends and the evolution of PSUs and rack architecture for AI servers.

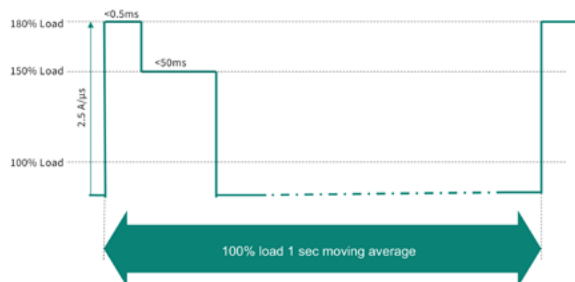


Figure 1: Example peak power profile demanded by AI GPUs

Peak power demand in next generation AI server racks

Figure 2 shows the next generation of server rack architecture in this evolution. As the rack power rises above 300 kW, the power components are separated from the IT components in a power sidecar that contains the power supply units (PSUs), the battery backup units (BBUs), and the capacitor backup units (CBUs).

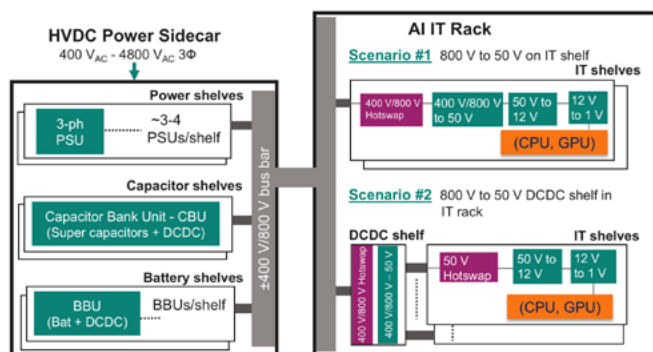


Figure 2: Next generation AI server rack architecture

With PSU power reaching up to 30 kW, with 3-phase AC input and high voltage DC (HVDC) output, the power sidecar can extend the rack power up to 1.3 MW. To put this rack power increase in perspective, it is around 10 or even 20 times the rack power of the current generation of server racks.

Considering all GPUs working synchronously in the same IT rack and also with other IT racks in the same datacenter cluster, demanding peak power as shown in Figure 1, we must expect a large current transient on the grid and in the datacenter's front-end power distribution, such as the medium voltage transformers, protection devices, etc.

This overloading of the grid can be illustrated by simulating a PSU input current during the peak power event. Figure 3 shows a PLECS simulation of a traditional two-stage PSU during a peak load event. Here, the energy is first supplied from the bus capacitor causing its voltage to drop, and as the PFC voltage controller tries to recover its output voltage, the controller will command its inner current loop with a higher reference current, causing the line current to overshoot higher than the nominal rated current.

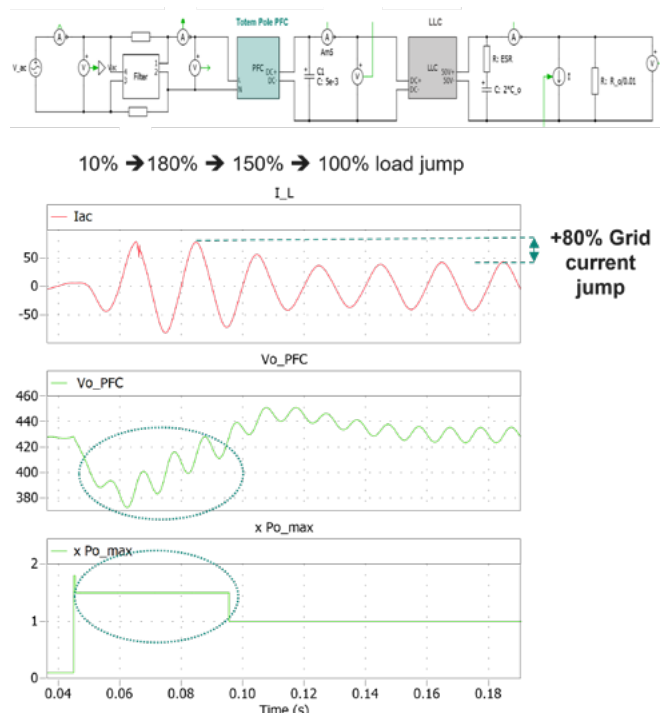


Figure 3: Simulation of a traditional 2-stage PSU during peak load event

To limit grid current transients, the sidecar’s input energy must be buffered from the AI peak loads, which is the main function of the CBU shown in Figure 4. A CBU consists of a capacitor bank with a bidirectional DC-DC converter to discharge the capacitors’ energy to the DC bus during AI peak load, and then charge the capacitors during the GPU’s idle times, which will smooth out the peak power demand from PSUs and therefore the grid side.

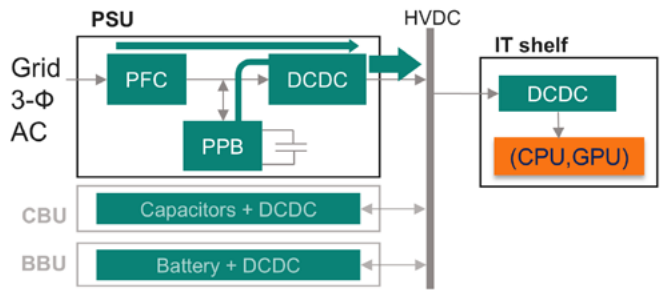


Figure 4: Rack power partition

Although CBUs can offer energy storage needed for peak shaving, they need separate shelves, and consume valuable space in the rack. Additionally, they may need to be compatible with, and to communicate with the PSU shelves, to manage rack power. Alternatively, energy buffer circuits can be integrated inside the PSU to offer the same functionality as the CBU as shown in Figure 4, allowing the rack to eliminate or reduce the need of extra capacitor shelves. Energy buffer circuits can increase the energy utilization in the PSU bulk capacitor by allowing it to discharge deeper while maintaining regulation of the bus voltage without affecting the DC-DC stage design, as detailed in the following section.

Power Pulsation Buffer (PPB) to support GPU peak load profiles
As GPUs draw a higher peak power and generate high load transients, the Power Pulsation Buffer functions as an efficient, high-density energy storage between the PFC and the DC-DC stages, and can support peak loads without overloading the upstream grid. PPBs can be integrated inside single-phase or three-phase PSUs, and can have different implementations, some of which are shown in Figure 5. The PPB bridge circuit can be 2-level or 3-level, and they can also be in series or in parallel. These bridge switches can be rated 440 V, 650 V, or 1200 V, designed with SiC, depending on the circuit type and the bus voltage.

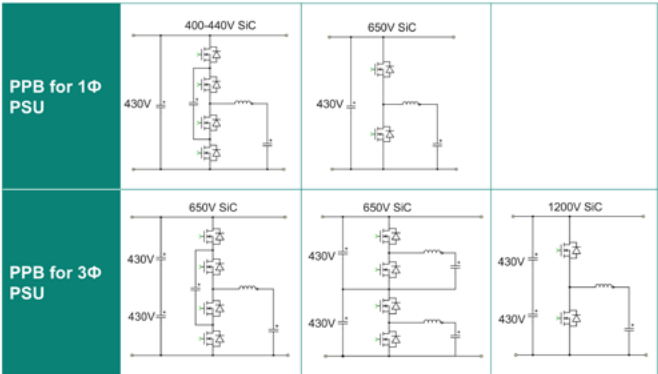


Figure 5: Different implementations of Power Pulsating Buffer in 1-ph and 3-ph PSU

Figure 6 shows an example 3-ph HVDC PSU with interleaved 3-level PPB. It shows a PLECs simulation of a peak-power event; with and without the PPB. From the figure, it is clear how the PPB provides energy during the peak-load event while maintaining the grid power limited to 110% of the PSU rated power.

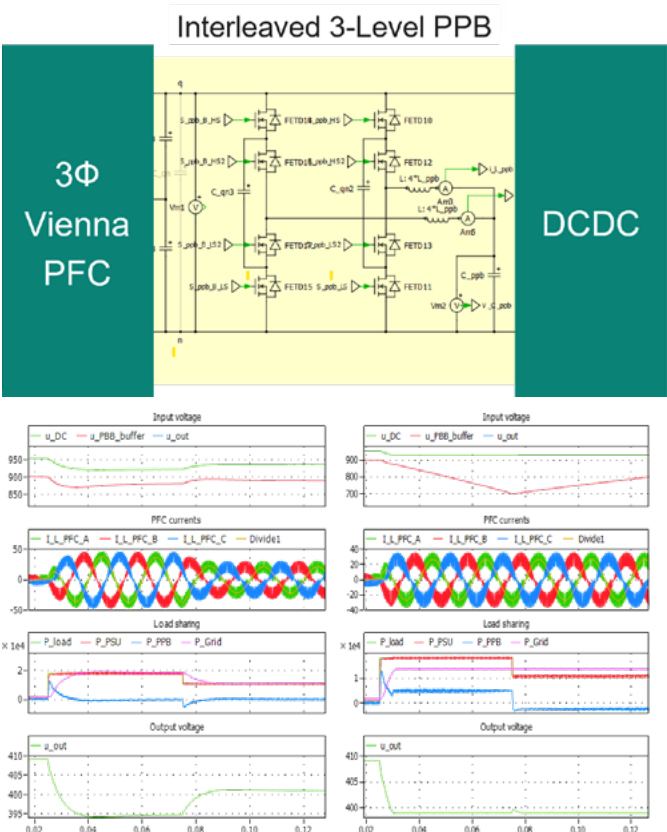


Figure 6: Simulation of peak load event: Without PPB (left) and with PPB (right) in 3-ph HVDC PSU

Control and operation of PPB
PPB can be operated continuously during normal operation, exchanging energy between the storage capacitor and the bus capacitor. Alternatively, it can be idle in normal operation and only operating on-demand during peak power events. Table 1 shows a comparison of both these PPB operation options.

PPB on-demand operation	PPB continuous operation
<ul style="list-style-type: none">- Good utilization of stored energy- Can support load jumps- Active only during hold-up and peak power → no additional losses of PPB- Components sized for short event operation- No grid frequency cancellation → DCX not possible, LLC must regulate small range of V_{in} fluctuation- Used for third harmonic injection in 3-ph PFC- Stable input and output voltages- Controlled re-rush current	<ul style="list-style-type: none">- Good utilization of stored energy- Can support load jumps- Active all the time → additional losses of PPB operation- Components need to be sized for steady state operation- Grid frequency cancellation → allows for optimum DCX with fixed frequency and high efficiency- Grid frequency cancellation is more suitable for 1-ph PSUs, but cannot be used for third harmonic injection in 3-ph PFC- Stable input and output voltages- Controlled re-rush current

Table 1: Comparison of PPB operation options

Learn more about how Power Pulsation Buffer can improve SMPS performance via Infineon’s PSU reference designs at

www.infineon.com/aipsu

Selecting the Right SiC MOSFET Device: A Key to Efficient Zero-Voltage Switching

Zero-voltage switching enables efficient power conversion at high frequencies. While ZVS significantly reduces switching losses, some residual losses still remain. Researchers from FAU Erlangen-Nürnberg benchmarked 1200 V SiC MOSFETs through calorimetric loss measurements at frequencies up to 350 kHz. Their findings help designers select the optimal SiC devices for their high-frequency soft-switching applications.

By Thomas Lehmeier, Yan Zhou, Martin März, Institute of Power Electronics, Friedrich-Alexander-Universität Erlangen-Nürnberg, and Ajay Poonjal Pai, Head of WBG Innovation, Munich, Sanan Semiconductor

Why is the selection of an appropriate SiC device essential in ZVS applications?

Zero-voltage switching (ZVS) in a power converter is a key technique for reducing switching losses while mitigating electromagnetic interference, thereby enabling high switching frequencies of up to hundreds of kilohertz. ZVS is achieved by minimizing the voltage-current overlap during switching transitions through circuit parasitics or small passive-reactive components. Although ZVS significantly reduces switching losses, it does not eliminate them. In [1], it has been demonstrated that the remaining losses are influenced by the MOSFET's intrinsic parameters (such as gate resistance, parasitic capacitances, etc.), as well as the gate driver's drive strength and timing. The goal was to evaluate today's leading 1200 V SiC power MOSFETs under ZVS in a half-bridge up to 350 kHz, providing clear device-selection criteria for designers of ultra-efficient, high-density soft-switching converters.

Testing Methodology Using a Transient Calorimetric Approach

Accurately estimating power losses from voltage and current measurements using double-pulse tests is highly challenging due to the rapid switching of WBG devices. Compared to electrical approaches, calorimetric measurement methods typically offer greater accuracy, making them more suitable for this context. To shorten the measurement time, a transient calorimetric method is employed. This method involves measuring the linear temperature rise $\Delta\theta$ of a thermal mass — such as a copper block serving as a thermal capacitance C_{th} — heated by the transistor over a specified time Δt (which is significantly shorter than the copper block's thermal time constant). This allows for the estimation of total power losses in the semiconductor device using:

$$P_{\text{loss, total}} = C_{th} \frac{\Delta\theta}{\Delta t} \tag{1}$$

Test-Bench Setup

A 15-gram copper block is soldered to the back of each tested transistor to increase the thermal capacitance, as depicted in Figure 1(a). A half-bridge test circuit supplying an inductive load is used to assess the residual ZVS losses, as shown in Figure 1(b). The two switches, S_{HS} and S_{LS} , are operated using Triangular Current Mode (TCM) modulation to achieve ZVS turn-on for both the high-side and low-side switches. The transistors' dead-time is kept as short as possible to minimize the current flowing through the intrinsic body diodes. To further minimize conduction losses in the body diode during the dead-time, a SiC Schottky diode is connected

in parallel with each transistor. The measurement setup utilizes three cylindrical air coils L , each with a distinct inductance value, to evaluate power losses at various switching frequencies ranging from 70 kHz to 350 kHz. The external gate turn-off resistor is set to zero, as is commonly practiced in soft-switched applications. The gate driver used in this study provides a maximum gate current of 10 A. The primary circuit and test parameters are listed in Table 1.

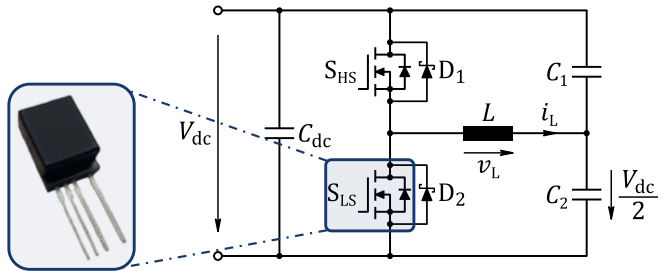


Figure 1: (a) Black-painted copper block soldered to a transistor. (b) Circuit diagram of the experimental setup featuring two transistors under evaluation.

Parameter / Component	Value
DC-link voltage V_{dc}	800 V
DC-link capacitance C_{dc}	40 μ F
DC-link capacitance $C_1 = C_2$	20 μ F
Switching frequency f_{sw}	[70 160 240 350] kHz
Inductance L	[14 28 61] μ H (air coil)
Gate turn-on voltage $V_{gs(on)}$	18 V
Gate turn-on voltage $V_{gs(off)}$	5 V
Gate resistance $R_{g(on)}/R_{g(off)}$	4 Ω / 0 Ω
Dead-time T_{dead}	120 ns
SiC Schottky diode D_1, D_2	SDS120J002D3

Table 1: Experimental Circuit and Test Parameters.

Figure 2 illustrates an exemplary heating process in which the low-side switch is equipped with a copper block. Temperature measurements were taken on matte black painted surfaces to minimize surface reflections and thereby enhance the accuracy of thermal imaging. The temperature data were recorded using an infrared thermographic camera with an average sampling rate of 15 Hz. The slope of the recorded thermal profiles, along with C_{th} , determines the total power losses of the device.

Accelerate your xEV design



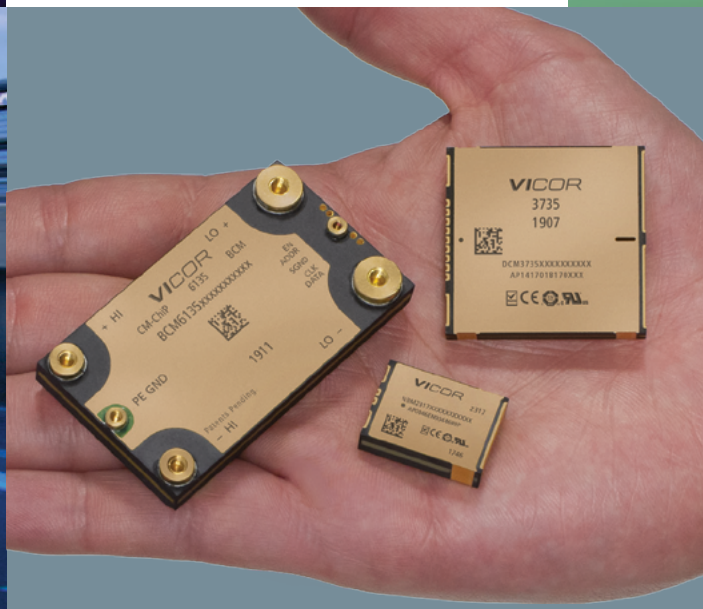
400/800V onboard charging compatibility



convert high voltage to 48V or 12V



efficiently bridge 48V and 12V systems



smallest, lightest power solutions

vicorpower.com/automotive

VICOR

High performance power modules

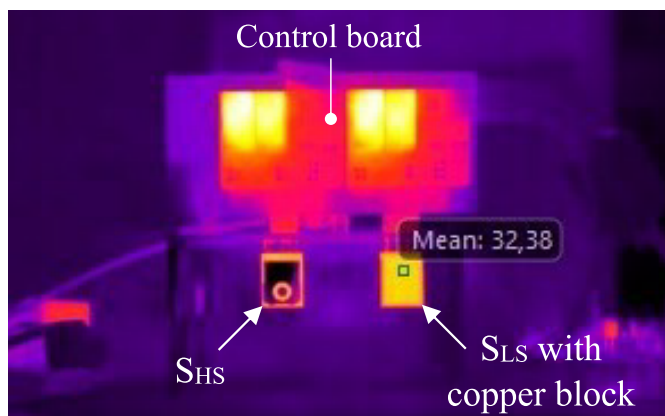


Figure 2: Thermal imaging of a heating process. The measurement window is positioned at the center of the MOSFET die.

Experimental Results

Nine standard TO-247-4 SiC MOSFETs, labeled T1 to T9, along with a TO-247-4 SiC JFET cascode device T10, are included in the study. All devices have a maximum blocking voltage of 1200 V and similar $R_{ds(on)}$ values. Sanan's planar structured transistor (SMS1200016M [2]) is designated as T1 in the measurement series. The remaining transistors T2 to T10 are commercially available devices that reflect the latest advancements in semiconductor technology. Table 2 summarizes the key characteristics of these devices.

Each device under test was operated for five seconds, starting at room temperature. Figure 3 presents the increase in copper block temperature obtained from thermal imaging.

The measurement series emphasizes the importance of selecting an appropriate transistor for soft-switched applications using ZVS: After five seconds, transistors T1 and T2 exhibit a temperature increase of only 4 K, which is roughly half the increase of 7.5 K

observed in transistor T10. The temperature profiles were recorded for each current level I_{sw} at two different inductance values, corresponding to two distinct switching frequencies. Based on the temperature curves from thermal measurements, the conduction losses can be subtracted during post-processing, allowing for the calculation of the residual switching energies under ZVS opera-

ID	Device	Structure	$R_{ds(on)}$ in m Ω	$R_{g,int}$ in Ω	C_{iss} in nF @ $V_{ds} = 1$ V	C_{oss} in nF @ $V_{ds} = 1$ V	V_{th} in V	$\tau_{g(off)}$ in ns ($R_{g,int} \cdot C_{iss}$)
T1	SiC MOSFET	Planar	16	0.9	7.2	5.8	2.8	6.5
T2	SiC MOSFET	Planar	15	1.1	6.3	8.9	4.0	6.9
T3	SiC MOSFET	Planar	11	1.2	7.7	5.8	2.7	9.2
T4	SiC MOSFET	Unknown	21	0.8	6.7	5.3	2.5	5.4
T5	SiC MOSFET	Planar	14	1.4	9.1	6.4	3.0	12.7
T6	SiC MOSFET	Trench	14	3.7	5.4	3.9	4.2	20.0
T7	SiC MOSFET	Planar	14	2.6	8.5	4.6	2.5	22.1
T8	SiC MOSFET	Trench	17	3.0	3.3	3.1	4.2	9.9
T9	SiC MOSFET	Planar	15	1.6	5.9	5.7	3.1	9.4
T10	SiC JFET Cascode	Planar	16	0.8	9.1	25.2	4.7	7.3

Table 2: Specifications of the SiC Transistors with TO-247-4 Package under Evaluation.



embeddedworld
Exhibition & Conference

CONNECTING THE
EMBEDDED COMMUNITY

10–12.3.2026

NUREMBERG, GERMANY

Redeem your ticket voucher
GG4ew26 now!
embedded-world.de/en/codes



Media partners

elektroniknet.de

Markt & Technik

Elektronik

Elektronik
automotive

Elektronik
•medical

**NÜRNBERG
MESSE**

tion. The gate metallization losses were determined to be in the range of 0.5 to 2 μJ , which can be neglected in this study. Figure 4 presents the residual switching losses as a function of the switched current for all evaluated transistors.

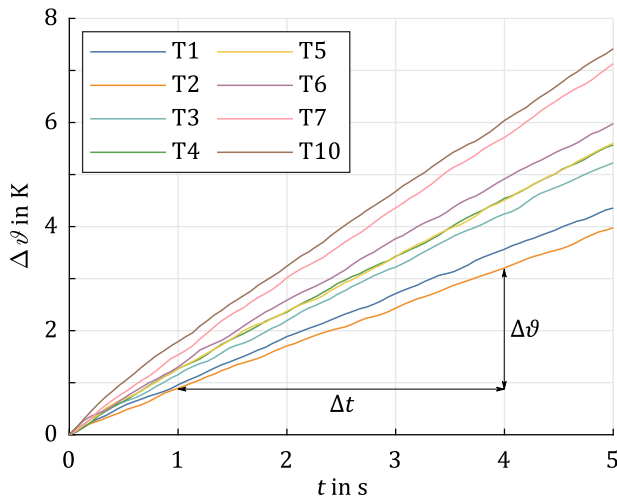


Figure 3: Measured copper block temperature profiles over five seconds for various transistors switching at 40 A.

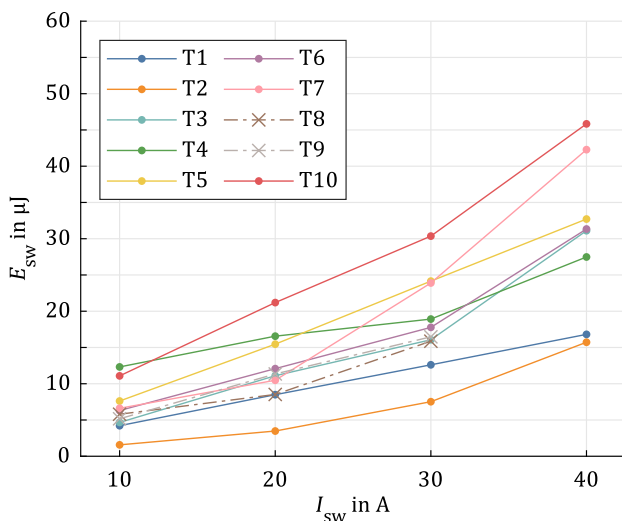


Figure 4: Calculated residual switching energies for the evaluated devices at different switched currents.

E_{sw} rises linearly to slightly more than proportional with increasing I_{sw} . Transistors T1 and T2 demonstrate the best performance in the investigation, while T7 and T10 show the worst results. In particular, the most suitable transistors for ZVS operation cause only about one-third of the switching energy compared to the worst. Minor anomalies in the E_{sw} -curves indicate slight measurement inaccuracies.

So, what's the device selection criterion in ZVS applications?

Notably, the transistor's unit cost did not correlate with its performance in the measurement series conducted. Instead, device-specific parameters determine the performance under ZVS conditions. A lower internal gate resistance $R_{g,int}$ and a higher ratio of V_{gs} to V_{th} result in higher gate discharge currents.

For a given gate current, devices with lower input capacitance C_{iss} lead to a rapid gate-source voltage decay (small gate discharge constant $\tau_{g(off)}$), and therefore remain in conduction for a shorter interval, resulting in a lower (V-I)-overlap. Consequently, transistors T1, T2, T3, and (at high load) T4 demonstrated superior performance.

Moreover, a larger output capacitance C_{oss} slows the vds rise during switching transitions, also reducing the overlap between voltage and current. For example, transistor T2 with its relatively high C_{oss} demonstrated particularly low losses compared to the others. In practical applications, further performance improvements can be achieved by adding an external NP0 MLCC capacitor in parallel to drain-source. This increases the effective capacitance and reduces voltage slew-rates, which particularly benefits otherwise lower-performing transistors. Beyond that, other transistor parameters such as transconductance and reverse transfer capacitance C_{rss} also impact the ZVS losses, although these effects are considered secondary.

The key findings highlight that minimizing $R_{g,int}$ and C_{iss} , while maximizing C_{oss} , leads to the optimal ZVS switch. Sanan's transistor portfolio is distinguished by its exceptionally low $R_{g,int}$ down to 0.9 Ω , and a carefully optimized input-to-output capacitance ratio. This synergy enables ultra-fast channel closure and a gentle voltage rise, reducing the (V-I) overlap during turn-off and minimizing residual switching losses under ZVS conditions.

The full article was published in the proceedings of this year's PCIM Conference [1].

The full article was published in the proceedings of this year's PCIM Conference [1].

References

- [1] T. Lehmeier, Y. Zhou, M. März, and A. P. Pai, "Influence of SiC MOSFET Device Parameters on Zero-Voltage Switching Losses," in Proc. PCIM Europe, Nuremberg, Germany, 2025, pp. 1928–1934.
- [2] Sanan Semiconductor, "1200 V 16 mΩ SiC Power MOSFET: SMS1200016M data-sheet," Rev. 1.0.0, 2024.

www.sanan-semiconductor.com

WÜRTH ELEKTRONIK
MORE THAN YOU EXPECT



HUGE PEAK, STRONG BEAD!

Chip beads with ultra low R_{DC} with specified peak current capability.

www.we-online.com/mps8



© ei505

WE are here for you!

Join our free webinars on:
www.we-online.com/webinars

Solving DC/DC Power Challenges in Military Avionics Through Modularity (Part 2)

After outlining the key standards for military and avionics power supply design in part 1, this part 2 turns to one of their most demanding challenges: managing input bus electrical overstress. The wide bus voltage range, transients, spikes, and undervoltage conditions all present a strict set of constraints for the power electronics designer. This part 2 of the story breaks down, how overvoltages are characterized in these standards and provides engineers with practical methods to suppress them. It looks at spikes and surges and explains, how a transient limiter works.

By Christian Jonglas, Technical Support Manager, GAIA Converter

When it comes to spikes and surges, it always comes back to two basic characteristics: duration and energy. What is the difference between these two and what does this mean for the design engineer?

Spikes

What is referred to as “spike” in this article is an over-voltage that lasts less than 1 ms. When the duration exceeds this value, it is common to refer to the event as a “surge.” Understanding this distinction is crucial because each kind of over-voltage requires treatment by a different device. Typically, spike protection is expected to implement a clamping device such as a Transient Voltage Suppression (TVS) diode, a Metal Oxide Varistor (MOV), or a gas discharge tube. This is possible because the relatively short duration of spikes means they contain an amount of energy that can be handled by a single clamping component. To select any clamping device's protection, three parameters must be considered that will be provided by the standard: the peak voltage, the duration, and the energy or the source impedance.

Let's take as example the injected voltage spikes described into the MIL-STD-1275F. The table 3 in part 1 of this story shows a spike with the following specifications: ± 250 V 70 μ s and 200 mJ. This is referring to the envelope of the transient spike described into the standard (Figure 1 below). Over the course of the last three revisions of Mil-STD-1275, the maximum energy specified increased from 15 mJ in revisions C and D to 200 mJ in revision E, and finally returned to 200 mJ in revision F.

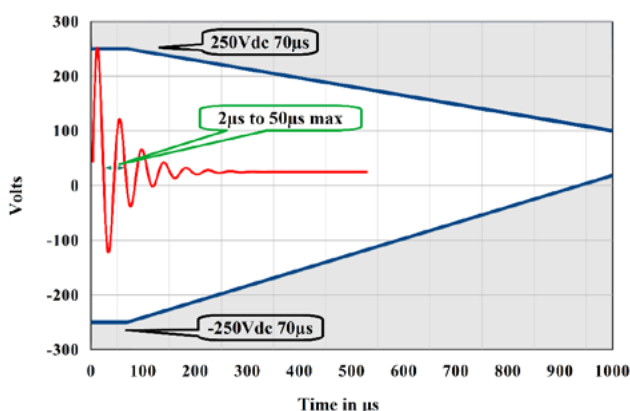


Figure 1: The graph defined into Mil-Std-1275F describes only the envelope of the spikes (blue line). The spike waveform is shown here above (red line).

We have the peak voltage, the pulse duration, and the energy—but to properly match the clamping protection to our design, one more parameter is needed: the minimum clamping voltage, which is the voltage threshold at which the device begins to conduct significant current. According to the MIL-STD-1275F standard, the most severe threat to the clamping device itself is a 100 V surge with a 50 ms duration. To prevent damage from excessive current flow during this extended event, the protection device must begin clamping at or slightly below 100 V. We can now select a clamping device rated to trigger at 100 V and capable of withstanding 200 mJ of energy.

However, this energy is not delivered instantaneously. A reasonable assessment of the waveform (red curve) indicates that the initial, most aggressive surge—the first arch—contains less than 66 mJ of this total 200 mJ energy. This first arch has extreme characteristics such as a very fast rise time of up to 50 ns (a slew rate of 5 V/ns to reach 250 V) and a minimum duration estimated at 1 μ s (a half-period of 500 kHz), that is expected to be softened by the input impedance of a power supply. Using a conservative approximation of 66 mJ dissipated over 25 μ s, we can consider a 2.64 kW power and 10.56 A peak current under 250 V. With these requirements defined, we can evaluate suitable clamping devices:

- SMCJ78CA (Littelfuse)[2.1]: This device could be a candidate. Its maximum clamping voltage is 126 V at its peak pulse current of 11.9 A. While it appears to meet the current requirement, its clamping voltage is too high to protect any downstream circuitry rated for only 100 V.
- SMDJ78CA (Littelfuse)[2.2]: This is a more robust solution. With a peak current capability of 23.8 A, it provides significant margin over the calculated 10.56 A requirement. This ensures reliable operation and provides effective protection for circuits with a 100 V maximum rating.
- 5KP78CA (Littelfuse)[2.3]: If board space is not a constraint, a higher-power component like this offers maximum margin and “peace of mind.” Thanks to its vastly higher current handling (40.5 A).

Of course, these results can be revised to a lower value if the power supply input is capacitive, as the capacitive impedance can handle a non-negligible part of the spike's energy. It is noticeable that the qualification test procedure requires a minimum of 100 spike injections applied each at a rate of one every second. Sometimes, spikes are applied between ground and plus or minus termination. In this case some safety considerations may indicate if TVS are allowed or not. Figure 2 shows the position of the spike suppressor at the front side of the power architecture.

The Premier Global Event in Power Electronics

APEC 2026

SAVE THE DATE

MARCH 22-26, 2026

SAN ANTONIO, TX



The clamping protection devices function by overloading the spike source to maximize the voltage drop across its internal impedance. Consequently, a TVS diode, MOV, or gas tube will be ineffective if the spike source exhibits zero internal impedance. However, clamping protection is useless in some cases, as transient spike voltages generated by a high-impedance source can be attenuated simply with a capacitor or LC filter. For example, consider the DO160G Section 17 specification: a 600 V/10 μ s spike into a 50 Ω source impedance. When this spike is applied to any GAIA converter filter in the FGDS series, the 600 V transient is reduced to just a few volts, well within the tolerance of the downstream converter. As an example, the FGDS-2A-50V, when subjected to this 600 V spike, exhibits a transient impedance of approximately 0.7 Ω , limiting its output voltage rise to no more than 35 V (Figure 3).

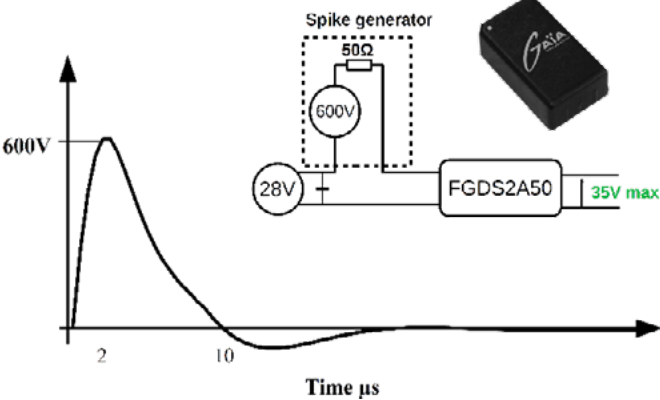


Figure 3: Thanks to the 50 Ω internal impedance, the DO160 600V spike can be dampened directly by a FGDS-2A-50V EMI filter.

Surges

When clamping a surge transient voltage, relying on overloading the surge source to cause a voltage drop is no longer viable because the source impedance is usually very low or the surge duration is too long. In such cases, the energy contained in the surge is too high for a single clamping component that will be damaged. The most common approach for handling transient surges is to insert a series element into the input bus that introduces a voltage drop when input voltage reaches a given level. This method imply the transient protection needs to pass-through the total current drawn

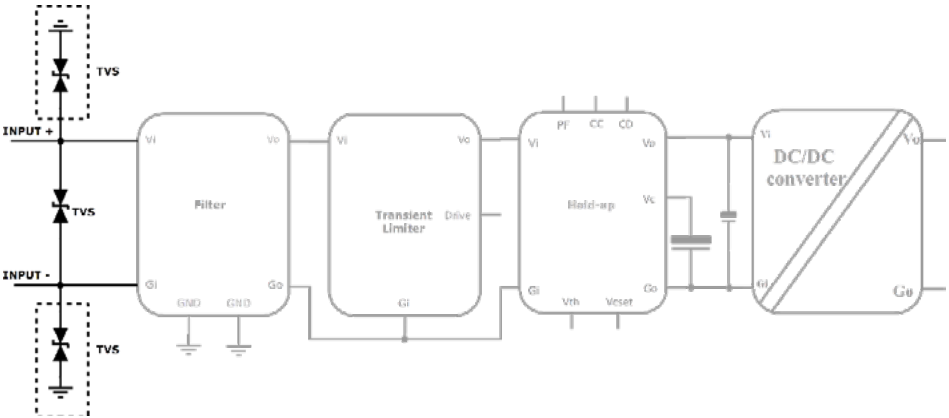
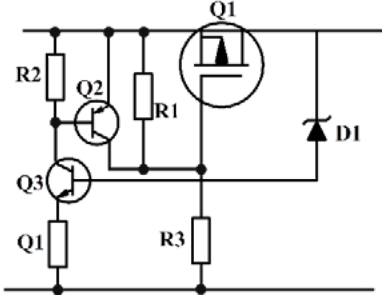


Figure 2: The spike protections such as TVS are connected between input+ and input- of a power architecture, and can also be populated across inputs and ground.

Figure 4: A series element such as the Q1 of this transient limiter allows to handle long lasting overvoltage



by the downstream converter. Figure 4 presents a basic example of a discrete P-MOSFET-based transient voltage limiter. Choosing a discrete solution over a ready-to-use COTS based modular approach introduces three key challenges:

- **Safe Operating Area (SOA) Compliance:** The MOSFET will operate in its resistive mode during the surge event. This requires the designer to verify that the selected transistor operates within its SOA. Since the SOA is typically specified at 25 $^{\circ}$ C, the designer must extrapolate the data across the full temperature range of its reliability application, from -40 $^{\circ}$ C to 105 $^{\circ}$ C.
- **P-MOSFET choice:** While many P-MOSFETs are available for low-power applications (below 50–80 W), higher power projects typically require N-MOSFETs. Implementing a surge limiter with an N-MOSFET using discrete components leads to a much more complex design.
- **Thermal Management:** Managing heat generated by the MOSFET during clamping adds significant design complexity and requires complex thermal calculation.

Although driving circuits for N-MOSFET-based transient limiters are now commercially available, ensuring Safe Operating Area (SOA) compliance across temperature ranges, thermal management, and other military qualifications remains challenging for designers pursuing discrete solutions. Adopting a modular approach with Commercial Off-The-Shelf (COTS) products significantly simplifies the

COTS REF.	LGDS-50	FLHG-60	LGDS-100	LHUG-150	LGDS-300	LGDS-600
parameters						
output power	50W	60W	100W	150W	300W	600W
Surge voltage/time	50V/100ms	100V/100ms	202V/100ms	100V /100ms	100V/ 100ms	202V/350ms
Max output voltage	38	65	42	78	42	38
Standard	DO160 MilSTD704	DO160 MilSTD704 MilSTD1275 MIL-STD-461	DO160 MilSTD704 MilSTD1275 DefStan 61-5 (6)	DO160 MilSTD704 MilSTD1275	DO160 MilSTD704 MilSTD1275	DO160 MilSTD704 MilSTD1275 DefStan 61-5 (6)
MTBF @ 40 $^{\circ}$ C	2500 000 Hours	1700 000 Hours	1300 000 Hours	891 000 Hours	1300 000 Hours	1300 000 Hours
Multiple Functions Module		yes		yes		

Table 1: From 50 to 600 W, the GAIA Converter transient limiters come in potted metallic case board mounted modules enabling compliance to the main defense and avionic standards.

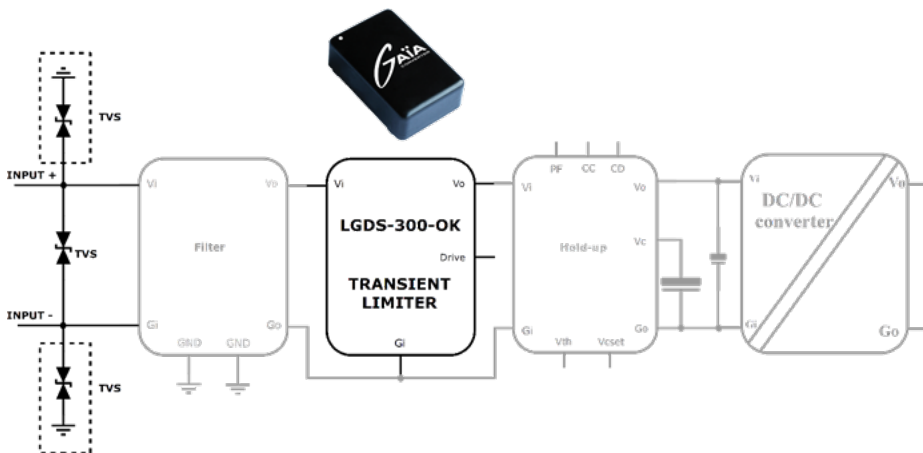


Figure 5: In this power supply architecture, the LGD-300-OK transient limiter, placed after the EMI filter that allows the surge to pass, limits any surge from 50 to 100 VDC to a lower voltage acceptable for the converters, while reducing the inrush current.

designer's task and accelerates development timelines for any project. GAIA Converter offers transient limiters with voltage capabilities from 80 V to 202 V, meeting most industry standards. These modules feature output clamping voltages compatible with a wide range of DC/DC converters and power ratings from 50 W to 600 W. Housed in encapsulated metallic cases, these board-mounted modules are fully qualified for military and avionic applications. Designed for high reliability, they achieve very high Mean Time Between Failure (MTBF) figures. Some variants integrate additional functions such as reverse polarity protection, inrush current limiting, hold-up support, and (in the latest models) integrated EMC filtering. An overview of GAIA Converter's COTS transient limiters is provided in Table 1.

Avoiding Transient Limiter

Just as effective input filtering can eliminate the need for spike protection by dampening over-voltage below a DC/DC converter's maximum limit, high-performance DC/DC converters with wide input ranges may similarly obviate surge protection devices. For example, GAIA Converter's MGDD-80-N-E (80 W, 9–80 VDC input) and MGDS-100-M-C (100 W, 10–100 VDC input) can withstand transient inputs up to 80 VDC (per DO-160) and 100 VDC (per MIL-STD-1275), respectively, without damage. This resilience stems from their use of current-mode control in the regulation loop. Unlike converters using voltage-mode control—which only responds to input surges after the output voltage rises, risking brief output overshoot—this current-mode control proactively monitors input current and adjusts regulation, preventing output disturbances.

What's next?

As established in Part 1 of this series, military and avionic standards define the maximum levels of electromagnetic interferences (EMI) alongside surges and spikes, that a power supply must comply to. For switching-mode power supplies (SMPS), these disturbances also represent a significant source of emissions creating an additional design challenge. The upcoming Part 3 of this story will break down the various modes of electromagnetic interference (EMI) propagation and describe methods to contain it, with a focus on using EMC filters.

References

- [2.1] <https://www.littelfuse.com/assetdocs/tvs-diodes-smcj-datasheet?assetguid=37388813-0d6d-4329-969b-1aa8b7614ac1>
- [2.2] <https://www.littelfuse.com/assetdocs/tvs-diodes-smdj-datasheet?assetguid=2d9772b3-822b-4362-914d-b74e0a706638>
- [2.3] <https://www.littelfuse.com/assetdocs/tvs-diodes-5kp-datasheet?assetguid=b1ddd6a2-fccb-4327-bea1-7d77c0793479>

www.gaia-converter.com

ARCEL
POWER ELECTRONICS

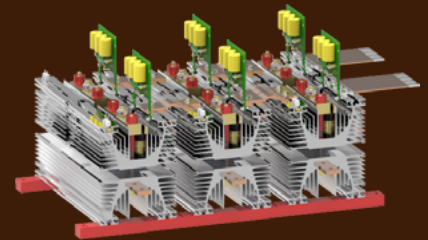
WE BUILD
POWER STACK



AC/DC

Press-pack

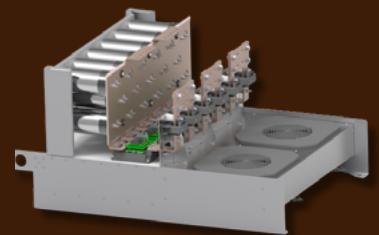
1000A – 400Vac (B6C)



DC/AC

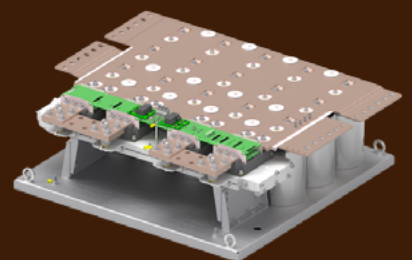
3ph Inverter

1500A – 400Vac (B6CT)



DC/DC

2000A – 800Vdc (L1CT)



Email



Ghislain GINOT
Sales manager

WWW.ARCEL.FR

An Exploration of Surface Mount Power Packaging Technologies for SiC MOSFETs

The adoption of Wide-Bandgap (WBG) devices is driven by innovation in device technology and packaging. New and ongoing challenges in device technology require manufacturers to continually enhance and upgrade their devices. Surface mount packages for Silicon Carbide (SiC) MOSFETs and diodes offer several advantages over through-hole packages. Today, this is primarily driven by the need for compact, efficient systems that run cool. A SiC device lends itself to these benefits with its higher efficiency and current density.

By Vipin Gaonkar, Principal Applications Engineer, High-Power Solutions Business Unit, Microchip Technology

Benefits

Historically, the 3-terminal TO-247 package has been the workhorse in power converters, accommodating large die but falls short in leveraging the performance advantages of WBG technology. The 4-terminal TO-247, or TO-247-4L, introduced the Kelvin source for reduced loop inductance and improved gate drive signal quality. However, it offered minimal improvements in thermal performance.

Within the surface mount family of discrete packages, designers may choose between top or bottom-side cooled packages. The selection criteria are driven by the following primary factors:

1. **Power Density** – Maximizes continuous and peak power capability from a given die while maintaining sufficient creepage and clearance distances
2. **Electrical Performance** – Minimizes parasitic inductance, reducing the overshoot and ringing as well as the overall switching losses
3. **Ease of Use** – Simplifies circuit board design while improving the design for manufacturability
4. **Availability** – Industry-standard packages offer the benefit of multi-sourcing while unique packages offer designers opportunities for differentiation

Table 1 summarizes JEDEC recognized surface mount packaging options that are generally available from multiple vendors.

Package	Approx. Dimensions (mm)	Approx. Creepage (mm)	Cooling	Notes
D2PAK	15 x 10 x 4.3	6.6	Bottom-side	Heat conduction through circuit board
TOLL	10 x 11 x 2.3	3.15	Bottom-side	
PSMT (TOLT)	10 x 15 x 2.3	3.0	Top-side	Low inductance, high power density
QDPAK	15 x 21 x 2.3	4.8	Top-side	

Table 1: Package Characteristics

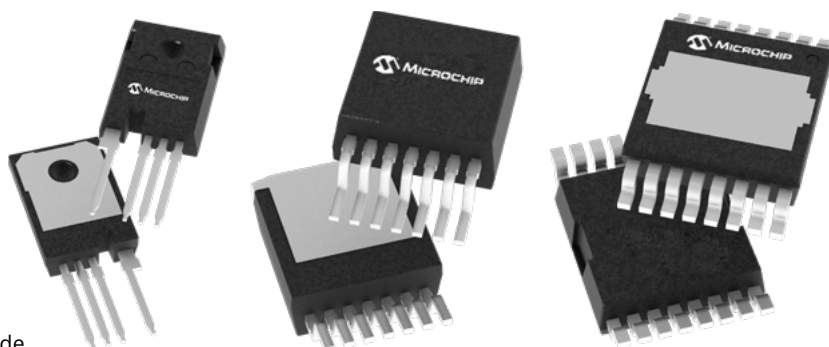


Figure 1: TO-247-4LN (left); D2PAK (center); PSMT (right)

Ease of use

Balancing design considerations, such as thermal performance, assembly and reliability, is important when selecting a package. Top-side cooled package feature options, such as positive and negative standoff, drive the circuit board layout design, thermal design, and assembly process. The standoff represents the z-axis offset from the bottom of the package body to the bottom of the leads.

With positive standoff, the leads sit flush on the printed circuit board (PCB), creating a gap between the package body and the board. This requires thicker Thermal Interface Material (TIM) to account for the gap and its tolerance and ensures proper compression for optimal thermal conductivity. However, excessive compression can stress solder joints, potentially leading to fatigue and reliability issues over time.

The negative standoff feature mitigates the reliability risk on solder joint fatigue by significantly reducing the stress on the device leads. With a negative standoff, the package body makes direct contact with the PCB substrate. A gap of 0.01–0.11 mm is maintained between the bottom of the package body and the bottom of the leads.

The thickness and thermal performance of the TIM depends on the package height and lead tolerance. A negative standoff minimizes the effect of lead tolerance, as solder fills the gap between the lead and the PCB pad. This allows the package body to consistently rest flat on the PCB, minimizing variations in TIM thickness due to tolerances. As a result, the junction-to-ambient thermal resistance is optimized and closely controlled, reducing solder joint stress and associated fatigue while improving long-term reliability.

Improving power density

This section presents simulation results comparing D2PAK and PSMT packages. The simulation aims to evaluate heat flux and cooling performance, using heat conduction through the PCB and TIM for bottom-side cooled D2PAK devices, and through the TIM and heatsink for top-side cooled PSMT devices.

A 100 μm thick TIM is applied between the PCB and the heat sink in the simulation with the D2PAK, and between the device and heat-sink in the case of the PSMT simulation. Figure 2 below is a representation of the thermal conduction path.

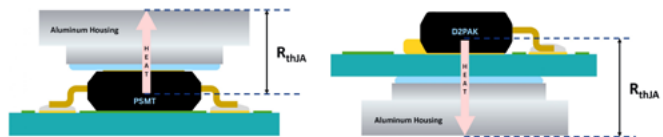


Figure 2: Thermal path in PSMT vs D2PAK

Simulations were performed in free convection at 25°C and 85°C. Shown in Figure 3 are results from the 85°C simulation for the PSMT and D2PAK packages. The PSMT package simulation showed a 25% - 35% lower junction temperature than the D2PAK. A top-side cooled package offers a better thermal path, resulting in a lower junction temperature and higher power density system.

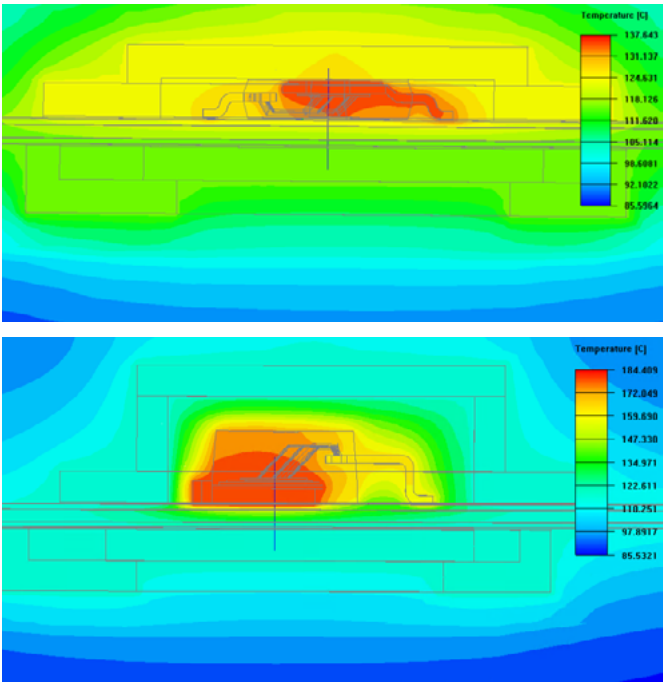


Figure 3: Thermal simulation results of PSMT (top) and D2PAK (bottom)

Impact of Creepage & Parasitic Inductance

Below are the simulation results for power loop inductance for different SiC power packages.

Package	Creepage	Inductance
TO-247-4LN	8.45 mm	31.97 nH
D2PAK	6.6 mm	29.89 nH
PSMT (TOLT)	3.0 mm	14.13 nH

Table 2: Packages simulation results

In designing high voltage systems, creepage distance is an important design parameter. The legacy TO-247 evolved from 3 lead (TO-247-3L) to 4 lead (TO-247-4L) to 4 lead with notch (TO-247-4LN) increasing the creepage from 3.0 mm to 3.8 mm to 8.45 mm.

While important, there are design solutions for creepage, such as introducing a notch in the PCB or conformal coating. Table 2 provides a summary of the three packages. Parasitic inductance is a significant factor impacting power conversion efficiency. Parasitic inductance exists in both power and gate loops, influencing overall device performance. In high-frequency power converters utilizing SiC MOSFETs, parasitic inductance becomes increasingly problematic, resulting in greater energy losses, increased voltage overshoot and elevated Electromagnetic Interference (EMI) due to ringing. The impact of parasitic inductance can be visualized in the waveforms of Figure 4 by the voltage overshoot during switching.

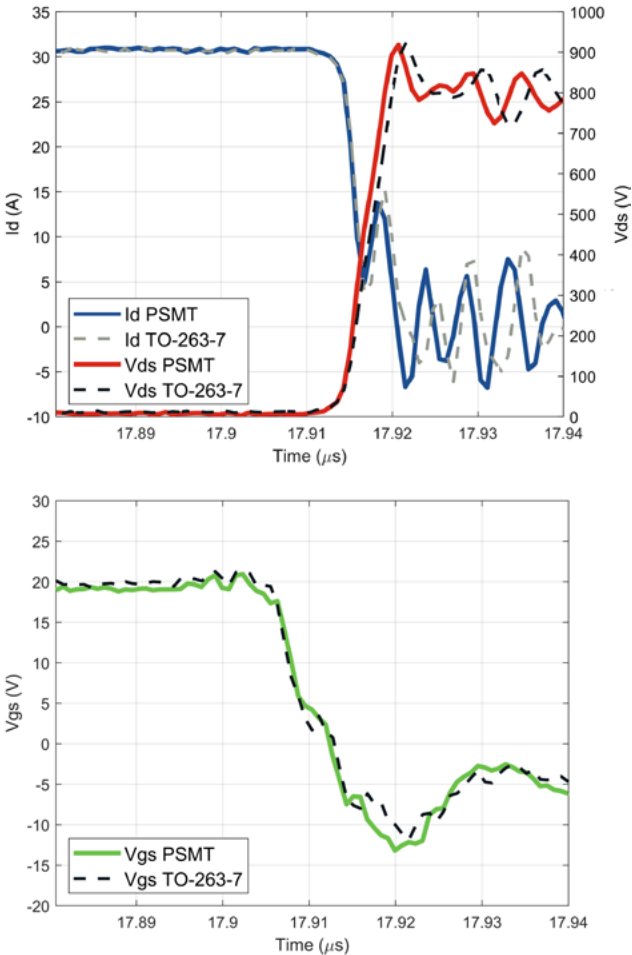


Figure 4: Switching waveforms comparing the D2PAK vs the PSMT

Top-side cooled packages, such as PSMT and QDPAK, provide notable benefits compared to bottom-side cooled options, such as D2PAK and TOLL. By separating the thermal and electrical paths, these devices enable system designers to reduce parasitic inductance and optimize thermal management. This separation allows for more flexible and efficient power loop routing. With the electrical path independent from the thermal path, designers can better minimize inductive losses, support faster switching speeds in their applications and increase power density.

Summary

Top-sided cooled package offers excellent thermal improvements over legacy discrete packages. If the designer is trying to optimize switching or simplify their manufacturing, Microchip has a wide array of other packages offered in voltage ranges of 700V to 3300V.

Beyond discrete packaging, as power requirements increase, integration could be key to solving the power density or switching efficiency problems.

Configuring Four-Switch Buck-Boost μ Module Regulators for Step-Up, Step-Down, or Inverting Output

A four-switch buck-boost power module integrates the controller, MOSFETs, power inductor, and capacitors within a 3D integrated package. This article demonstrates the ability of such a μ Module to operate in various topologies, including buck (step-down), boost (step-up), and inverting buck-boost configurations for negative output applications.

By Ling Jiang, Senior Manager, Wesley Ballar, Senior Engineer, and Anjan Panigrahy, Product Applications Engineer, Analog Devices; and Henry Zhang, ADI Fellow

Many power conversion applications need to support wide input or output voltage ranges. Analog Devices has a high current, high efficiency, fully integrated four-switch buck-boost power module for such applications. This device integrates the controller, MOSFETs, power inductor, and capacitors within an advanced 3D integrated package, enabling compact design and robust performance. This μ Module[®] regulator delivers high power density, high efficiency, and a good thermal performance across a wide range of input and output voltages.

Four-Switch Buck-Boost Topology as a Buck Regulator

ADI has introduced multiple 40 V step-down μ Module regulators. Figure 1 highlights the available regulators capable of supporting a maximum load current exceeding 4 A. However, these buck regulators are limited in their voltage and current range. By employing the newly released four-switch buck-boost μ Module regulator, the LTM4712, as a step-down converter, the operating range can be significantly extended, simplifying system design for engineers.

The four-switch buck-boost converter can be effortlessly configured as a buck converter without requiring any special adjustments. When $V_{IN} > V_{OUT}$, the internal controller keeps power FET M3 off and M4 continuously on. M1 and M2 regulate the output, operating like a standard buck converter, as illustrated in Figure 2.

Figure 2: Utilizing the device as a buck regulator.

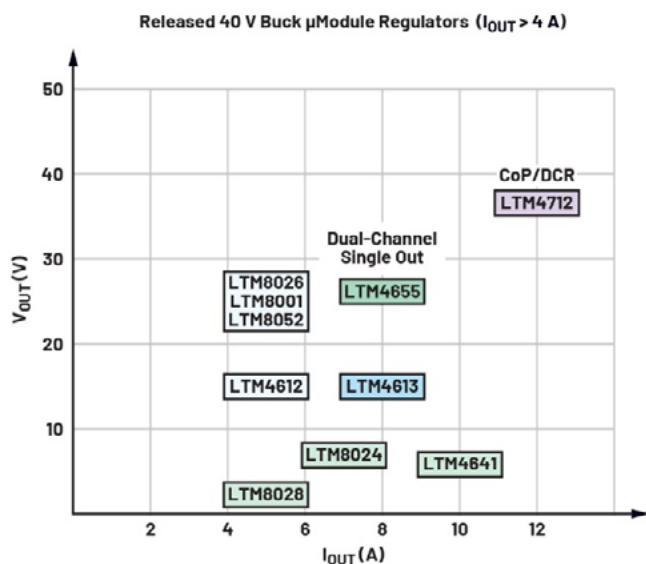
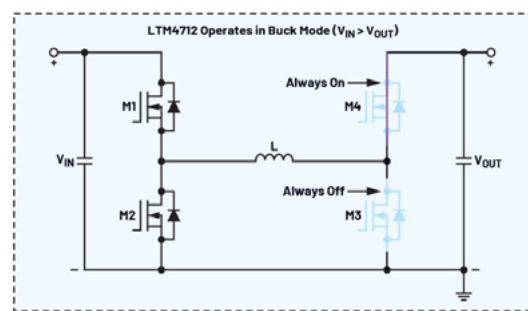


Figure 1: 40 V_{IN} (>4 A) buck μ Module regulators.

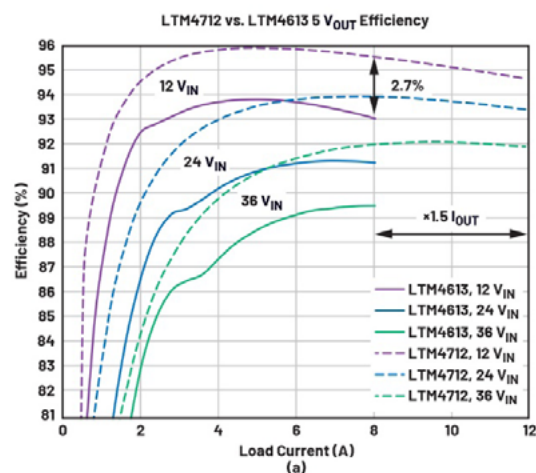
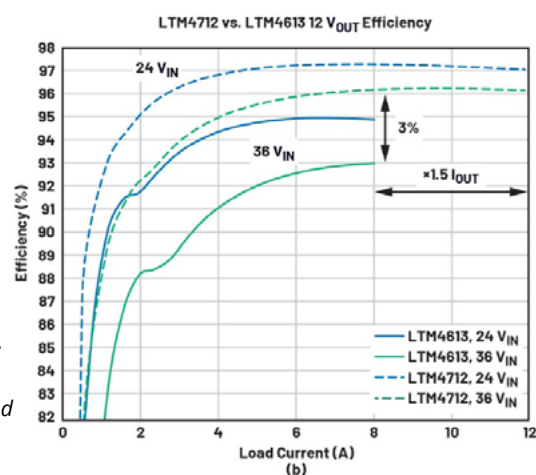


Figure 3: Buck mode efficiency and current capability comparison: (a) 5 V_{OUT} efficiency and (b) 12 V_{OUT} efficiency.



Compared to the previous step-down regulator, the LTM4613, the current device achieves higher power efficiency, despite the additional conduction loss introduced by M4, as shown in Figure 3. This improvement is made possible by advancements in MOSFET and inductor technologies.

The thermal comparison without forced cooling, shown in Table 1, underscores the efficiency advantage of the buck-boost converter. Despite delivering significantly higher power than the buck regulator, the new device operates at a cooler temperature with a similar footprint area.

Operating Condition	Parameters	LTM4712	LTM4613
12 V _{IN} /5 V _{OUT}	Max I _{OUT}	12 A	8 A
	Efficiency at I _{MAX}	94.7%	93%
	Thermal at I _{MAX}	58°C	70°C
36 V _{IN} /12 V _{OUT}	Max I _{OUT}	12 A	6 A
	Efficiency at I _{MAX}	96.2%	93%
	Thermal at I _{MAX}	80°C	101°C

Table 1: Buck mode thermal performance comparison, T_A = 25 °C, no forced cooling.

Four-Switch Buck-Boost as a Boost Regulator

As shown in Figure 4, ADI has previously released one 40 V boost μModule regulator. While the LTM4656 supports a maximum current of 4 A, the recently released four-switch buck-boost converter can handle a higher load current when it functions as a step-up regulator.

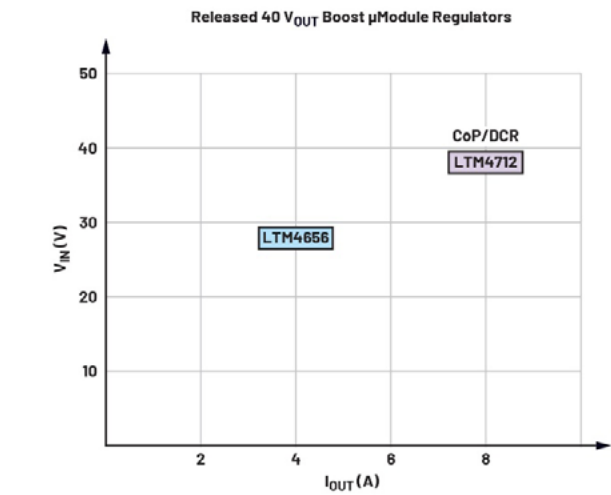


Figure 4: ADI 40 V boost regulator family.

When using the four-switch buck-boost converter in applications where V_{IN} < V_{OUT}, internal switch M1 remains on, while M2 stays off. M3 and M4 naturally regulate the output as a typical boost converter as shown in Figure 5. Unlike standard boost converters, which lack output short-circuit protection, the four-switch buck-boost offers inherent short-circuit protection. If the output is shorted to ground, M1 and M2 begin switching as a buck converter, limiting the current flowing from input to output. The maximum short circuit current is restricted by either the R_{SENSE} resistor placed in the input or output paths, or the peak inductor current limit, whichever

is lower. In addition, during the initial fast V_{IN} ramping up stage, a conventional boost converter usually has uncontrolled, high inrush current through the boost diode to charge up C_{OUT}. As the four-switch buck-boost always starts in buck mode when V_{OUT} is low, its input inrush current is tightly controlled and limited by the soft start of the inductor current. In summary, the four-switch buck-boost offers a more reliable step-up converter than a conventional boost regulator.

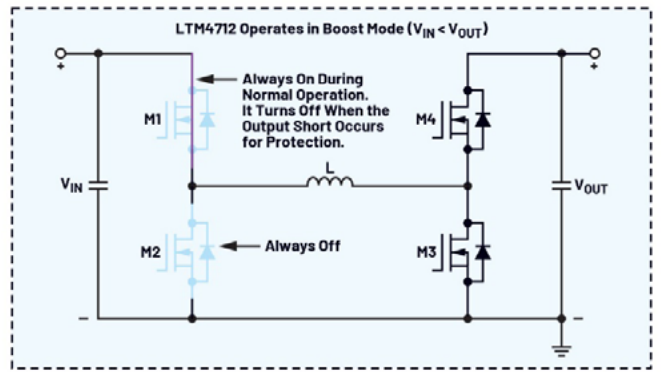


Figure 5: Utilizing the device as a boost regulator with inherent output short protection.

Figure 6 and Table 2 compare the efficiency, power capability, and thermal performance between the four-switch buck-boost μModule regulator and the buck μModule regulator. The first device demonstrates higher efficiency, extended current handling, and significantly better thermal performance. Both regulators share the same 16 mm × 16 mm footprint.

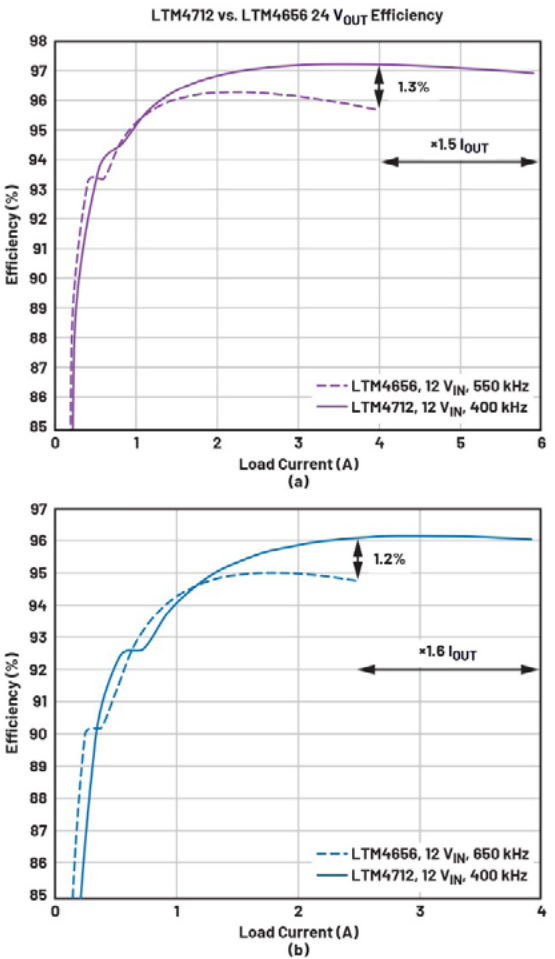


Figure 6: Boost mode efficiency and current capability comparison: (a) 24 V_{OUT} efficiency and (b) 36 V_{OUT} efficiency.

Operating Condition	Parameters	LTM4712	LTM4656
12 V _{IN} /24 V _{OUT}	Max I _{OUT}	6 A	4 A
	Efficiency at I _{MAX}	96.9%	95.7%
	Thermal at I _{MAX}	69°C	81°C
12 V _{IN} /36 V _{OUT}	Max I _{OUT}	4 A	2.5 A
	Efficiency at I _{MAX}	96.1%	94.8%
	Thermal at I _{MAX}	84°C	89°C

Table 2: Boost mode thermal performance comparison, T_A = 25 °C, no forced cooling.

Four-Switch Buck-Boost as an Inverting Buck-Boost Regulator for Negative Output Voltage

Similar to standard buck converters, the four-switch buck-boost can also be configured in an inverting buck-boost topology for negative output applications. As shown in Figure 7, M1 and M2 switch complementarily, with M3 off and M4 on during this operation. Note that the maximum voltage, V_{MAX} = |V_{IN}| + |V_{OUT}|, must be less than 40 V, which is the maximum voltage rating for the device. The magnitude of the DC through the inductor, I_L, is given by I_L = I_{OUT}/(1-D), where D is the duty cycle of the phase leg with M1 and M2, and M1 is the primary switch.

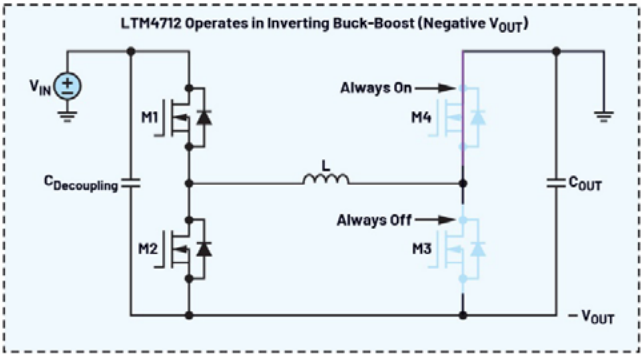


Figure 7: The device configured as an inverting buck-boost regulator.

Figure 8 illustrates an example circuit of the inverting configuration, designed for a 24 V input and -12 V output, capable of delivering up to 10 A of load current. Figure 9 presents the efficiency curves obtained from bench testing.

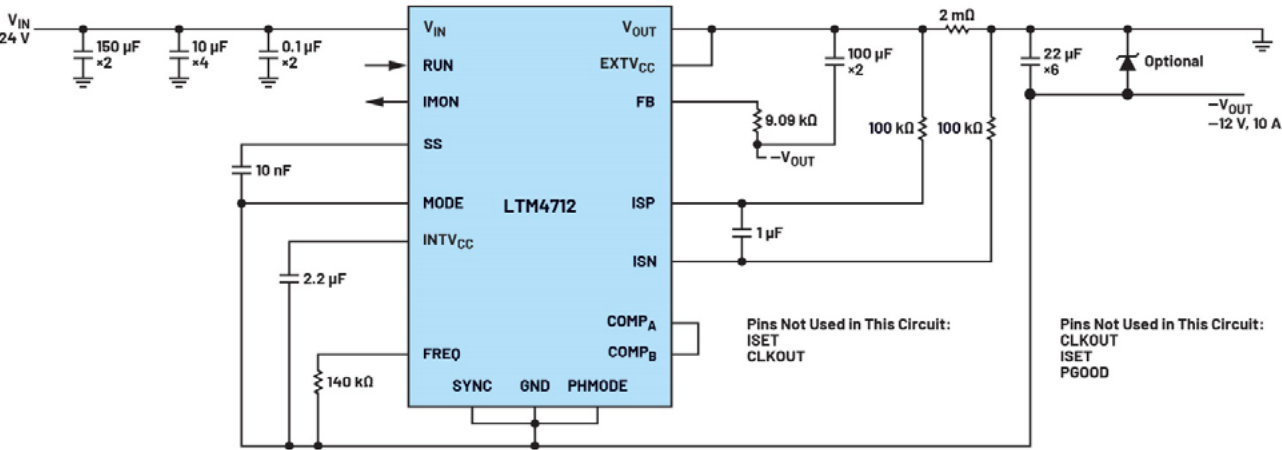


Figure 8: Example circuit of an inverting configuration.

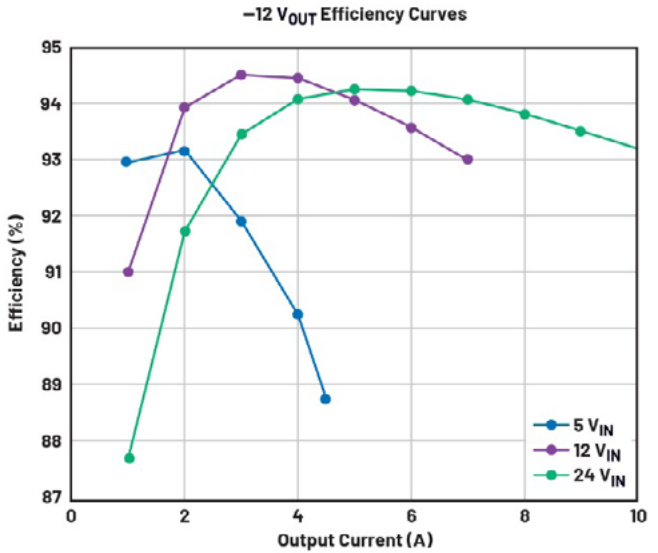


Figure 9: Bench tested efficiency curves for -12 V_{OUT}.

In the inverting buck-boost converter, the output voltage may rise slightly above zero during startup. This same behavior is observed when configuring the four-switch buck-boost regulator in inverting mode.

Figure 10 illustrates the mechanism behind the reversal of the output voltage during startup. When the input supply is turned on, but before all four MOSFETs begin switching, the input current starts charging the output capacitor in reverse through two paths: via the C_{IN} decoupling capacitors placed across M1 and M2, and through the INTV_{CC} capacitor path. If C_{IN} or C_{INTVCC} are significantly larger than C_{OUT}, a higher reverse output voltage is likely to occur.

However, an inherent clamping circuit is present inside of the µModule regulator, as shown in Figure 11. V_{SD3} and V_{SD4} represent the source-to-drain voltages of M3 and M4, respectively. When -V_{OUT} > V_{SD3} + V_{SD4}, the body diodes of M3 and M4 conduct, taking over the charging current. These two body diodes create a natural clamping circuit. In other words, the maximum reverse output voltage is V_{SD3} + V_{SD4}.

Figure 12 displays the bench-tested reversed output voltage waveforms during startup. In Figure 12a, the magnitude of reversed -V_{OUT} is approximately +0.75 V, with a limited C_{IN} (50 µF) presented in the circuit compared to C_{OUT} (330 µF). When increasing C_{IN} to 350 µF, a higher reserved -V_{OUT} of +1.5 V is observed, as shown in Figure 12b.

The ratio of C_{IN} to C_{OUT} can be adjusted to minimize the positive output voltage before reaching the internal clamping voltage, $V_{SD3} + V_{SD4}$. Additionally, an external low forward drop clamping Schottky diode can be added at the output to limit the positive voltage to a desired level, as shown in Figure 8.

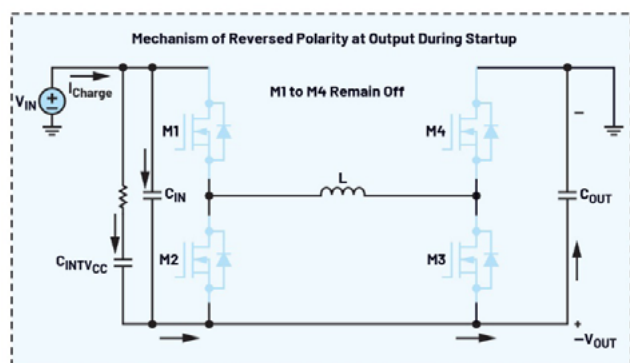


Figure 10: Charging current flow paths during startup.

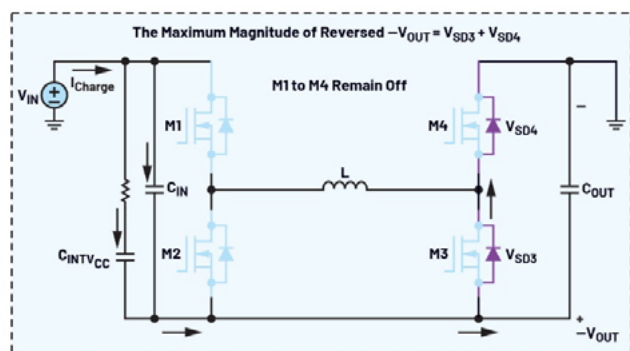


Figure 11: The natural clamping circuit in the four-switch buck-boost.

Conclusion

The four-switch buck-boost regulator can naturally be used as either a step-down or step-up regulator without requiring any special configurations. Bench testing has verified that the newly released buck-boost μ Module delivers the highest efficiency, best thermal performance, and extended current capability compared to other available buck or boost μ Module regulators. Additionally, this four-switch buck-boost can be easily configured as an inverting buck-boost regulator for applications requiring a negative output. High efficiency has been confirmed through bench tests.

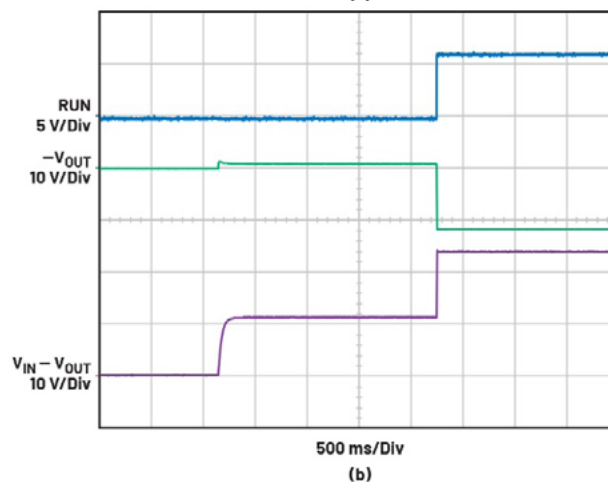
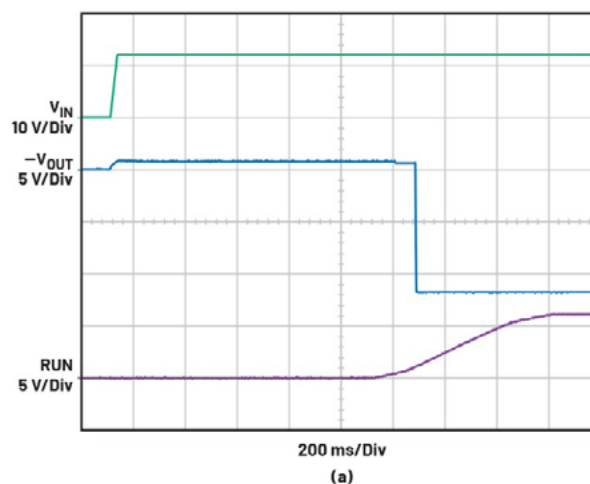


Figure 12: Reversed $-V_{OUT}$ waveforms during startup: (a) relatively small C_{IN} (50 μ F) compared to C_{OUT} (330 μ F) and (b) relatively large C_{IN} (350 μ F) compared to C_{OUT} (330 μ F).

Reference

Jiang, Ling, Wesley Ballar, Anjan Panigrahy, and Henry Zhang. "μModule Regulator Achieves Highest Power Efficiency." Electronic Products, October 2024.

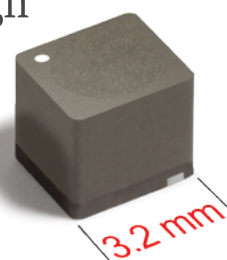
www.analog.com



KTA3030 Series

Low-Voltage, High-Current Power Inductors

- Peak current capabilities of 56 A and above with soft saturation
- Inductance as low as 40 nH for fast transient response and high power in single- or multi-phase converter applications
- DCR as low as 0.83 mΩ and exceptionally low AC losses
- Ideal for modern CPUs, GPUs, ASICs, and SoCs in servers, data centers, automotive, and other power applications



Request Free Samples @ coilcraft.com

Current Sensor for Protection and Control of Wide Bandgap Power Electronics

Allegro MicroSystems introduced “the industry’s first commercially available magnetic current sensor to achieve 10 MHz bandwidth



featuring Allegro’s advanced XtremeSense™ TMR (tunneling magnetoresistance) technology”. The ACS37100 TMR current sensor helps power system designers master the control signal chain and unlock the full potential of fast-switching GaN and SiC FETs. Tailored to the needs of electric vehicles (xEVs), clean energy power conversion systems, and AI data center power supplies, the automotive grade ACS37100 achieves a 50 ns response time, providing the high-fidelity data needed for optimal efficiency and protection in demanding high-frequency applications. At sub-megahertz frequencies, conventional magnetic current sensors lack the speed and precision to provide the high-fidelity, real-time data required for stable control and protection loops. This can leave advanced systems vulnerable to damage and may prevent them from operating at their full potential. The ACS37100 is engineered to solve this control challenge. The device delivers a noise of 26 mA_{RMS} across the full 10 MHz bandwidth. Integrated reinforced isolation is 5 kV for 60 seconds per UL 62368-1 while the internal conductor resistance is specified with 1.2 mΩ.

www.allegromicro.com

Supporting Wide Bandgap R&D

The Microtest Group, a manufacturer of test systems and testing of chips on packages and silicon wafers, launched two turnkey platforms for power device characterization: Quasar²⁰⁰ and Pulsar⁶⁰⁰. Developed by ipTEST, Microtest’s UK subsidiary, the two platforms are claimed to “set a new benchmark in precision testing”. Quasar²⁰⁰ and Pulsar⁶⁰⁰ are designed for academic researchers and engineers developing new semiconductor products. With a plug-and-play approach, they simplify experimental workflows by eliminating the need for custom equipment and reducing manual operations such as soldering and complex test setups. This enables users to obtain accurate, publication-ready results with traceable precision. They speed up datasheet generation, facilitate correlation with production testers, and ensure safe validation of next-generation devices. Quasar²⁰⁰ is suitable for evaluating Si, GaN, and SiC devices. Its counterpart, Pulsar⁶⁰⁰, extends these capabilities to ultra-high current applications, well-suited for testing SiC inverters and automotive systems, supporting short-circuit tests up to 1,000 ADC and more than 10,000 AAC. Both platforms offer up to ±0.1% mea-

QUASAR²⁰⁰ AND PULSAR⁶⁰⁰



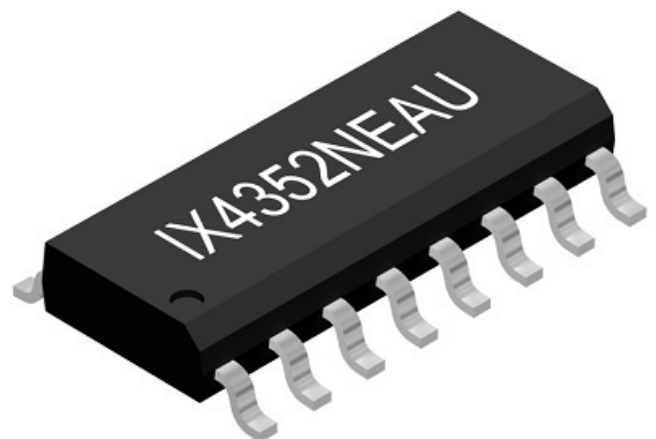
surement accuracy across all voltage and current waveforms, with typical parasitic inductance below 30 nH in AC tests. UKAS (United Kingdom Accreditation Service)-traceable calibration and comprehensive audit logs ensure reliability, consistency, and compliance from lab benches to production lines.

www.microtest.net

Gate Driver simplifies SiC and IGBT Designs

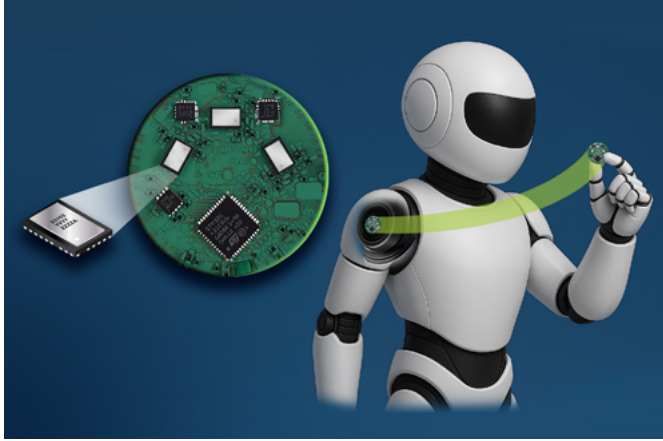
Littelfuse released the IX4352NEAU automotive-qualified low-side gate driver designed to meet the growing demands of SiC MOSFET and IGBT control in electric vehicle (EV) powertrain and DC/DC converter applications. According to the company the IX4352NEAU is “the first AEC-Q100-qualified low-side gate driver to offer an integrated and adjustable negative gate drive bias, eliminating the need for an external negative voltage rail or the costly DC/DC converters typically required to suppress parasitic turn-on of high-speed power devices”. It offers an adjustable negative gate drive bias (down to -10 V) which improves dv/dt immunity, suppresses parasitic turn-on, and ensures faster turn-off of SiC MOSFETs and IGBTs. Furthermore, it offers 9 A peak source and sink drive capability (separate pins), integrated protections and 3.3 V TTL/CMOS-compatible inputs. The devices are AEC-Q100 qualified.

www.littelfuse.com



Reference Design combines Power, Sensing, and Control for Robot Joints and UAVs – fitting in A1 Robot Motor

Efficient Power Conversion Corporation (EPC) launched the EPC91120, a 3-phase brushless DC (BLDC) motor drive inverter optimized for humanoid robot joints. "Featuring EPC's EPC23102 ePower™ Stage IC, the EPC91120 delivers superior efficiency, high power density, and precise motion control in a compact 32 mm-

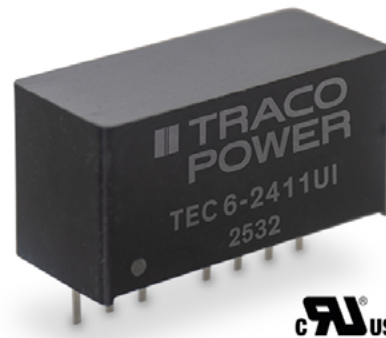


diameter footprint designed to integrate directly within robotic motor assemblies", the company reports. The EPC91120 evaluation board integrates three EPC23102 GaN monolithic half-bridge ICs with an on-board microcontroller, current and voltage sensing, magnetic encoder interface, and RS485 communication. The system operates from 15 V to 55 V_{DC}, delivering up to 21 A peak (15 A_{RMS}) continuous current and 42 A peak (30 A_{RMS}) pulsed. With a 100 kHz PWM switching frequency and only 50 ns dead time, the EPC91120 achieves exceptional efficiency and dynamic performance, ideal for humanoid robot joint motors and other high-precision motion applications. The board was specifically designed to fit the mechanical dimensions of the Unitree A1 robot motor, enabling direct evaluation in real-world robotic systems. Under natural convection cooling at 26 °C ambient, the EPC91120 delivers 7 A_{RMS} per phase without a heatsink and up to 15 A_{RMS} when integrated into the humanoid joint motor casing as a heatsink. Experimental results demonstrate total system efficiencies exceeding 80 % from DC input to mechanical output, validating the design for high-torque, low-weight robotic joints.

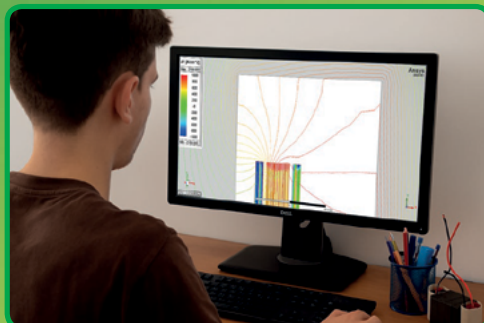
www.epc-co.com

Ruggedized 6 W DC/DC Converters with 8:1 Inputs

The TEC 6UI series from TRACO power comprises isolated DC/DC converters featuring an 8:1 input range. These converters are engineered to seamlessly replace and serve as an alternative to existing 2:1 and 4:1 input converter series. With an input voltage range of 9 to 75 V_{DC}, the TEC 6UI supports a broad spectrum of standard bus voltages, reducing the need for multiple model variants within a single application. Each model includes built-in protection such as short circuit protection, overcurrent limitation, undervoltage lock-out, and remote-control functionality. The converters are certified for an operating temperature range of -40 °C to +80 °C in accordance with IEC/EN/UL 62368-1 and are capable of functioning at altitudes up to 5000 m. Housed in a SIP-8 plastic case, the TEC 6UI series is well-suited for space-constrained applications. Available in both single and dual output configurations with an I/O isolation of 1600 V_{DC}, these converters are suited for a wide range of industrial applications.



www.tracopower.com



**VALIDATING SIMULATIONS
ENHANCING PRODUCTION**



**SIRIO INDUCTIVE COMPONENTS
YOUR PARTNER.
FROM DESIGN TO MANUFACTURING.**



For standard components
visit our website
www.sirio-ic.com

Schottky Barrier Diode combining low V_F and I_R

ROHM has developed a Schottky barrier diode that overcomes the traditional V_F / I_R trade-off. This way, it delivers high reliability protection. The RBE01VYM6AFH represents the concept of leveraging the low- V_F characteristics of rectification SBDs for protection purposes. By adopting a proprietary architecture, ROHM has achieved low I_R that is typically difficult to realize with low V_F designs. As a result, even under harsh environmental conditions, the device meets market requirements by delivering V_F of less than 300 mV (at $I_F=7.5$ mA even at $T_a = -40^\circ\text{C}$), and an I_R of less than 20 mA (at $V_R = 3$ V even at $T_a = 125^\circ\text{C}$). These exceptional characteristics not only prevent circuit damage caused by high photovoltaic voltage generated when powered OFF, but also significantly reduce the risk of thermal runaway and malfunction during operation. The AEC-Q101 qualified diode is housed in a compact flat-lead SOD-323HE package (2.5 mm \times 1.4 mm) that offers both space efficiency and excellent mountability.

www.rohm.com

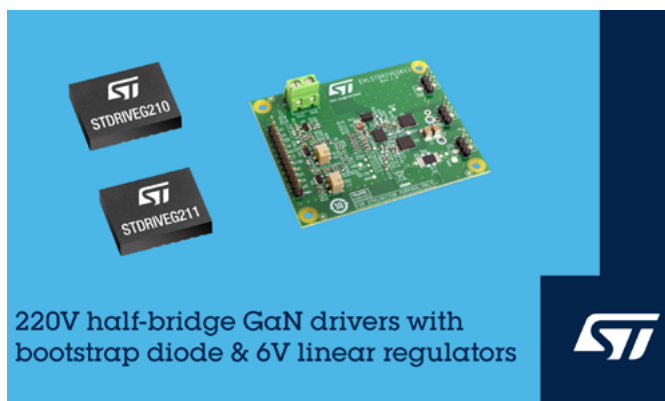


GaN Half-Bridge Gate Drivers

STMicroelectronics' STDRIVEG210 and STDRIVEG211 half-bridge gallium nitride gate drivers are tailored for systems powered from industrial or telecom bus voltages, 72 V battery systems, and 110 V AC line-powered equipment. Rated for maximum rail voltage of 220 V, the drivers integrate linear regulators to generate high-side and low-side 6 V gate signals and provide separate sink and

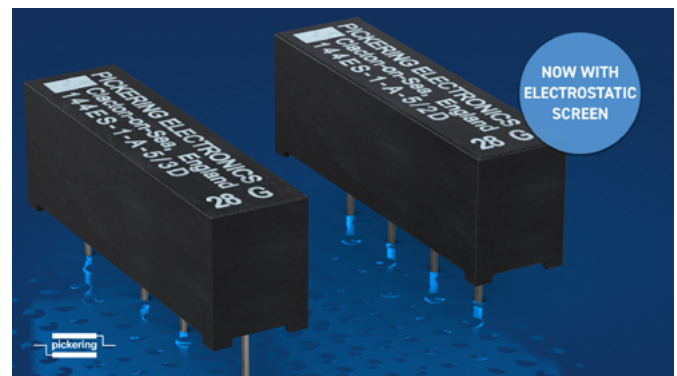
source paths for optimum control. The STDRIVEG210 is featured for power-conversion applications such as server and telecom supplies, battery chargers, adapters, solar micro-inverters and optimizers, LED lighting, and USB-C power sources. Suitable both for resonant and hard-switching topologies, its 300 ns startup time permits to minimize the wake-up time especially during intermittent operation (burst mode). The STDRIVEG211, equipped with overcurrent detection and smart shutdown, targets motor drives in power tools, e-bikes, pumps, and servos, as well as class-D audio amplifiers, in addition to power supplies. Both devices have an integrated bootstrap diode to supply high-side driver.s The separate gate-driving paths can sink 2.4 A and source 1.0 A for fast switching transitions and dV/dt tuning. Protection features include interlocking to prevent cross conduction, while the high-side and low-side drivers have a short propagation delay with 10 ns matching time for low dead time operation. Under-voltage lockout (UVLO) prevents operating in low-efficiency or dangerous conditions and the STDRIVEG211, which is oriented towards motor-drive applications, has additional high-side UVLO protection.

www.st.com



Reed Relais switches up to 80 W

Pickering Electronics has upgraded its Series 144 high power reed relays switching up to 80 W while stacking on a 0.25-inch pitch to include a new variant with an electrostatic shield between the switch and the coil to help minimize noise. Electrostatic screening protects against noise that can otherwise occur between the coil drive and high voltage circuits. This new screening option is in addition to Pickering's internal mu-metal screen, which helps eliminate problems that would otherwise be experienced due to magnetic interaction when devices are closely stacked. Miniature, ultra-high packing density reed relays usually have a switching rating of up to 10 W and 0.5 A, but some applications demand higher switching power and higher carry current specifications. Suitable applications for the Series 144 include mixed signal semiconductor testers, photovoltaic and EV charging, mining gas analysis, medical electronics, in-circuit test equipment, and high voltage instrumentation. As dry reed relays, Series 144 offers an eco-friendlier option than mercury-wetted reed relays. For many applications, it also provides a superior alternative to electromechanical relays (EMRs), where its low-level performance and high isolation significantly improve efficiency and reliability. And compared to EMRs, reed relays deliver



faster switching speeds and longer mechanical lifespans. 1 Form A, 2 Form A and 1 Form B configurations are available, with 5 V, 12 V or 24 V coils offered, all with optional internal diode protection. Additional build options are also available on request, including many pin configurations.

www.pickeringrelay.com

650 V Super Junction TOLL Package Products with Integrated Kelvin Source

Magnachip Semiconductor released two 650 V Super Junction MOSFET (SJ MOSFET) products, adopting the TO-Leadless (TOLL) package, that are designed to meet the high-power and high-current requirements of premium consumer electronics such as premium TVs, gaming monitors, AI laptop adaptors and chargers. Current Magnachip products with TOLL packaging, such as the 80 V – 200 V eXtreme Trench MOSFETs, use a 3-pin configuration. The 650 V SJ MOSFETs have a 4-pin Kelvin configuration, which minimizes the effects of parasitic inductance on the gate-source return path, thereby improving switching stability and overall

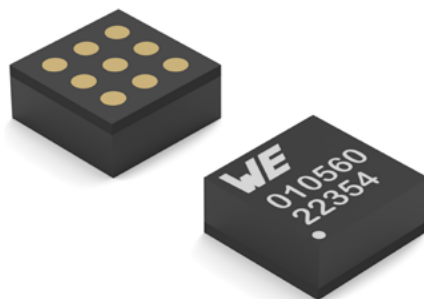


power efficiency by reducing gate oscillation (ringing). Compared to a conventional D2PAK package, the 4-pin TOLL package delivers more than a 100 % increase in current capability, a 24 % reduction in footprint and a 48 % reduction in height. Therefore, the 4-pin TOLL package is suitable for smaller PCB and high-power density applications, which demand high power efficiency and effective heat dissipation performance. For example, the MMTB65R099RFRH device suited for a drain-source voltage of 650 V operates with a maximum $R_{DS(on)}$ of 99 m Ω .

www.magnachip.com

MicroModule Series expanded

The MagI³C-VDMM power module product family from Würth Elektronik continues to grow: The three variable step-down MicroModules for input voltages from 2.5 V to 5.5 V and adjustable output voltages from 0.6 V to 4 V are available in pin-compatible 1 A, 2 A, and 3 A versions. The modules achieve a peak efficiency of up to 96 %. With a quiescent current of 4 μ A, they are also suitable for battery-powered applications. MagI³C-VDMM power modules represent a fully integrated DC/DC power supply that includes a switching regulator with integrated MOSFETs, as well as a controller, compensation, and a shielded inductor – all in a single package. The modules, which can replace linear regulators, are equipped with integrated protection circuits. They protect against



thermal overload and electrical damage caused by overcurrent, short circuit and undervoltage. Depending on the load, they automatically switch between pulse frequency modulation (PFM) and pulse width modulation (PWM) modes.

These mode transitions allow optimal efficiency and output voltage ripple at all load currents. To save energy, the power module can be set to resting mode using an additional pin. Together, the Power-GOOD and EN functions also enable power sequencing. These MagI³C-VDMM power modules measure 3.5 x 3.5 x 1.5 mm³ in an LGA-9 package. The devices are suitable for point-of-load DC/DC applications, industrial and medical equipment, test and measurement devices, for powering DSPs, FPGAs, MCUs and MPUs as well as I/O interfaces. In the operating temperature range from -40 °C to 105 °C the modules comply with EN55032 (CISPR-32) Class B for radiated emissions.

www.we-online.com

Reflow-suitable Package for SiC Devices in High-Power Applications

High-power applications such as electric vehicle charging, battery energy storage systems, and commercial, construction and agricultural vehicles (CAVs) are driving the demand for higher system-level power density and efficiency to meet increasing performance expectations. At the same time, these requirements introduce new design challenges, including reliable operation under harsh environmental conditions, robustness against transient overloads, and optimized overall system performance. To address these challenges, Infineon Technologies has launched the CoolSiC™ MOSFETs 1400 V G2 in the TO-247PLUS-4 Reflow package. The devices support higher DC-link voltages and enable improved thermal performance, reduced system size and enhanced reliability.



The package technology supports reflow soldering at 260 °C for up to three cycles and enables reliable operation with junction temperatures up to 200 °C. This 1400 V voltage class provides additional margin for faster switching and simplifies protection measures against overvoltage. This eliminates the need for power derating and contributes to overall system robustness. The CoolSiC MOSFETs 1400 V G2 in the TO-247PLUS-4 Reflow package are available in $R_{DS(on)}$ classes from 6 to 29 m Ω and suitable for applications where high power density is crucial. Infineon also offers CoolSiC MOSFETs 1400 V in a TO-247-4 package with high creepage. $R_{DS(on)}$ classes for this portfolio range from 11 to 38 m Ω .

www.infineon.com

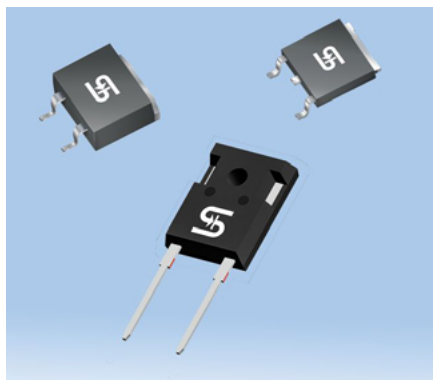
1700 V GaN Technology for 800 V_{DC} AI Data Centers

Power Integrations outlined the benefits of its PowiGaN™ gallium-nitride technology for next-generation AI data centers. The capabilities of 1250 V and 1700 V PowiGaN technology for 800 V_{DC} power architectures are explained in a new white paper from Power Integrations. This white paper details the performance advantages of Power Integrations' industry-first 1250 V PowiGaN HEMTs, illustrating their field-proven reliability and their ability to meet the power-density and efficiency requirements (>98 %) of the 800 V_{DC} architecture. Further, the paper demonstrates that a single 1250 V PowiGaN switch delivers greater power density and efficiency compared to stacked 650 V GaN FETs and competing 1200 V SiC devices.

www.power.com



1,200 V Automotive-Grade Low-Loss Diodes



Taiwan Semiconductors introduced a series of automotive-grade, low-loss diodes offered in industry-standard packages. The 1,200 V PLA/PLD series, with ratings of 15 A, 30 A or 60 A, all feature maximum forward voltages of 1.3 V, a reverse leakage of less than 10 μ A at 25 °C and junction temperatures of up to 175 °C. Available in three popular packages (ThinDPAK, D2PAK-D and TO-247BD), the 1,200V diodes enable easy

drop-in replacement to improve efficiency in existing designs. Applications include three-phase AC/DC converters, server and computing power systems, EV charging stations, on-board battery chargers, Vienna rectifiers, totem pole and bridgeless topologies, inverters and UPS systems, and general-purpose rectification in high-power systems of various types.

www.taiwansemi.com

Power-Management Solutions for scalable AI Infrastructures



Texas Instruments (TI) debuted design resources and power-management chips to help companies meet growing artificial intelligence (AI) computing demands and scale power-management architectures from 12 V to 48 V to 800 V_{DC}. A typical example is a reference design for a 30 kW AI server power-supply unit featuring a three-phase, three-level flying capacitor power factor correction converter paired with dual delta-delta three-phase inductor-inductor-capacitor converters. Another example is a Gallium-nitride intermediate bus converter capable of delivering up to 1.6 kW of output power in a quarter-brick (58.4 mm by 36.8 mm) form factor based on TI's LMM104RM0 converter module offering over 97.5 % input-to-output power-conversion efficiency and the possibility for active current sharing between multiple modules.

www.ti.com

Advertising Index

Absopulse	35	GVA	19	Sanan	C3
APEC	43	HIOKI	13	Semikron Danfoss	17
ARCEL	45	Hitachi Energy	35	SIRIO ELETTRONICA	53
Coilcraft	51	Infineon	33	Texas Instruments	21
COMSOL	31	ITG Electronics	23	Toshiba	11
ed-k	C2	Mitsubishi Electric	25	Vicor	39
Efficient Power Conversion (EPC)	C4	MPS	9	Vincotech	27
Electronic Concepts	1	PCIM	30	Würth Elektronik eiSos	3, 41
Embedded World	40	Plexim	15		
Fuji Electric Europe	29	ROHM	7		

Sanan - Your Partner for Wide Band Gap Solutions



- Power SiC MOS FETs
- Power SiC SBDs
- Power SiC & GaN foundry services
- Full turnkey manufacturing platform



www.sanan-semiconductor.com/en

Europe sales.europe@sanan-ic.com
Hong Kong sales.hk@sanan-e.com
Japan sales.jp@sanan-e.com
Korea sales.kr@sanan-e.com
✉ **Americas** sanan-semi@luminus.com

 **San'an**

We're selling micro Ohms.

And the fewer, the better.



EPC2373
15 V, 470 $\mu\Omega$
3.3 x 2.6 mm

470 $\mu\Omega$



epc-co.com



<https://l.ead.me/EPC2373>